The Synthesis and *In Vitro* Evaluation of Short Interfering RNA Containing Triazole Functionalized Sphingolipid-Based Derivatives

by

Charlene A. Fernandez

A thesis submitted to the
School of Graduate and Postdoctoral Studies in partial
fulfillment of the requirements for the degree of

Master of Science in Applied Bioscience

Faculty of Science

University of Ontario Institute of Technology (Ontario Tech University)

Oshawa, Ontario, Canada

December 2021

THESIS EXAMINATION INFORMATION

Submitted by: **Charlene A. Fernandez**

Master of Science in **Applied Bioscience**

Thesis title: The Synthesis and *In Vitro* Evaluation of Short Interfering RNA Containing Triazole Functionalized Sphingolipid-Based Derivatives

An oral defense of this thesis took place on November 18, 2021 in front of the following examining committee:

Examining Committee:

Chair of Examining Committee	Dr. Janice Strap
Research Supervisor	Dr. Jean-Paul Desaulniers
Examining Committee Member	Dr. Denina Simmons
External Examiner	Dr. Hendrick de Haan, University of Ontario Institute of Technology (Ontario Tech University)

The above committee determined that the thesis is acceptable in form and content and that a satisfactory knowledge of the field covered by the thesis was demonstrated by the candidate during an oral examination. A signed copy of the Certificate of Approval is available from the School of Graduate and Postdoctoral Studies.

ABSTRACT

RNA Interference (RNAi) is a natural cellular process that silences the expression of a target gene in a sequence-specific manner by mediating targeted mRNA degradation. One of the main challenges in RNAi research is developing an effective delivery system for siRNAs. Recently, fatty acid conjugated siRNAs have shown promising potential as safe and effective method to deliver oligonucleotides to extrahepatic cells. A class of fatty acids that we are interested in are sphingolipids, they are a class of lipids containing a backbone of sphingoid bases and aliphatic amino alcohols. Sphingolipids show potential as lipid-conjugated siRNAs as they are important structural and functional components of plasma membranes of eukaryotic cells.

Here, we design a library of siRNAs containing propyl-triazole modified sphingosine at various locations of the sense and antisense strand of the reporter gene firefly luciferase and evaluate its gene-silencing abilities in both the presence and absence of a transfection carrier.

Keywords: sphingolipids; siRNA; gene-silencing; cellular uptake; RNA interference

AUTHOR'S DECLARATION

I hereby declare that this thesis consists of original work of which I have authored. This is a true copy of the thesis, including any required final revisions, as accepted by my examiners.

I authorize the University of Ontario Institute of Technology (Ontario Tech University) to lend this thesis to other institutions or individuals for the purpose of scholarly research. I further authorize University of Ontario Institute of Technology (Ontario Tech University) to reproduce this thesis by photocopying or by other means, in total or in part, at the request of other institutions or individuals for the purpose of scholarly research. I understand that my thesis will be made electronically available to the public.

_____ Charlene Fernandez

STATEMENT OF CONTRIBUTIONS

All of the studies reported in this dissertation were performed by myself under the supervision of Dr. Jean-Paul Desaulniers. For the oligonucleotide synthesis, Dr. Lidya Salim generated the RNA sequences using the synthesizer.

I hereby certify that I am the sole author of this thesis and that no part of this thesis has been published or submitted for publication. I have used standard referencing practices to acknowledge ideas, research techniques, or other materials that belong to others. Furthermore, I hereby certify that I am the sole source of the creative works and/or inventive knowledge described in this thesis.

ACKNOWLEDGEMENTS

First, and foremost I would like to extend my gratitude to Dr. Jean-Paul Desaulniers. This thesis was a very challenging at times, it has challenged my organic chemistry and biology knowledge, and you have kept me on track throughout every trial and turbulation. Thank you for providing the opportunity to continue research and growing my knowledge for chemical biology and nucleic acid chemistry. Thank you, JP.

Thank you to past and present members of the Desaulniers research group for their help directly or indirectly with my work. Lidya and Matthew, the both of you welcomed me into the group when I was in my third year of undergrad and I have learned a lot from you both. Ifrodet, we started in the Desaulniers group at the same time and have grown a lot as researchers, and I'm thankful for your constant enthusiasm towards research. Autumn, our projects were quite different, but you always brought a positive outlook and I'm thankful for the different ideas we can bounce off of. Andrew, I'm grateful for the additional guidance you've provided inside and outside of the lab.

Many thanks to Dr. Eva Goss and Synthose for providing a great opportunity to collaborate on this challenging but rewarding project. Without your ideas, guide and optimism we wouldn't have had successful outcomes.

I would like to thank Dr. Denina Simmons, as a member of my Masters committee, I appreciate your time, effort and enthusiastic ideas throughout the entire project.

A special thank you to Richard, Gen, and Mike for all the chats and help over the last few years, I truly appreciate your time, effort, and snacks.

Thank you to the members of the Easton and Zenkina group, you have all kept me educated and entertained during the last few years. Hopefully we'll be able to share more Skip-bo and Uno matches, Nintendo Switch tournaments and pints of cider in the coming years.

To my parents, thank you for all of your love and support over the entirety of my university career. Thank you for consistently pushing me to achieve greatness, I would not have made it this far without your support.

Lastly, I would like to thank my girlfriend Rana. I cannot begin to express how lucky I feel to have you by my side, and I know I could not have accomplished any of this work without your love, and encouragement. Thank you for listening to me talk about more organic chemistry, mechanisms, and biology than an electrochemist should ever have to. Thank you for constantly reminding me to never dim my light to make others comfortable.

There are many others who I would like to thank, however, in the interest of space I simply say that I appreciate all of the support and love offered by my friends. It's often your kind words, love and support that help keep me going.

TABLE OF CONTENTS

LIST OF FIGURES

CHAPTER 1

CHAPTER 3

LIST OF TABLES

LIST OF SCHEMES

LIST OF ABBREVIATIONS AND SYMBOLS

A: Adenosine

Ago2: Argonaute2

ASGPR: Asialoglycoprotein receptor

ASO: antisense oligonucleotide

BCL2: B-cell lymphoma protein 2

bp: base pair

C: Cytosine

CD: Circular dichroism

CPG: Controlled pore glass

EDTA: Ethylenediaminetetraacetic acid

DCM: dichloromethane (CH_2Cl_2)

DIPEA: *N*,*N*-diisopropylethylamine

DMAP: 4-(dimethylamino)pyridine

DMEM: Dulbecco's modified Eagle medium

DMF: *N*,*N*-dimethylformamide

DMSO: dimethylsulfoxide

DMT: 4,4'-dimethoxytrityl

DNA: 2'-deoxyribonucleic acid

ds: double-stranded

dsRNA: double-stranded RNA

dsRBD: double-stranded RNA binding domain

dT: 2'-deoxythymidine

EMAN: methylamine 40% wt. in H_2O and methylamine 33% wt. in ethanol (1:1)

ESI-MS: Electrospray ionization mass spectrometry

EtOAc: Ethyl acetate

EtOH: Ethanol

FDA: US Food and Drug Administration

FBS: Fetal bovine serum

G: Guanosine

GalNAc: *N*-acetylgalactosamine

J: Coupling constant (Hz)

LNP: Lipid nanoparticles

MALDI-TOF: Matrix assisted laser desorption ionization – time of flight

MeCN: Acetonitrile

MeOH: Methanol

miRNA: microRNA

mRNA: Messenger RNA

nt: nucleotide

NMR: Nuclear magnetic resonance

OH: hydroxyl

ONs: Oligonucleotides

PACT: Protein kinase RNA activator

PCR: Polymerase chain reaction

PIWI: P-element-induced wimpy tested domain

PS: Phosphorothioate

RISC: RNA-induced silencing complex

RNA: Ribonucleic acid

RNAse: ribonuclease

RNAi: RNA interference

rt.: Room temperature

S1P: Sphingosine-1-phosphate

S1PR: Sphingosine-1-phosphate receptor

siRNA: Small interfering RNA

t: Triplet

T: Thymidine

TBDPS: *tert*-butyldiphenylsilyl

TCA: Trichloroacetic acid

TEA: Triethylamine

THF: Tetrahydrofuran

TLC: Thin-layer chromatography

ΔT_m: Change in Melting Temperature

T_m: Melting temperature

TRBP: Transactivation response RNA binding protein

tRNA: Transfer RNA

U: Uridine

UV: Ultraviolet

wt: Wild-type

Chapter 1: Introduction

1.1 DNA *versus* RNA

Deoxyribonucleic acid (DNA) is the hereditary material in humans and almost all organisms; it holds instructions an organism needs to develop, live, and reproduce.[1] DNA, along with ribonucleic acid (RNA) and proteins, is one of three major macromolecules that are essential for life. DNA consists of two long polymers made up of monomeric units called nucleotides. A nucleotide is comprised of a 5-carbon sugar, a nucleobase (base), and a phosphate group, shown in **Figure 1.1 (A)**. There are four different bases in DNA, purine base: adenine (A) and guanine (G); pyrimidine bases: cytosine (C) and thymine (T).[2]

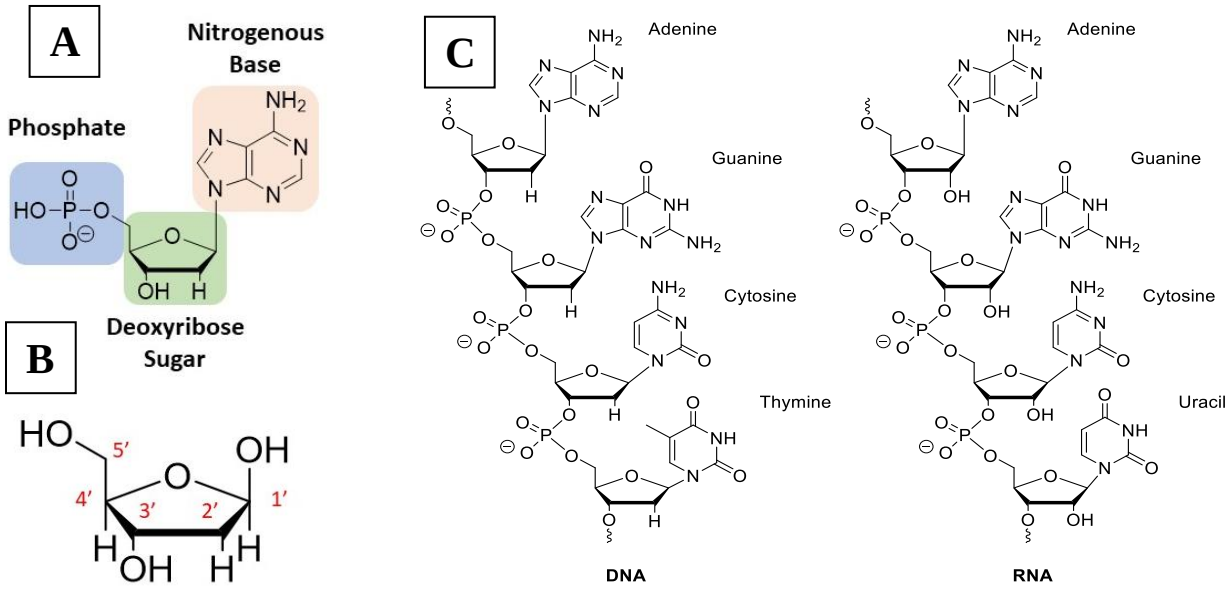

Figure 1.1: (A). Structure of a nucleotide with 3 main components: phosphate, nitrogenous base, and deoxyribose sugar. **(B).** Deoxyribose sugar with indications of numbered 1' to 5'. **(C).** Natural structure of DNA and RNA.

The carbons within the deoxyribose ring are numbered 1' to 5', shown in **Figure 1.1 (B)**. Within each monomer, the phosphate is linked to the 5'-carbon of the deoxyribose and the nitrogenous base is linked to the 1'-carbon by a N-glycosidic bond. In the DNA strand, the

phosphate residue forms a link between the 3'-hydroxyl (OH) of one deoxyribose and the 5'-hydroxyl of the next, this linkage is called a phosphodiester bond.

The order of the nucleobases determines the genetic code, which subsequently specifies the sequence of the amino acids within proteins for building and maintaining an organism; similar to how the order of letters in the alphabet can appear in a certain order to generate words or sentences. In the DNA double helix, the two strands run in opposite directions illustrated in **Figure 1.2 (B)**. The ends of the DNA strands are called the 5' (five prime) and 3' (three prime) ends. The 5'-end has a terminal phosphate group, while the 3'-end has a terminal hydroxyl group.

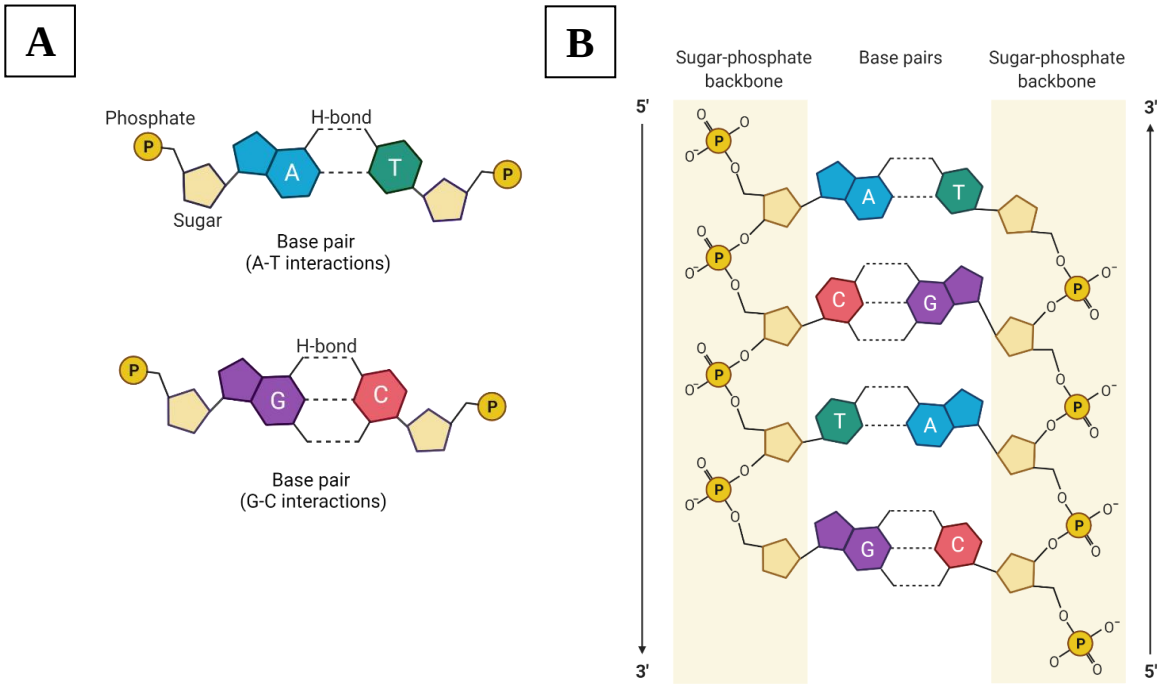

Figure 1.2. (A): Purines and pyrimidines, with hydrogen bonding indicated by the dashed line. **(B).** The DNA double helix, with sugar phosphate backbone and nitrogenous bases.

In **Figure 1.2 (B)**, one strand is running 5' to 3' top to bottom, whereas the other strand is running 3' to 5' top to bottom. The two sequences interact via hydrogen bonds engaging in complementary base pairing. The purines form hydrogen bonds to pyrimidines, with A bonding

only to T, and C bonding only to G, shown in **Figure 1.2 (A)**. The base pairs are stabilized by hydrogen bonds; adenine and thymine form two hydrogen bonds, whereas cytosine and guanine form three hydrogen bonds.

Similar to DNA, RNA is another macromolecule that is essential for all known forms of life. RNA is known to be involved in several important roles in the cell; messenger RNA (mRNA) translating DNA to make proteins, transfer RNA (tRNA) brings amino acids to the ribosome during protein synthesis, microRNA (miRNA) provides non-specific transcriptional control, and short interfering RNA (siRNA) provides highly specific knockdown of a target mRNA.[3] Although there are a few similarities between DNA and RNA, they differ from one another in three basic respects illustrated in **Figure 1.1 (C)**. First, RNA utilizes uracil as a nitrogenous base, instead of the thymine used in RNA. Second, RNA nucleotides possess a hydroxyl group at the 2'position, while DNA is deoxygenated at that position to a proton. The addition of a hydroxyl group impacts the structural conformation of the sugar by adopting a C3'-*endo* conformation. This occurs due to the gauche effect between the 2'-hydroxyl and the 4'-oxygen on the sugar.[4] Lastly, there are nearly 200 chemical modifications for RNA, whereas DNA's modifications are limited.[5, 6] Shown in **Figure 1.1 (C)** is the chemical structure comparison of natural DNA and RNA.

One of the most important pathways in molecular biology is the 'Central Dogma'. The central dogma is a two-step process in which the genes on the DNA are transcribed into RNA and translated into a sequence of amino acids that generate a protein. Shown in **Figure 1.3** is an illustration of the pathway.

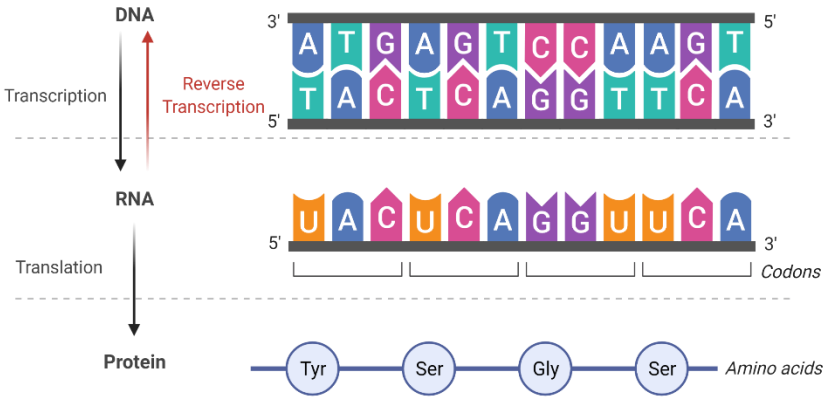

Figure 1.3: The flow of genetic information. The arrows represent steps where DNA or RNA is being used as a template to direct the synthesis of another polymer, either RNA or protein. Created with BioRender.

The process involves two major steps: transcription and translation. The pathway begins with unwinding the DNA double helix, where it can either undergo replication in preparation for cell division or generate RNA via transcription.[7] In transcription, an enzyme called RNA polymerase uses DNA as a template for the synthesis of a complementary RNA. This leads to the dissociation of RNA polymerase from the DNA template and the release of the RNA product, mRNA. The mRNA is exported from the nucleus and associates with itself with ribosomes before it can begin translation.[8] In translation, the sequence of the mRNA is decoded to specify the amino acid sequence of a polypeptide. Specifically, the nucleotides of the mRNA are read in triplets called codons. As a ribosome latches on to an mRNA, it will find the "start codon" then gradually build a chain of amino acids based on the sequence, one codon at a time. Ribosomes depend on a group of specialized tRNA molecules. tRNAs contain 3 nucleotides that can match with the codon and deliver their amino acid cargo. This process repeats many times with the ribosome moving down the mRNA one codon at a time until it reaches a "stop codon" and releases the polypeptide.

Since the 1970's there has been an excitement and interest with manipulating gene expression in living cells through targeting the previously described pathway.[9] This led to the discovery of oligonucleotides (ONs), short DNA or RNA molecules that have the ability to inactivate genes involved in disease processes. Traditional medicine targets post-translational

molecules such as proteins, whereas ONs can be designed to target a specific mRNA at the pre-translational level, affording a new specific means of gene suppression.[9] There is a great interest in utilizing this therapeutic design as a means to treat diseases that were deemed "untreatable".[10] There are a couple of pathways oligonucleotides use such as antisense oligonucleotides (ASO) and RNA interference (RNAi). In this thesis, we will be focussing on the RNAi pathway.

1.2 RNA Interference (RNAi)

RNAi is a natural cellular process that silences gene expression by promoting the degradation of mRNA (**Figure 1.4**).[11] This process plays an important role in gene regulation and as a defense mechanism against invading viruses. RNAi was first discovered in 1988 by Fire and Mello in their Nobel prize winning study investigating the mechanisms for effective gene inhibition by exogenous RNA in *Caenorhabditis elegans.*[12] Their observations found that RNAi is an evolutionarily conserved mechanism of gene-specific process in which the degradation of the target mRNA is guided by a complementary double-stranded RNA (dsRNA). It appeared later, that the same process occurs throughout the eukaryotic kingdom. This led to the discovery of a class of dsRNAs that exhibited gene silencing abilities called short interfering RNA (siRNA). Since then, siRNAs have rapidly become a widely used tool for molecular biology gene knock-down experiments and has dominated the medicine world by targeting disease genes previously considered "undruggable".[13]

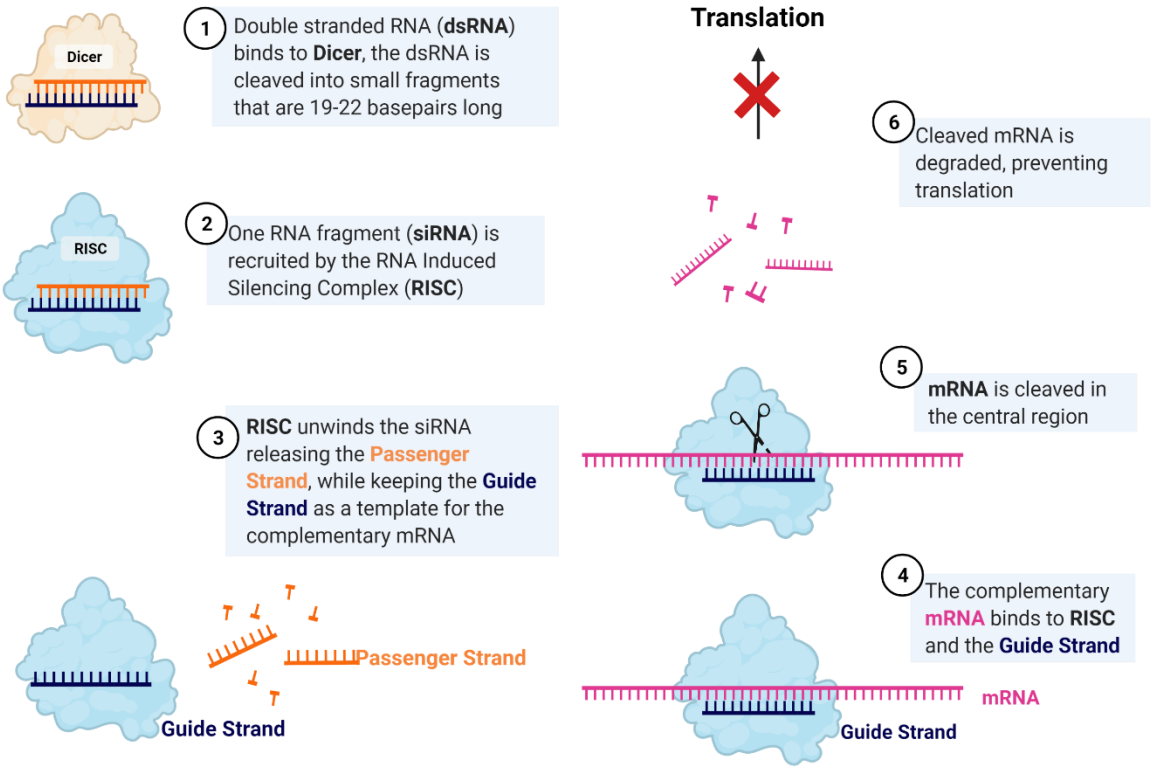

Figure 1.4: The RNA interference pathway. Created with BioRender.

1.2.1 siRNA and RNAi in Mammals

The RNAi pathway begins with the introduction of a dsRNA into the cytoplasm via transcription from cellular genes or infecting pathogens. A specialized ribonuclease (RNase) enzyme named Dicer cleaves the dsRNAs into smaller dsRNA molecules. This short dsRNA molecule is known as short interfering RNA (siRNA). siRNAs are 19-22 nucleotides in length and possess a definitive two-base pair overhang on the 3' end of each strand. The small fragments are then bound to an Argonaute2 (Ago2) protein that is specific for dsRNAs that are in the A-form helical conformation. The binding of the Ago2 initiates the formation of the RNA induced silencing complex (RISC), it's an assembly of dsRNA binding proteins such as protein kinase RNA activator

(PACT) and transactivation response RNA binding protein (TRBP). The RISC senses the relative thermodynamic asymmetry between the ends of the siRNA. The binding is enhanced by the presence of the 5'-phosphate, while hydroxyl groups inhibit binding.[14] As a result of the asymmetric binding, the guide strand is preferentially loaded into active RISC, and the passenger strand is degraded.[15, 16] The guide strand is utilized as a template to target the complementary mRNA.[17] Once the duplex is formed between the guide strand and the complementary mRNA, the mRNA is cleaved at the phosphodiester bond between base pairs 9 and 10 counting from the 5'-end of the guide strand. The resulting cleaved mRNA dissociates from the RISC and can no longer be translated into the encoded protein.[7] This pathway can be initiated in two ways: synthetic siRNAs can be transfected into cells using transfecting agents, or native long endogenous dsRNA is processed by Dicer into siRNA.[18] Dicer and Ago2 are essential enzymes involved in the RNAi pathway. Dicer has two distinct RNase motifs: dsRNA binding domain (dsRBD) and an N-terminal ATP-dependent RNA helicase domain.[19] The dsRBD binds dsRNA together, and is present in RNA editing, RNA transport, RNA processing and RNA silencing.[20] Meanwhile, the RNA helicase domain uses ATP to catalyze the cleavage or remodeling of long dsRNA.[21] Additionally, Argonaute2 endonuclease is an essential enzyme involved in the RNAi pathway as it cleaves the sense strand from the duplex. [22 23] The endonuclease is comprised of four main domains: the N-terminal domain (N), the P-element-induced wimpy tested (PIWI) domain, the PIWI/Argonaute/Zwille (PAZ) domain, and the middle (MID) domain[24-27] as is shown in **Figure 1.5**.

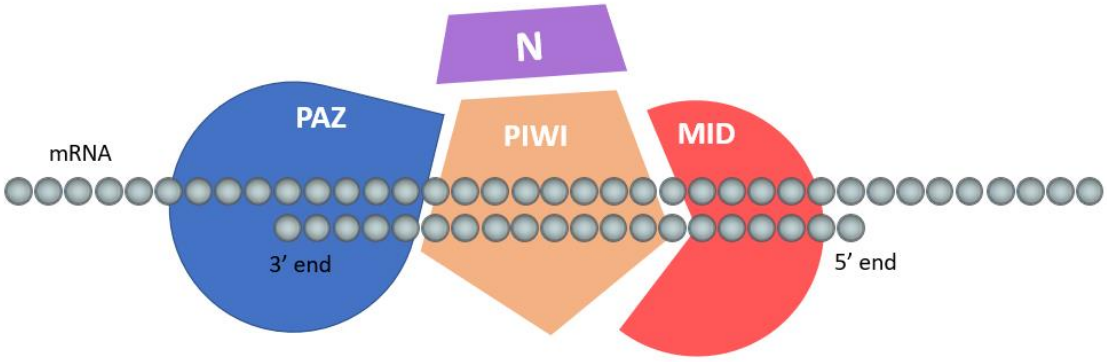

Figure 1.5: Argonaute2 catalytic region with an antisense RNA and target mRNA. Created with BioRender.

Argonaute2 forms a bilobal scaffold composed of MID-PIWI and N-PAZ lobes that are connected by linkers. The bilobal structure binds to guide and target molecules along a nucleic acid-binding channel. The PIWI domain is a structural homologue of the RNase H catalytic domain and contributes to endonuclease splicing activity for the target strand.[28 29] The MID domain interacts directly with the 5'-end of the guide strand by recognition of the phosphorylated first nucleotide.[30, 31] The PAZ domain contains a hydrophobic pocket of an oligosaccharide-binding-like fold and associates with the 3'-end of the guide strand.[32-34] The N-terminal is the least well characterized of the four domains although there is some insight to its purpose. In previous studies, the N-terminus domain prevents the extension of base pairing of the guide and target strands at the 3'-region of the guide.[35, 36] In addition, biochemical studies of human Argonaute (*Hs*Ago) showed that the N-terminal domain facilitates the unwinding of the guide/target duplex during RISC assembly.[37] There are many interacting regions of the domains and enzymes, therefore it is important to keep this in mind when chemically modifying siRNAs in order to retain function for purposes such as molecular biology tool or a potential therapeutic agent.

1.2.2 RNAi Limitations

Over the last decade, there has been a lot of success with the use of RNAs as therapeutics as they have changed the medicinal world with their ability to target disease genes previously considered "undruggable".[38] It was not until about 20 years later, in 1989, the first antisense oligonucleotide therapeutic, Fomvivirsen (marketed as Vitravene) was FDA approved to treat cytomegalovirus. Fifteen years after, in 2013 the second antisense oligonucleotide therapeutic Mipomersen (marketed as Kynamro) was FDA approved to treat homozygous familial hypercholesterolemia. With more than two decades after the natural gene-silencing mechanism of RNAi was elucidated, siRNA-based therapeutics have broken into the pharmaceutical market. Currently, there are three therapeutics already approved and many others in advanced stages of drug development pipeline. In 2018, Patisiran (marketed as Onpattro) was the first FDA approved siRNA drug to treat polyneuropathy in people with hereditary transthyretin-mediated amyloidosis. In November 2019, Givosiran (marketed as Givlaari) was the second siRNA therapeutic to be FDA approved for the treatment of adults with acute hepatic porphyria. The third siRNA therapeutic to be FDA approved was Lumasiran (marketed as Oxlumo) in November 2020 for the treatment of primary hyperoxaluria. Although we can see the success of siRNA therapeutics now, it took nearly 20 years to develop the first siRNA-based drug due to the natural structure of RNA led to enzymatic degradation, polyanionic nature of RNA physiological pH and off-target effects. There are three main regions on the RNA that have led to the drawbacks of RNA therapeutics: 2'-hydroxyl group on the ribose sugar, phosphodiester backbone and nucleotide base.

Natural RNA is easily degraded within every organism due to the presence of exo- and endo-nucleases in the blood serum, as the phosphodiester backbone linkages on the RNA are subject to being natural substrates.[39] The phosphodiester bond is also susceptible to hydrolysis at physiological pH since phosphorous is oxophilic; the oxygen in water can attack the electron deficient center.[40] The 2'-hydroxyl group on the ribose sugar can also perform a nucleophilic attack on the closest phosphorous atom to undergo a self-hydrolysis.[41]

The hydroxyl group present on the phosphodiester linkage has a pk_a value close to zero, indicating that under physiological conditions deprotonation will occur, resulting in a polyanionic backbone.[40] This hinders RNA's ability to cross the cellular membrane due to the negatively charged moieties on the surface of the cellular membrane.[42] The charge density of the RNA inhibits its ability to associate with serum proteins such as albumin, resulting in strands becoming hydrolyzed.[43]

Considering the siRNA antisense strand relies on Watson-Crick base pairing to identify target mRNA, it is possible that other mRNA sequences that are similar to the target may undergo accidental degradation.[44] Duplexes with a mismatch are able to form RISC tolerable substrates and result in off-target silencing.[44] Occasionally when an siRNA associates with RISC, there is an error in strand selection and the active RISC is formed with the guide strand resulting in solely off-target effects.[45]

One of the main challenges siRNA drug development faces is site-specific delivery.[3, 46] As previously mentioned, the large anionic siRNA molecules must overcome a variety of physiological barriers to reach the cytoplasm in target cells. siRNA drugs have shown their success by increasing their stability and specificity with delivery systems such as formulation-mediated delivery and numerous chemical modifications, which will be the main focus of this dissertation herein.

1.2.3 Chemical Modifications of siRNAs

For a number of years, nucleic acid chemists have investigated and synthesized chemically modified oligonucleotides with the goal of avoiding the drawbacks natural RNA faces while maintaining potent gene silencing abilities. With the recent success of siRNA therapeutics, the research community has a better understanding of how to achieve both goals.

Using well-established nucleic acid synthetic methods synthesizing oligonucleotides and implementing chemical modifications at specific positions is straight-forward. In order to accomplish this, the oligonucleotides are built one base pair at a time by using a controlled-pore

glass (CPG) support.[47] A method that is commonly used is the dimethoxytrityl (DMT)-phosphoramidite solid phase synthesis, shown in **Figure 1.6**.[48] DMT-phosphoramidite uses a 5'-triphenyl alcohol protecting group and a 2'-phosphite group to precisely build specific sequences and allowing modifications to be specifically incorporated into the oligonucleotide through modified phosphoramidites.

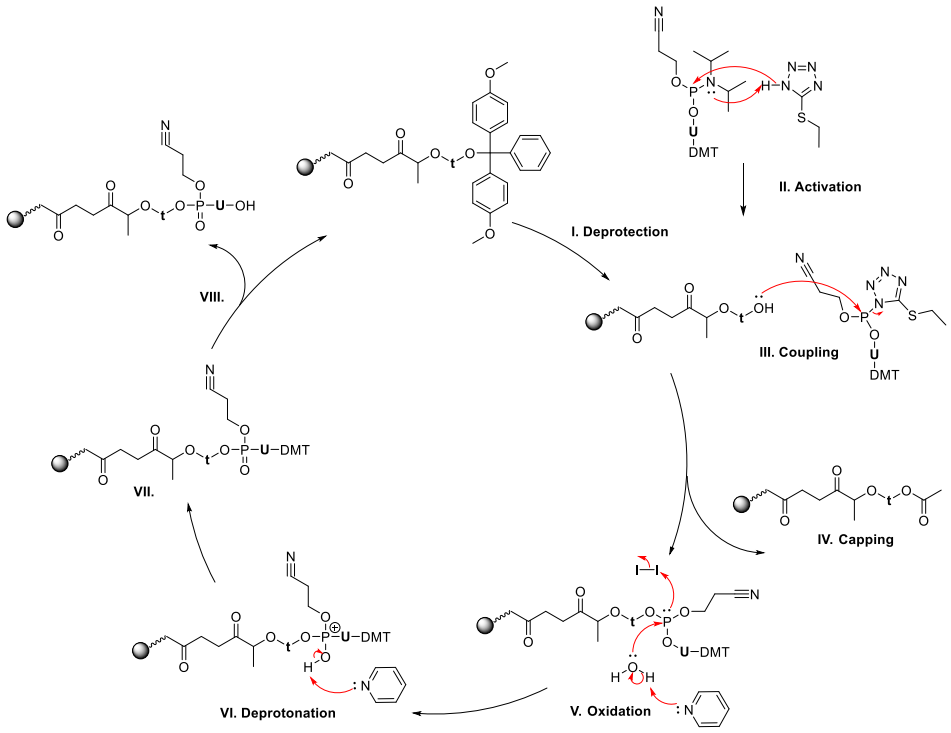

Figure 1.6. DMT-Phosphoramidite oligonucleotide synthesis for solid-phase RNA synthesis.

The CPG solid support typically has a DMT protected dT base attached to the support, as a result the fully automated synthesis proceeds in the 3' to 5' direction. The first step (I) detritylation, it is the acid-mediated deprotection of the 5'-DMT group. This is accomplished by using trichloroacetic acid, producing a primary alcohol that will couple with the next nucleobase. The trityl cation that is generated, is resonance stabilized by the methoxy groups, allowing it for easy cleavage.[49] In order for the subsequent base to couple, it must be activated (II) with ethylthiotetrazole, which is an excellent leaving group that allows for displacement of

diisopropylamine. Since phosphorous is oxophilic, the free primary alcohol readily attacks the phosphite center of the activated base coupling to the nucleobases (III).[50] The free bases must then be capped (IV) with a protective acetyl group, to prevent unwanted reactions or incorrect sequences. This generates a phosphite linkage that must be oxidized to phosphate, to accomplish this, phosphorous undergoes a nucleophilic attack on iodine (V).[50] The intermediate is readily deprotonated by another pyridine molecule (VI), generating the stable phosphate (VII).[49] The oligonucleotide can undergo one of two steps: continue the cycle by coupling successive bases, or terminate the cycle by undergoing a cleavage and deprotection (VIII).

Over the last couple of decades, there is a variety of chemical modifications for oligonucleotides, with more constantly emerging. The types of modifications are categorized into three categories: backbone modifications, ribose sugar modifications and nucleobase modifications.[46] Shown in **Figure 1.7** is a summary of various chemical modifications for oligonucleotides. Several of these structures will be described in depth in the following paragraphs.

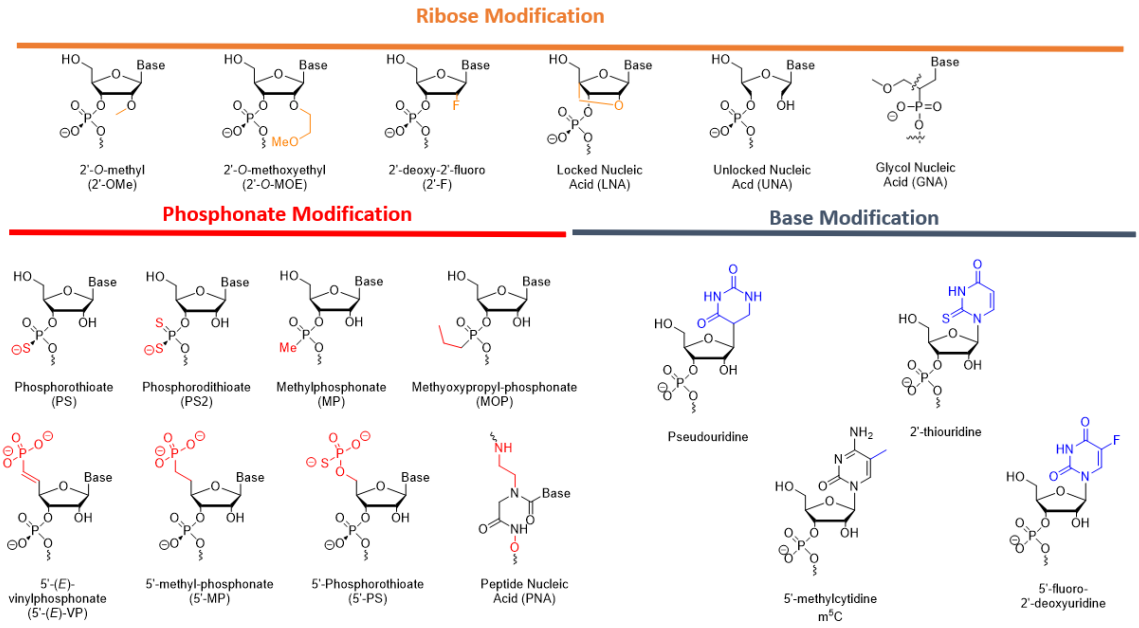

Figure 1.7: Structures of chemical modifications and analogs utilized for siRNA and ASO.

One of the earliest-discovered and most commonly utilized modifications is the replacement of the highly charged, unstable phosphodiester backbone with a phosphorothioate (PS) backbone.[51] This is achieved by replacing one of the non-bridging oxygen atoms on the phosphate group with a sulfur atom. Additionally, the PS linkage increases oligonucleotide's hydrophobicity, resulting in increased circulation time, increased half-life, and more favorable pharmacokinetics.[52-54] Although previous studies have shown that PS modification reduces the binding affinity between the oligonucleotide and its target sequence to some extent and aggravates chemistry-related toxicities with a high PS content, PS modifications are still vital and necessary for siRNA modifications.[55, 56] In addition, other modifications have been identified and successfully used to replace the phosphodiester group on oligonucleotides and change the properties, this includes: phosphorodithioate (PS2), methylphosphonate (MP), methoxypropylphosphonate (MOP), and peptide nucleic acid (PNA).[57] The PS2 modification has shown to increase the affinity between RISC and siRNA.[58] The site-specific incorporation of MP and MOP modifications are used to mitigate the hepatotoxicity of antisense oligonucleotides.[59, 60] Furthermore, PNA is typically used to modify detection probes for capturing and detecting certain nucleic acid targets.[61]

Ribose sugar modifications are useful for controlling the ribose ring puckering. Sugar puckering is an important physical property for oligonucleotides because they affect the binding affinity with complementary sequences, duplex conformation, and enzyme substrate toleration.[62] The sugar conformation is directed by the steric forces and electronegative characteristics of the sugar substituents.[63] In RNA the 2'-hydroxyl and 3'-oxygen drive the conformation to a C_3'-*endo*, sometimes referred to as the "North" conformation.[63] There are many sugar modifications that are well tolerated in RNAi the most common modifications are at the 2' position to protect the siRNA from participating in nuclease-mediated cleavage, endoribonuclease degradation and enhance stability.[64, 65] Most commonly, the OH group is modified with a 2'-fluoro (2'-F), 2'-O—methyl (2'-OMe), or a 2'-O-methoxyethyl (2'-MOE).[66] Notably, 2'-OMe is a naturally occurring ribose sugar

and the most frequently used modification as it can enhance stability, increase affinity for its target mRNA and reduce immunogenicity in the body.[67] Based on 2'-OMe, a series of analogs have been identified, among which 2'-MOE is the most favorable.[64] The 2'-MOE modification has shown higher binding affinity for RNA than 2'-OMe, which further increases the capability of the modified siRNA to resist nuclease attack.[68] Another widely used 2'-OH modification is 2'-F, as the highly electronegative fluorine causes the modified siRNA to readily adopt a C_3'-endo conformation, providing considerable benefits in binding affinity with ΔT_m of 2.5ºC per modified nucleotide.[41] In addition, 2'-carbon, 4'-carbon or the whole sugar ring can undergo modifications, resulting in molecules including unlocked nucleic acid (UNA), locked nucleic acid (LNA), glycol nucleic acid (GNA), and tricyclo-DNA (tcDNA). With the UNA modification, the RNA results in higher flexibility and thermal destabilization due to the unconnected 2' and 3' carbons. UNAs have the ability to block the entry of passenger strands and promote RISC loading of the guide strand through its asymmetrical characteristics.[69] Similarly, GNA can be used to remove off-target effect-induced hepatotoxicity by including the modification in the seed region of the siRNA guide strand.[70] LNA's modification involves forming a bridge between the 2'-oxygen and the 4' carbon, this "locks" the ribose into the preferred C_3'-*endo* conformation and significantly increasing the affinity of base pairing. [71]

The final category of chemical modifications are the nucleobases as they have shown to have an impact on the thermal stability of duplexes, the off-target effects and mitigate immunostimulation.[72] In addition, substitutions of pseuodouridine, 2-thiouridine, N6-methyladenoine, 5-methylcytidine or other base analogs of uridine and cytidine residues can reduce innate immune recognition while making antisense oligonucleotides more resistant to nucleases. Modifying siRNA with *N*-ethylpiperidine triazole-modified adenosine analogs have shown to reduce the immunogenicity of siRNA.[73-75] Moreover, the addition of fluorescent modifications has gained attention as they can be used for fluorescence-based detection or monitoring cellular uptake

and trafficking of siRNA in cells. An example of this is the addition is 6′-phenylpyrrolocytosine (PhpC) as it is a cytosine mimic and exhibits excellent base pairing fidelity, thermal stability and high fluorescence.[76] Moreover, many other less common base analogs have been used in siRNA modifications as their applications have helped better understand the mechanism of gene silencing and develop new methods to overcome drawbacks.[77]

1.3 Barriers of Oligonucleotide Delivery

siRNAs have promising potential as therapeutics, with the success of three FDA-approved siRNA drugs and several others in late-stage clinical trials targeting various disease genes. However, the single most critical factor limiting the utility of siRNAs as therapeutics is delivering siRNAs to its intracellular target site.[78] Unfortunately, the siRNAs' potential is limited by their physicochemical characteristics and instability with plasma half-lives. On top of their own characteristics, other barriers are dependent on the target tissue or organ, and administration routes.

1.3.1 Localized *versus* Systemic Delivery

There are two main administration routes utilized to deliver siRNA therapeutics to the target organ or tissue: local administration, and systemic administration. With localized delivery, siRNAs are applied directly to the target organ or tissues, this method results in high bioavailability at the target site and has fewer barriers compared to systemic delivery. Localized or topical administrative routes can deliver siRNA therapeutics to several organs such as eyes, mucous membranes, localized tumors, and skin.[79] Additionally, lung infections can be treated with local siRNA delivery; direct installation of siRNA through intranasal or intra-tracheal routs permits direct contact with epithelial cells of the lungs.[80]

In contrast, systemic delivery of siRNAs such as intravenous injection, have various challenges that limit the siRNA bioavailability at the target site.[81] As previously mentioned, due to

the physicochemical characteristics of siRNA such as anionic charge, large molecule, and size, their potential is limited. Once the siRNAs are intravenously injected, they can be rapidly degraded by nucleases present in plasma, tissues, and the cytoplasm.[82] Due to the anionic charge of the siRNA molecules, it is nearly impossible to cross the biological membrane. Lastly, at the systemic level, delivery is compromised by rapid clearance due to the kidneys. These barriers limit the application of siRNA-based therapeutics. However, there are two broad strategies that have been utilized to address these challenges in order to improve the delivery system of siRNA: formulation-based delivery or conjugated-based delivery. An ideal delivery system is biocompatible and non-immunogenic, allowing for specific cellular transport and entry. Clinically acceptable siRNA delivery systems should be carefully designed to improve the stability of siRNAs after administration into the body, to deliver siRNA specifically to the desired tissue site, and to facilitate the cellular uptake of siRNA within target cells.[83]

1.3.2 Formulation-Based Delivery

Lipid nanoparticles (LNPs) are the most successful formulated-based siRNA delivery strategy[46] As an example, LNPs were used to deliver Patisiran, the first siRNA drug to treat polyneuropathy in adults with hereditary transthyretin amyloidosis (hATTR).[84] They are made up of cationic, ionizable and helper lipids such as cholesterol, 2-distearoyl-sn-glycero-3-phosphocholine (DSPC), 1,2-dimyristoyl-rac-glycero-3-methoxypolyethylene glycol-200, and D-Lin-MC3-DMA, which promotes RNA packing, increase stability, and allow for passage through the lipid bilayer.[3] siRNAs are encapsulated within the LNP, protecting them from degradation. Other formulation-based approaches are currently in development, including complexes with cationic transfection agents, liposomes, dendrimers, and micelles (**Figure 1.8)**.[85] However, there are various drawbacks to the formulated approach such as toxicity, size, and invasive administration.[86] The excipients used to generate this system are highly toxic, resulting in the need

for patients to be pre-treated with anti-inflammatory drugs.[86] The method of administration is invasive and time-consuming as it requires a medical professional to administer the therapeutic through an intravenous infusion.[55] Lastly, due to the large size of the LNPs they are limited to clearance organs with fenestrated or discontinuous endothelium such as the liver and spleen. There are researchers developing improved formulations to over these drawbacks. However, the future of delivery seems to lie in conjugated-based approaches.[66]

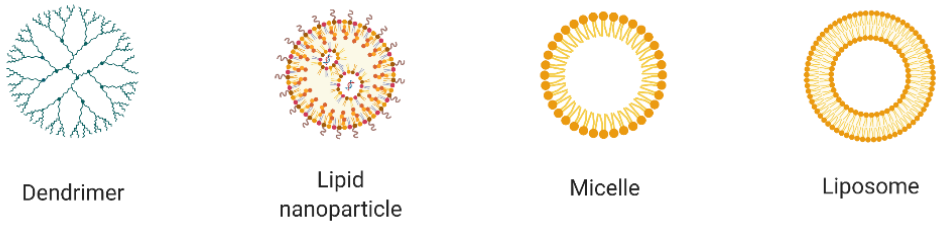

Figure 1.8. Overview of various formulation-based approaches for oligonucleotide therapeutics.

1.3.3 Conjugation-Based Delivery

Covalent conjugation of siRNAs with other ligands and molecules are used to improve delivery and uptake. In contrast to LNPs, ligand-siRNA conjugates can transport siRNA to specific tissues and cells by specific recognition and interactions between the ligand such as carbohydrates, aptamers, small molecules etc., and the surface receptor.[82] This method results in increased bioavailability, efficacy and decreased off-target effects. Furthermore, conjugates tend to be less toxic and less immunogenic, due to their size.[66]

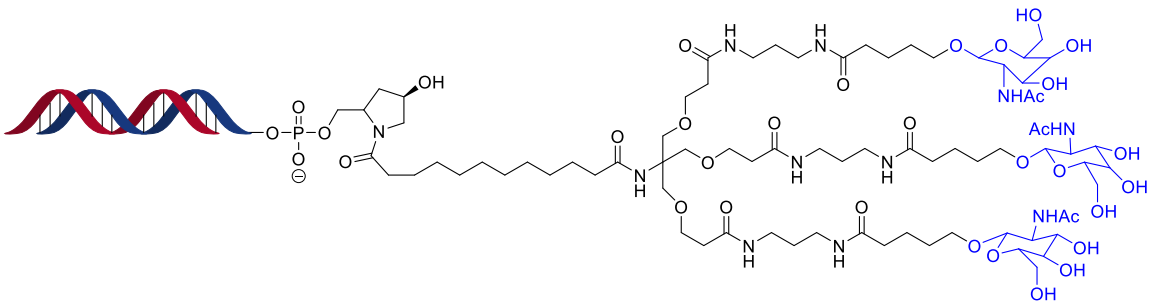

Figure 1.9: Structure of the triantennary GalNAc conjugate used in several drug candidates from Alnylam Pharmaceuticals.

To date, the most advanced therapeutic siRNA conjugate system is a trimer of *N*-acetylgalactosamine (GalNAc), as it eagerly binds to the Asialoglycoprotein receptor (ASGPR) on hepatocytes. GalNAc-siRNA conjugates have dominated the development of oligonucleotide therapeutics to treat liver diseases due to their potent and durable gene silencing abilities that last 6-9 months.[87,88] This conjugate approach has led to the success of three US Food and Drug Administration (FDA) approved therapeutics: Givosirin, Lumasirin, Inclisiran, and many therapeutics in clinical programs.

With the success of GalNAc delivery oligonucleotides to the liver, there is a need to deliver therapeutics to other sites in the body. Oligonucleotide therapeutics have potential for the treatment of muscle-related diseases. When locally injected, oligonucleotides exhibit potent target gene reduction in a small portion of the muscle, its limited distribution minimizes its potential as a therapeutic. When injected systemically, oligonucleotides naturally accumulate in the liver, ultimately being discarded. However, there is promising potential with lipid conjugated siRNAs.

1.3.4 Lipid Conjugation-Based Delivery

The second widely used class of conjugates are lipids such as cholesterol and fatty acids. Lipid conjugates enhance the circulation time, improve systemic delivery, and exhibits productive silencing of oligonucleotides to other target tissues and organs beyond the liver. [89] One of the most well-studied lipid moieties enabling efficient cellular and tissue delivery following direct oligonucleotide conjugation is cholesterol (**Figure 1.10)**. Cholesterol constitutes 15-30% of cellular membranes and intercalates into lipid membranes upon co-incubation with cells. With this in mind, there are two methods cholesterol conjugates promote siRNA uptake. The first, cholesterol conjugate intercalates into the plasma membrane and the oligonucleotide is internalized by endocytosis. The second, cholesterol conjugates bond to circulating plasma lipoproteins and siRNA uptake is driven by interactions with lipoprotein receptors. Cholesterol-conjugated siRNAs

are able to deliver oligonucleotides to muscle after systemic administration. However, to achieve sustainable silencing, 50 mg/kg of cholesterol conjugated siRNAs are required. Although,

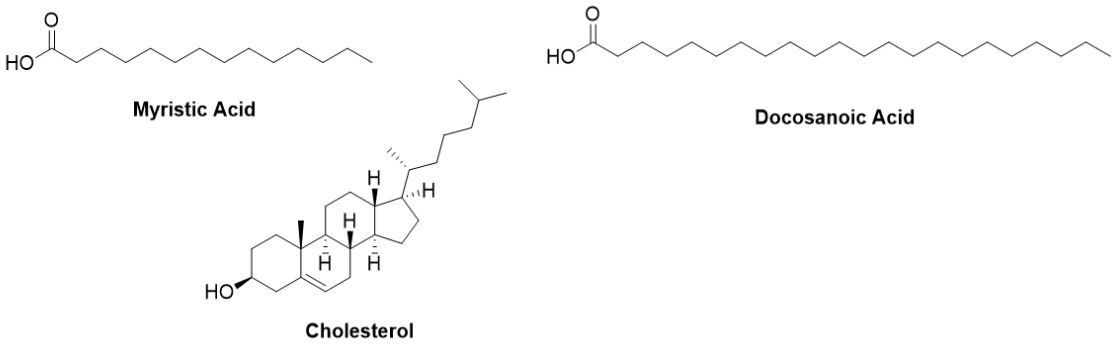

cholesterol conjugates exhibit therapeutic potential, they are limited due to their toxicity at high concentrations.[90]

Figure 1.10: Structure of various lipids.

More recently, fatty acids have gained attention due to their involvement in the contractile work of skeletal and cardiac cells and are transported efficiently across the muscular endothelium barrier to reach muscle cells.[91] The majority of fatty acids in the plasma are bound to serum album and there are seven binding sites for long-chain non-esterified fatty acids, drugs, ions and other metabolites. Albumin interacts with a variety of receptors such as glycoprotein Gp60, Gp30 and Gp18,(SPARC), the Megalin/Cublin complex, and the neonatal Fc receptor (FcRn)[91] Albumin's interaction with these receptors is responsible for its recycling and cellular transcytosis.This is an attractive property of albumin as it can "self-deliver" therapeutics across tissues and cellular barriers. The mechanism is illustrated in **Figure 1.11.**

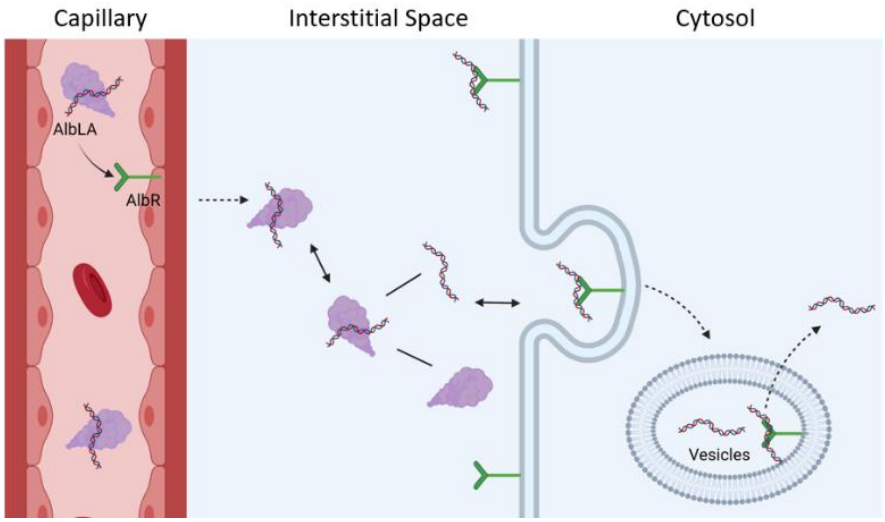

Figure 1.11: Schematic representation of route taken by lipid conjugated RNAs from the capillary to cytosol in muscle. AlbLA: albumin bound lipid; AlbR: albumin receptor. Created with BioRender.

Although fatty acid conjugated siRNAs have been investigated recently, there have been a few studies that exhibit their promising delivery ability. A study performed in 2019 by Biscans *et al*., compared the distribution and silencing activity in a variety of tissues including muscles. A variety of conjugates such as cholesterol, myristic acid (Myr), docosanoic acid (DCA), and docosahexanoic acid, were investigated and DCA moieties showed enhanced cardiac and skeletal muscle delivery after systemic administration in mice.

1.4 Sphingolipid Modified Nucleic Acid

A class of lipids that are of interest are sphingolipids (**Figure 1.12)** which are one of the major classes of eukaryotic lipids. A few examples include ceramide, sphingosine, and sphingosine-1-phosphate (S1P). Sphingolipids are found throughout the body; they are primarily located in nerve cell membranes and make up approximately 25% of the lipids in the myelin sheath.[92] Although they were initially identified in the brain tissue, some sphingolipid sub-classes are found in other parts of the body including spleen and blood. Sphingolipids are key components of cellular and subcellular eukaryotic membranes. This class of lipids are involved in signal transduction pathways that mediate cell growth, differentiation, multiple cell functions and apoptosis.[93] The bioactive lipid, ceramide, has shown high potential for cancer treatments as an anti-cancer agent, cancer cell suppressor or a biomarker.[94-96]

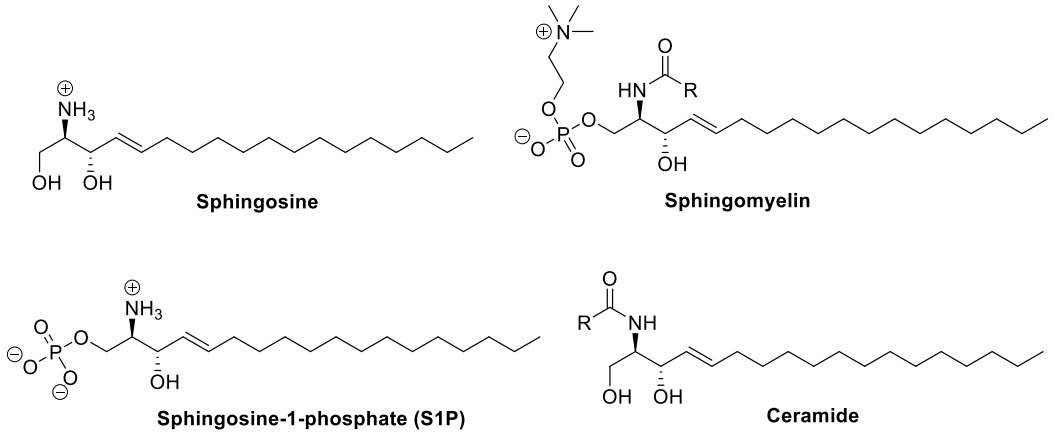

Figure 1.12. Various lipids in the Sphingolipid family.

As sphingolipid metabolism plays an important part in several pathologies, the pathway of this metabolism has been widely studied. Many of the biochemical pathways of synthesis and degradation have been identified successfully along with the enzymes involved. Sphingolipids are involved in a couple of metabolic pathways such as the *de novo* pathway and the sphingomyelin pathway shown in **Figure 1.13 (A).** In the sphingomyelin pathway, sphingosines are catalyzed by

kinases to generate S1P. However, uncontrolled activity of the kinases leads to increase in growth and survival of cancer cells, while inhibiting apoptosis and resistance to chemotherapeutic agents. S1P is a signaling sphingolipid involved in a class of G-Protein Coupled Receptors named sphingoshine-1-phosphate receptors (S1PR) illustrated in **Figure 1.13 (B).** S1P regulates a variety of cellular processes in mammals such as migration, survival, and proliferation.[96] As a result, sphingolipids' involvement in cellular regulating pathways, various disorders have been linked to the sphingolipid metabolic pathways such as Alzheimer's, diabetes, and cancer.[97]

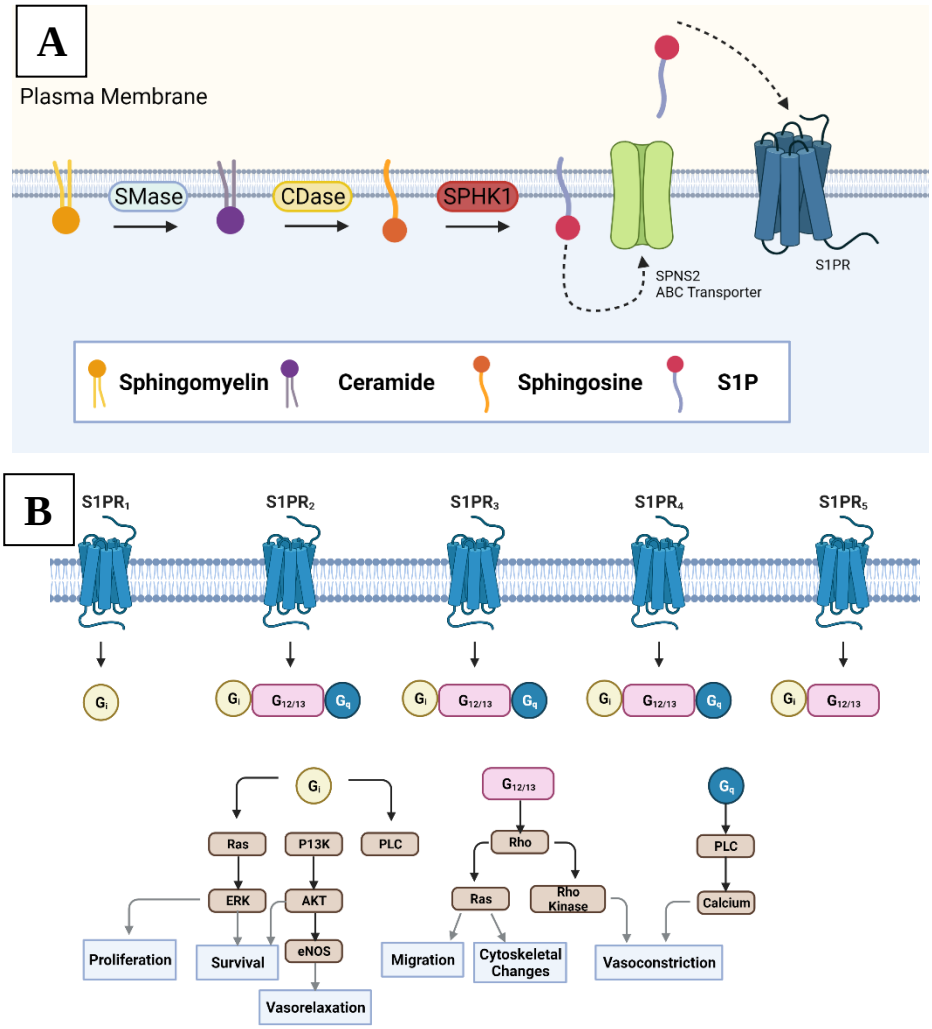

Figure 1.13: (A) Sphingomyelin pathway. **(B)** Summarized roles of various receptors in the S1PR class of G-Protein Receptors. Created with BioRender.

1.4.1 Modification Purpose and Benefits

Sphingosine and ceramide are naturally hydrophobic molecules that are components of eukaryotic membranes. These long carbon lipids hold potential as kinase inhibitors, biomolecular and delivery systems for oligonucleotides. However, there are drawbacks for sphingolipids due to their challenging synthesis and low availability, resulting in high costs.[98] As such, there is a need for improved and reproducible synthesis. As well as their utility as hydrophobic molecules to cross membranes has not been explored. One of the greatest challenges in using oligonucleotides involves its use in cellular systems. Oligonucleotides are negatively charged polymers, which make them particularly challenging to cross the negatively charged phospholipid bilayer. As such, this often limits their utility as tools and potential therapeutics. In order to overcome this limitation, efforts to label oligonucleotides with hydrophobic-based molecules has shown promising results. For example, cholesterol has been studied and used to label siRNAs to improve cell permeability, and its incorporation with liposomes or other nanoparticles.[89] The Desaulniers group recently generated a triazole-cholesterol phosphoramidite and published favorable gene silencing properties in the absence of a transfection carrier.[99] Additionally, other molecules, such as tocopherol and long carbon chain phosphoramidites have been synthesized and developed commercially. However, the main problem still persists, oligonucleotides have difficulty crossing cellular membranes across multiple cell types. Since sphingosines and ceramides are hydrophobic molecules that are components of eukaryotic cell membranes, there is interest in exploring their utility to allow for cellular membrane penetration.

1.5 Project Definition

Due to the possibilities obtained with the ability to silence genes at the pre-translational level, there is interest in investigating the potential of fatty acid conjugated siRNAs to deliver

oligonucleotides to extrahepatic sites.[91] As the library of chemical modifications continues to grow, there is the possibility that new siRNAs can be synthesized to enhance cellular uptake and delivery specificity, while decreasing degradation by nucleases.

This project will involve the investigation of synthesizing triazole-modified sphingosines and the incorporation of sphingosine spacers into RNA oligonucleotides. The synthesis of the sphingosine modification and incorporating it into RNA oligonucleotides will involve organic and catalytic chemistry to generate fair yields and safer alternatives. The modified RNA sequences will then be annealed with their compliment sequence strands to form siRNA duplexes. The siRNA duplexes will undergo hybridization testing to assess how the chemical modifications impact the thermal stability of the RNA duplex. The helical conformations will then be investigated to determine if the chemical modifications affect the helical conformation of the native alpha helical structure of wild type (wt) RNA duplexes. The modified siRNAs will be evaluated for their ability to silence gene expression utilizing the dual luciferase reporter system. This bioassay is a screening method that will be used to identify certain siRNA duplexes that exhibit potential with the sphingosine modification at certain positions. The modifications placed at the 3'-end, 5'end and central region of the sense strand will be further investigated for their cellular uptake abilities through a carrier-free luciferase assay. The gene silencing effectiveness of these siRNAs will be determined in the absence of a transfection carrier, which provides a more clinically relevant assessment of the delivery and gene silencing ability of siRNAs with these sphingosine modifications.

Finally, this project is in collaboration with Synthose Inc. a company in Toronto specializing in the synthesis of small molecules. The owner and co-founder, Dr. Eva Goss has been interested in using molecules such as sphingosine for biological applications. Thus, this project has been funded by an NSERC collaboration research and development (CRD) grant.

Chapter 2: Experimental

2.1 General Synthetic Method

Unless otherwise indicated all starting reagents used were obtained from commercial sources without additional purification. Anhydrous CH_2Cl_2 and THF were purchased from Sigma-Aldrich and run through a PureSolv 400 solvent purification system to maintain purity. Flash column chromatography was performed with Silicycle Siliaflash 60 (230-400 mesh). NMRs were performed on a Varian 400 MHz spectrometer. All ^{1}H NMRs were recorded for 64 transients at 400 MHz and all ^{13}C NMRs were run for 1500 transients at 101 MHz and all ^{31}P NMRs were recorded for 256 transients at 167 MHz. Spectra were processed and integrated using ACD labs NMR Processor Academic Edition.

2.2 Synthesis and Characterization of Organic Compounds

2.2.1 Synthesis of Imidazole-1-sulfonyl Azide Hydrochloride – Compound (1)

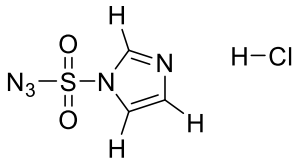

To an ice-cooled solution of sodium azide (13.0 g, 200 mmol) in MeCN (200 mL) was prepared and stirred for 10 minutes to dissolve the starting material. To this sulfuryl chloride (16.1 mL, 200 mol) was added drop-wise over the course of 10 minutes and the mixture stirred overnight at room temperature. Imidazole (25.9 g, 380 mmol) was added portion-wise to the ice-cooled mixture and stirred for 3 hours at room temperature. The mixture was diluted with EtOAc (400 mL), washed with H_2O (2 x 400 mL) then with saturated aqueous $NaHCO_3$ (2 x 400 mL). The organic layer was collected, dried over $NaSO_4$ and filtered. A solution of HCl in EtOH [obtained by the drop-wise addition of thionyl chloride (21.6 mL, 300 mmol) to ice-cooled dry ethanol (75 mL)] was added drop-wise to the filtrate. While stirring, the mixture chilled in an ice-bath, filtered and the filter cake was washed with EtOAc (3 x 100 mL) to give **compound 1** as white needles (26.1 g, 62%). ^{1}H NMR (400 MHz, DEUTERIUM OXIDE) δ 7.59 - 7.62 (m, 1 H) 8.01 (t, *J*=1.83 Hz, 1 H) 9.41 (s, 1 H); ^{13}C NMR (101 MHz, DEUTERIUM OXIDE) δ 137.7, 123.0, 123.0, 120.1, 118.9 ppm.

2.2.2 Synthesis of (*2S,3S,4R*)-2-azidooctadecane-1,3,4-triol – Compound (3)

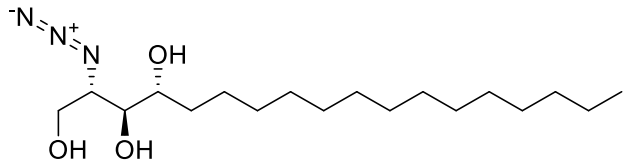

To a suspended solution of D-*ribo*-phytosphingosine (5 g, 15.7 mmol) and MeOH (150 mL), a solution of potassium carbonate (3.26 g, 32.9 mmol) and copper(II) sulfate (0.024 g, 0.15 mmol) in H_2O (50 mL) were added added. A solution of imidazole-1-sulfonyl azide hydrochloride **compound 1** (5.36 g, 30.5 mmol) in H_2O: CH_2Cl_2 (1:1 v/v, 50 mL) is added to the reaction mixture and stirred for 18 hours at room temperature. The reaction is extracted with CH_2Cl_2 (100 mL) and washed with H_2O (3 x 200 mL). The organic layer was collected, dried over Na_2SO_4 and concentrated *in vacuo* to afford a light blue powder which was purified by silica gel chromatography eluting with a gradient of MeOH/CH_2Cl_2 (5% MeOH in CH_2Cl_2 to 10% MeOH in CH_2Cl_2) to afford azido-phytosphingosine **compound 3** as a white powder (4.22 g, 78%); ^{1}H NMR (400 MHz, CHLOROFORM-d) δ 0.86 - 0.92 (m, 3 H) 1.25 - 1.37 (m, 22 H) 1.59 (br. s., 8 H) 3.65 (s, 1 H) 3.67 - 3.71 (m, 1 H) 3.76 - 3.79 (m, 1 H) 3.89 (dd, J=11.62, 4.52 Hz, 1 H) 4.01 (dd, J=11.74, 5.62 Hz, 1 H); ^{13}C NMR (101 MHz, CHLOROFORM-d) δ 77.2, 74.7, 72.5, 70.5, 63.1, 61.7, 50.9, 31.9, 31.9, 29.7, 29.6, 29.4, 25.8, 22.7, 14.1 ppm

2.2.3 Synthesis of (*2S,3S,4R*)-2-Azido-1-(*tert*-butyldiphenylsilyoxy)octadecane-3,4-triol – Compound (4)

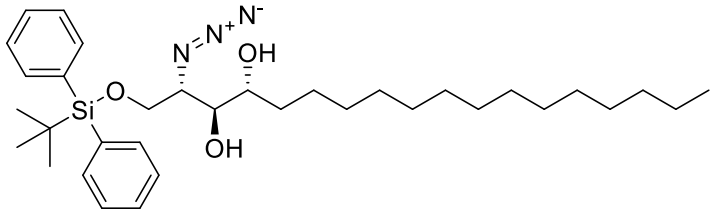

To a solution of azido-phytosphingosine (11 g, 32 mmol) in CH_2Cl_2 (150 mL) and DMF (35 mL), triethylamine (11.5 mL, 81.9 mmol), 4-DMAP (7.58 g, 62 mmol) and TBDPS-Cl (10.2 mL, 37.1 mmol) were added at 0 ºC and stirred at room temperature for 24 h. The reaction mixture was extracted with EtOAc (100 mL), washed with brine (100 mL x 3). The organic layer was collected, dried over Na_2SO_4 and concentrated *in vacuo*. The crude was purified by silica column chromatography using a hexane/EtOAc (5:1) as the mobile phase to afford the protected diol (16 g, 86%) as a colourless oil. ^{1}H NMR (400 MHz, CHLOROFORM-d) δ 0.90 (t, J=6.72 Hz, 3 H) 1.10 (s, 9 H) 1.22 - 1.39 (m, 28 H) 3.55 - 3.61 (m, 1 H) 3.65 - 3.73 (m, 2 H) 3.93 (dd, J=10.88, 5.99 Hz, 1 H) 4.06 (dd, J=10.76, 3.91 Hz, 1 H) 7.39 - 7.49 (m, 6 H) 7.71 (d, J=6.85 Hz, 4 H); ^{13}C NMR (101 MHz, CHLOROFORM-d) δ 135.6, 135.6, 132.6, 132.5, 130.0, 127.9, 127.9, 74.1, 72.4, 64.2, 63.4, 31.9, 31.9, 29.7, 29.7, 29.6, 29.4, 26.8, 26.7, 25.7, 22.7, 19.1, 14.1 ppm

2.2.4 Synthesis of (2*S*,4*S*,5*R*)-[2-Azido-2-(2,2-dioxo-5-tetradecyl-2,6-[1,3,2]dioxathiolan-4-yl)ethoxy]-*tert*-butyldiphenylsilane – Compound (5)

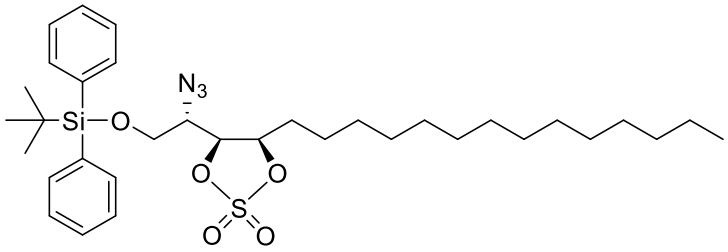

To a solution of the protected diol **4** (13 g, 22 mmol) in CH_2Cl_2 (120 mL), triethylamine (9.3 mL, 66 mmol) was added at 0 ºC. Thionyl chloride (1.89 mL, 26 mmol) was slowly added over the course of 10 minutes, the reaction mixture continued to stir at 0 ºC for 30 minutes, then diluted with EtOAc and washed with brine. The organic layer was collected, dried over Na_2SO_4 and concentrated *in vacuo* for 3 hours. The reaction mixture was dissolved in $CCl_4/CH_3CN/H_2O$ (45 mL, 1:1:1), to this solution were added $RuCl_3 \bullet 3H_2O$ (0.224 g, 0.858 mmol) and $NaIO_4$ (14.29 g, 66 mmol). The reaction was stirred for 2 h at room temperature, then extracted with EtOAc and washed with saturated $NaHCO_3$ solution. The organic layer was collected, dried over Na_2SO_4 and concentrated *in vacuo*. The crude was purified by silica column chromatography using a hexane/EtOAc (12:1) as the mobile phase to afford a protected cyclic sulfate (11.54 g, 80%) as a colorless oil. ^{1}H NMR (400 MHz, CHLOROFORM-d) δ 0.89 - 0.92 (m, 4 H) 1.09 - 1.12 (m, 9 H) 1.26 - 1.35 (m, 28 H) 3.71 (dt, J=10.03, 2.57 Hz, 1 H) 3.90 (dd, J=11.37, 5.26 Hz, 1 H) 4.05 (dd, J=11.25, 2.45 Hz, 1 H) 4.91 - 4.95 (m, 1 H) 4.99 (dd, J=11.25, 2.93 Hz, 1 H) 7.40 - 7.48 (m, 7 H) 7.67 - 7.71 (m, 4 H); ^{13}C NMR (101 MHz, CHLOROFORM-d): δ = 171.1, 135.6, 135.5, 135.2, 132.1, 131.9, 130.2, 130.1, 130.1, 128.0, 128.0, 127.8, 86.4, 79.8, 63.5, 60.4, 59.2, 31.9, 31.6, 29.6, 29.6, 29.4, 29.3, 29.3, 28.9, 28.1, 26.7, 26.5, 25.3, 25.2, 22.7, 22.6, 21.0, 20.7, 19.1, 14.2, 14.1 ppm.

2.2.5 Synthesis of (*2S,3R)-(E*)-2-Azido-1-(*tert*-butyldiphenylsilyoxy)octadec-4-en-3-ol – Compound (6)

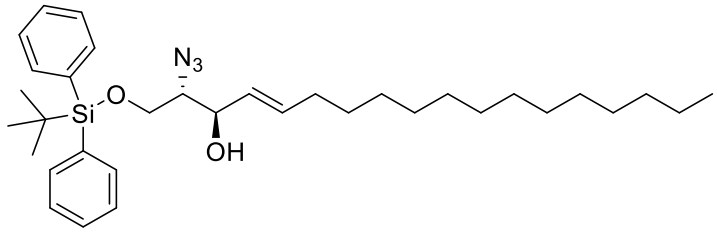

To a solution of cyclic sulfate **compound 5** (0.96 g, 1.49 mmol) in toluene (15 mL) were added Bu_4NI (0.59 g, 1.59 mmol) and DBU (0.281 mL, 1.88 mmol). The reaction was heated to reflux for 4 h, then cooled down to room temperature and concentrated *in vacuo*. The reaction mixture was dissolved in concentrated H_2SO_4 (72 µL), H_2O (30 µL) and THF (380 µL). The reaction was stirred for 3 h at room temperature, then extracted with EtOAc and washed with saturated $NaHCO_3$ solution and brine. The organic layer was collected, dried over Na_2SO_4 and concentrated *in vacuo*. The crude was purified by silica column chromatography using a hexane/EtOAc (10:1) as the mobile phase to afford **compound 6** (0.7 g, 81%) as a colorless oil. ^{1}H NMR (400 MHz, CHLOROFORM-d) δ 0.81 - 0.91 (m, 7 H) 0.98 - 1.07 (m, 33 H) 1.15 - 1.23 (m, 10 H) 1.23 - 1.34 (m, 22 H) 1.46 (sxt, J=7.38 Hz, 16 H) 1.62 - 1.74 (m, 21 H) 1.89 - 1.97 (m, 2 H) 3.27 - 3.36 (m, 15 H) 3.54 (dd, J=10.64, 8.93 Hz, 1 H) 3.73 (dd, J=10.76, 4.16 Hz, 1 H) 4.33 (dt, J=8.56, 3.91 Hz, 1 H) 4.79 (dd, J=7.70, 3.30 Hz, 1 H) 5.40 - 5.47 (m, 1 H) 5.63 - 5.72 (m, 1 H) 7.35 - 7.44 (m, 6 H) 7.65 - 7.72 (m, 4 H); ^{13}C NMR (101 MHz, CHLOROFORM-d): δ 135.5, 135.1, 130.0, 128.0, 77.5, 72.0, 32.0, 26.9, 19.6, 19.3, 14.2 ppm

2.2.6 Synthesis of (2*S*,3*R*)-(*E*)-2-Azidooctadec-4-ene-1,3-diol – Compound (7)

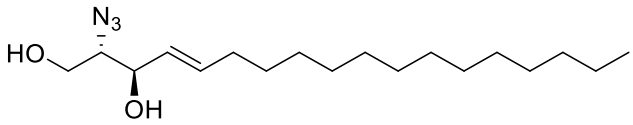

To a solution of **compound 6** (1.48 g, 2.54 mmol) in THF (13 mL) was added TBAF (1.24 mL, 5.26 mmol, 1.0 M solution in THF). The reaction stirred at room temperature for 1 h, then extracted with EtOAc and washed with water and brine. The organic layer was collected, dried over Na_2SO_4 and concentrated *in vacuo*. The crude was purified by silica column chromatography using a hexane/EtOAc (3:1) as the mobile phase to afford **compound 7** (0.79 g, 95%) as a colorless oil. ^{1}H NMR (400 MHz, CHLOROFORM-d) δ 0.79 - 0.84 (m, 3 H) 1.14 - 1.26 (m, 23 H) 1.29 - 1.38 (m, 2 H) 1.96 - 2.04 (m, 4 H) 3.41 - 3.47 (m, 1 H) 3.67 - 3.76 (m, 2 H) 4.16 - 4.21 (m, 1 H) 5.47 (ddt, J=15.41, 7.34, 1.47, 1.47 Hz, 1 H) 5.70 - 5.80 (m, 1 H); ^{13}C NMR (101 MHz, CHLOROFORM-d) δ 136.1, 128.0, 77.2, 73.8, 66.8, 62.6, 32.3, 31.9, 29.7, 29.7, 29.6, 29.5, 29.4, 29.2, 28.9, 22.7, 14.2, 14.1 ppm

2.2.7 Synthesis of (2S,3R,E)-2-azido-1-(bis(4methoxyphenyl)(phenyl)methoxy)octadec-4-en-3-ol – Compound (8)

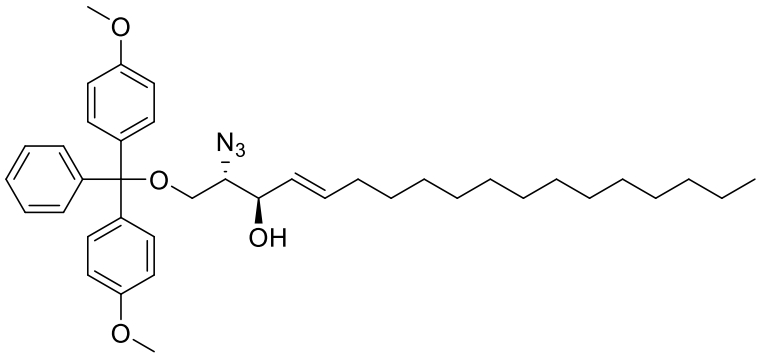

To a solution of **compound 7** (0.12 g, 0.368 mmol) in pyridine (0.12 mL, 1.5 mmol) were added at 0ºC DMAP (0.0045 g, 0.036 mmol) and DMT-Cl (0.137 g, 1.1 Eq). The reaction was stirred at 0 ºC for 2 h and at room temperature for 3 h. The reaction mixture was extracted with DCM and washed with saturated $NaHCO_3$ solution and brine. The organic layer was collected, dried over Na_2SO_4 and concentrated *in vacuo*. The crude was purified by silica column chromatography using a gradient of MeOH/CH_2Cl_2 (100% CH_2Cl_2 to 5 % MeOH in CH_2Cl_2) to afford **compound 8** (0.115 g, 50 %) as a light orange oil. ^{1}H NMR (400 MHz, CHLOROFORM-d) δ 7.63-7.80 (m, 4H), 7.37-7.51 (m, 6H), 5.67-5.85 (m, 1H), 5.46 (ddt, *J* = 15.4, 7.1, 1.5 Hz, 1H), 4.21-4.32 (m, 1H), 4.09-4.20 (m, 1H), 3.76-3.88 (m, 2H), 3.53 (dt, *J* = 6.3, 4.9 Hz, 1H), 1.99-2.12 (m, 3H), 1.93 (br d, *J* = 19.1 Hz, 1H), 1.76 (br s, 1H), 1.44 (br s, 1H), 1.24-1.35 (m, 18H), 1.06-1.18 (m, 10H), 0.85-0.99 ppm (m, 3H); ^{13}C NMR (101 MHz, CHLOROFORM-d) δ = 203.4, 158.6, 147.3, 139.5, 136.1, 134.8, 129.9, 129.7, 129.1, 128.7, 128.3, 128.0, 127.9, 127.8, 127.7, 127.7, 127.1, 113.6, 113.2, 113.0, 77.2, 73.8, 66.8, 62.6, 55.3, 55.3, 55.2, 32.3, 31.9, 29.7, 29.7, 29.7, 29.6, 29.5, 29.4, 29.2, 28.9, 26.6, 22.7, 14.1 ppm

2.2.8 Synthesis of (2S,3R,E)-1-(bis(4-methoxyphenyl)(phenyl)methoxy)-2-(4-propyl-1H-1,2,3-triazol-1-yl)octadec-4-en-3-ol – Compound (9-PT)

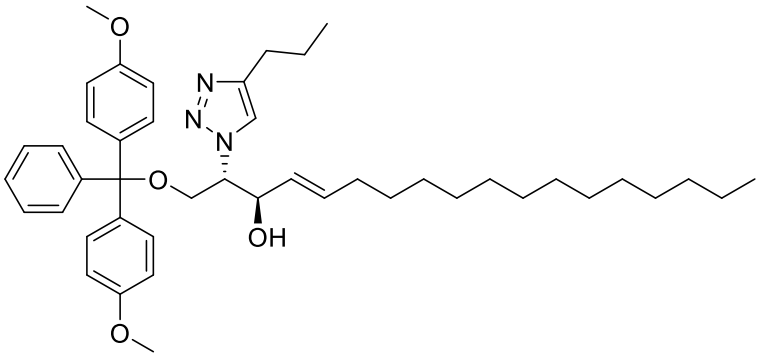

To a solution of **compound 8** (0.11 g, 0.175 mmol) in t-BuOH/H_2O (1 mL, 1:1) and TEA (0.048 mL, 0.35 mmol) were added copper (II)sulfate•pentahydrate (0.04 g, 0.175 mmol), sodium ascorbate (0.069 g, 0.35 mmol) and 1-pentyne (0.022 mL, 0.228 mmol). The reaction was stirred overnight at room temperature, it was extracted with CH_2Cl_2 and washed with brine. The organic layer was collected, dried over Na_2SO_4 and concentrated *in vacuo*. The crude was purified by silica column chromatography using a gradient of MeOH/CH_2Cl_2 (2 % MeOH in CH_2Cl_2 to 7 % MeOH in CH_2Cl_2) to afford the titled **compound 9-PT** (0.082 g, 67 %) as a colourless oil. ^{1}H NMR (400 MHz, CHLOROFORM-d) δ 7.29-7.38 (m, 5H), 7.27-7.28 (m, 1H), 7.16-7.22 (m, 4H), 6.83-6.89 (m, 4H), 5.81-5.87 (m, 1H), 5.52-5.60 (m, 1H), 4.25-4.30 (m, 1H), 3.80-3.85 (m, 8H), 3.53-3.57 (m, 1H), 2.06-2.12 (m, 2H), 1.23-1.37 (m, 36H), 0.87-0.93 ppm (m, 5H); ^{13}C NMR (101 MHz, CHLOROFORM-d) δ 129.1, 128.0, 127.9, 127.8, 127.7, 113.2, 113.0, 84.0, 77.2, 73.9, 66.8, 55.3, 53.4, 32.3, 31.9, 29.7, 29.7, 29.7, 29.4, 29.2, 28.9, 22.7, 14.1 ppm

2.2.10 Synthesis of (2S,3R,E)-1-(bis(4-methoxyphenyl)(phenyl)methoxy)-2-(4-propyl-1H-1,2,3-triazol-1-yl)octadec-4-en-3-yl (2-cyanoethyl) diisopropylphosphoramidite – Compound (10-PT)

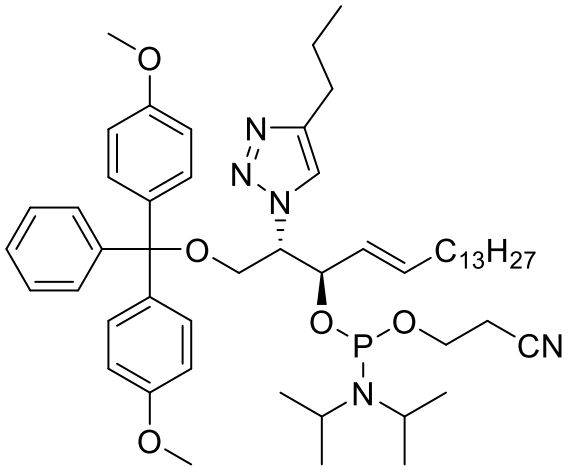

(10-PT)

A solution of **compound 9-PT** (0.25 g, 0.36 mmol) in 10 mL of dry THF was prepared in flame dried glassware. To this were added freshly distilled TEA (0.25 mL, 1.8 mmol) and 2-cyanoethyl-*N*,*N*-diisopropylchlorophosphoramidite (0.24 mL, 1.07 mmol). The reaction was stirred at room temperature for 3 h and concentrated *in vacuo* producing a colourless oil. The oil was purified using silica gel chromatography using EtOAc/Hexane (60% EtAOc in hexanes with 2% TEA) as as the mobile phase to afford **compound 10 -PT** (0.18 g, 57%) as a colorless oil. ^{1}H NMR (400 MHz, CHLOROFORM-d) δ 0.85 - 0.91 (m, 3 H) 0.91 - 1.00 (m, 4 H) 1.04 (d, J=6.85 Hz, 2 H) 1.08 - 1.20 (m, 16 H) 1.20 - 1.33 (m, 38 H) 1.60 - 1.72 (m, 2 H) 4.65 (d, J=7.34 Hz, 1 H) 4.73 (d, J=7.34 Hz, 1 H) 5.48 - 5.65 (m, 1 H) 6.76 - 6.83 (m, 9 H) 7.13 - 7.20 (m, 9 H); ^{31}P NMR (125 MHz, CDCl3) δ 149.29 (s, 1P), 148.91 (s, 1P), 148.86 (s, 1P), 148.27 (s, 1P), 148.22 (s, 1P), 148.03 (s, 1P), 147.97 (s, 1P), 147.85 (s, 1P), 147.91 (br t, *J* =

68.5 Hz, 1P), 147.43 (s, 1P), 147.37 (s, 1P), 16.11 (s, 1P), 12.16 (s, 1P). ESI-HRMS (ES+) m/z calculated for $C_{53}H_{78}N_5O_5P$: 895.5741 found 897.3534

2.3 Synthesis, Purification and Quantification of Oligonucleotides

Removal from Solid Support and Deprotection

All β-cyanoethyl 2'-O-TBDMS protected phosphoramidites, solid supports and reagents used in the synthesis of oligonucleotide strands were purchased from Chemgenes Corporation and Glen Research. All commercial phosphoramidites were dissolved in anhydrous acetonitrile to a concentration of 0.10 M. The chemically synthesized triazole sphingosine derivative phosphoramidites were dissolved in acetonitrile (anhydrous) to a concentration of 0.10 M. All sequences were synthesized via solid support phosphoramidite chemistry using Applied Biosystems 394 DNA/RNA synthesizer. The oligonucleotides were synthesized on 0.2 μM or 1.00 μM cycles kept under argon at 55 psi with 999 second coupling time. Antisense sequences were chemically phosphorylated at the 5'-end by using 2-2- (4,4'-dimethoxytrityloxy)ethylsulfonyl]ethyl-(2-cyanoethyl)-(N,N-diisopropyl)- phosphoramidite.

Oligonucleotide cleavage from the solid supports were completed by flushing the CPG column with 1.5 mL of EMAM (methylamine 40% wt. in H_2O and methylamine 33% wt. in ethanol, 1:1) (Sigma-Aldrich) for 1 hour at room temperature to remove the strands from the column. The oligonucleotides were further incubated overnight at room temperature in EMAM to deprotect the bases. The samples were concentrated on a Speedvac evaporator, then resuspended in 125 μL of 3HF-Et3N (Sigma-Aldrich) and 100 μL of DMSO and was incubated at 65 °C for 3 hours in order to remove the 2'-O-TBDMS protecting groups. The samples were concentrated on a Speedvac evaporator overnight.

Ethanol Precipitation and Desalting

The purification of the crude oligonucleotides starts with EtOH precipitation, followed by the desalting using Millipore Amicon Ultra 3000 MW cellulose centrifugal filters. were resuspended in 600 mL of chilled EtOH and 25 µL of 3 M NaOAc, the solution was mixed further via pipetting, vortexed thoroughly and placed in dry ice for 1 hour. The sample was centrifuged for 30 minutes at 12000 rpm at 4º and the supernatant was removed. The oligonucleotide pellets were resuspended in chilled EtOH, and the process was repeated two more times without the any addition NaOAc. The sample was concentrated using a Speedvac evaporator for 2 hours. The samples were resuspended in RNAse-free water and desalted through Millipore Amicon Ultra 3000 MW cellulose using a Speedvac evaporator until concentrated.

Oligonucleotides were used without further purification for annealing and transfection. Equimolar amounts of complimentary RNAs were annealed at 90 °C for 2 min in a binding buffer (75.0 mM KCl, 50.0 mM Tris-HCl, 3.00 mM MgCl2, pH 8.30) and the solution was slowly cooled to room temperature, resulting in siRNAs used for biological assays. A sodium phosphate buffer (90.0 mM NaCl, 10.0 mM Na_2HPO_4, 1.00 mM EDTA, pH 7.00) was used to anneal strands for biophysical measurements.

Quantification

The concentrated crude oligonucleotide sample was redissolved in 200 µL of DEPC treated nuclease-free water (Sigma-Aldrich). 1 µL of the RNA sample was added to 999 µL of water in a 1-mL quartz cuvette. The diluted sample was mixed thoroughly via pipetting and the absorbance was measured using a spectrophotometer (Thermo Scientific) at 260 nm. The optical density was calculated by multiplying the absorbance 37 value calculated by the spectrophotometer by the total volume of the stock oligonucleotide sample (200 µL)

2.4 Biophysical Characterization

The siRNA samples were prepared using equimolar amounts of each siRNA (5 µM) were annealed to their complimentary strand in various volumes of sodium phosphate buffer (90 mM NaCl, 10mM Na_2HPO_4, 1 mM EDTA, pH = 7) to each a total volume of 20 µL. The samples were heated to 90 ºC for 2 minutes, then allowed to cool down to room temperature.

2.4.1 Helical Conformation Analysis using Circular Dichroism

Circular dichroism studies were performed at 25 ºC over a wavelength range or 200 nm to 500 nm at a rate of 20 nm per minute. The siRNA samples were transferred to a 1 mm cuvette (QS), the average of three replicates were completed using a J-815 CD Spectrometer and data was recorded using Jasco's Spectra Manager 2.0 software.

2.4.2 UV-Monitored Thermal Denaturation of siRNA Duplexes

Melting temperatures (T_m) of each sample were measured by UV absorbance at 260 nm and were completed with a baseline of sodium phosphate buffer. The temperature was increased from 10 °C to 90 °C at a rate of 0.5 ºC per minute. T_m data was analyzed using Meltwin 3.5 software and the average of triplicate measurements is taken at the T_m of the duplex.

2.4.3 Procedure for HPLC Characterization

High performance liquid chromatography (HPLC) chromatograms were obtained using Waters 1525 Binary HPLC pump with Waters 2489 UV/Vis detector using the Empower 3 software. A reverse-phase column (C18 4.6 mm by 150 mm) was used. The conditions used were 5% acetonitrile in 95% 0.1 M TEAA (Triethylamine-Acetic Acid) buffer up to 100% acetonitrile over 25 minutes.

2.5 Cell Culture Maintenance

The cell line used for the biological analysis of the siRNAs is human epithelial cervix carcinoma cells, commonly referred to as HeLa cells. The cells were kept in cell culture flasks with

25.0 mL of DMEM with 10% fetal bovine serum and 1% penicillin-streptomycin (Sigma) in an incubator set for 37.0 ºC with a 5% CO_2 humidified atmosphere. Cells were passaged once cells had a confluency of 80-90% according to the following protocol. The culture flask was washed 3 times with 20 mL of 1X phosphate buffered saline (NaCl 137 mM, KCl 2.70 mM, PO_4^{3-} 10.0 mM, pH 7.40) and incubated with 5.0 mL of 0.25% trypsin (SAFC bioscience) for 4 min @ 37 °C to detach the cells from the flask. The cell solution was transferred to a 50.0 mL Falcon tube and diluted with 10.0 mL of DMEM and pelleted at 2,000 rpm for 5 minutes at room temperature. The supernatant was discarded, and the pellet was resuspended in 5.0 mL DMEM with 10 % FBS.

To obtain a cell count, a haemocytometer was used, followed by a dilution to make a final cell concentration of 1,000,000 cell per mL. The cell line is continued by adding 1.0 mL of the freshly passaged cells was added to a new culture flask that already contains 24 mL of DMEM with 10% FBS and 1% penicillin-streptomycin at 37.5 °C. The remaining cell solution was utilized for plating cells for assays.

2.6 Cell Based Assays

2.6.1 Plating and Transfection

For the luciferase assay, 50 µL of the 1,000,000 cells per ml solution were added to the wells of a 24 well plate already containing 350 µL of DMEM with 10% FBS per well at a cell density of 50,000 cells per well. After plates are prepared, they were incubated at 37 °C with 5% CO_2 for 24 hours. A mixture of 1µL siRNA, and 1 µL of Lipofectamine 2000 (and 100 ng of pGL3 and SV plasmid for luciferase assay) was prepared in Gibco's Opti-Mem Reduced Serum Medium to a total volume of 200 µL for Luciferase assay. A different solution is made for each siRNA and for every concentration. These solutions were then transferred to the well plates and incubated for another 24 hours.

For carrier-free luciferase assay, 10 µL of the 1,000,000 cells per ml solution was added to the wells of a 96 well plate that already has 150 µL of DMEM with 10% FBS per well at a cell

density of 10,000 cells. After plates are prepared, they were incubated at 37 °C with 5% CO_2 for 24 hours. A mixture of 1μL siRNA, and 1 μL of Lipofectamine 2000 (and 100 ng of pGL and SV plasmid for luciferase assay) was prepared in Gibco's Opti-Mem Reduced Serum Medium to a total volume of 100 μL. A different solution is made for each siRNA and for every concentration. These solutions were then transferred to the well plates and incubated for another 24 hours.

2.6.2 Dual-Luciferase Reporter Assay

For the luciferase assay, 50 μL of the 1,000,000 cells per ml solution were added to the wells of a 24 well plate already containing 350 μL of DMEM with 10% FBS per well at a cell density of 50,000 cells per well. After plates are prepared, they were incubated at 37 °C with 5% CO_2 for 24 hours. After the post transfection incubation period each well was washed with twice with 1X PBS and then 250 μL 1X Passive Lysis Buffer was added to lyse the cells over a period of 20 minutes on a shaker. Then 10 μL cell lysate was transferred to a CoStar 96 well plate (making triplicates of each lysate) immediately and a Synergy HT (Bio-Tek) plate luminometer was used to measure fluorescence. Fluorescence studies were done using the Dual-Luciferase Reporter Assay kit (Promega). According to the kit's protocol, 50 μL of Luciferase Assay Reagent II (LAR II) substrate was first added to induce firefly luciferase luminescence followed by the addition of 50 μL of Stop&Glo™ to quench firefly luciferase and induce *Renilla* luciferase luminescence. The firefly luciferase signal was normalized with the *Renilla* luciferase signal and the signal for the cells transfected with no siRNA were taken as 100% expression to which the other strands are compared.

2.6.3 Carrier-Free Luciferase Reporter Assay

For carrier-free luciferase assay, 10 μL of the 1,000,000 cells per ml solution was added to the wells of a 96 well plate that already has 150 μL of DMEM with 10% FBS per well at a cell density of 10,000 cells. After plates are prepared, they were incubated at 37 °C with 5% CO_2 for 24 hours. HeLa cells were seeded into 96-well plates containing 50 μL of DMEM (10% FBS 1% penicillin-streptomycin) at a cell density of $1.0x10^4$ cells per well. Plates were incubated for 24

hours at 37 C with 5% CO_2 humidified atmosphere. Prepare master mix by combining 200 ng pGL3 (2 µL), 50 ng (0.5 µL) pRLSV40 and 50 µL Opti-MEM Reduced Serum Medium per sample. Dilute 1 µL Lipofectamine 2000 TM in 49 µL Opti-MEM Reduced Serum Medium (in a microcentrifuge tube). Mix gently and incubate for 5 minutes at room temperature. Add 52.6 µL of master mix to diluted Lipofectamine. Mix gently with pipette. Add diluted lipofectamine-plasmid mixture to each well and allow the plate to incubate for 4 hours at 37 C with 5% CO_2 humidified atmosphere, after which the growth medium was discarded, and each well was washed twice with 1X PBS to ensure that no transfection reagent remained in solution. 50 µL DMEM (10% FBS, 1% penicillin-streptomycin) were added to each well. Each siRNA sample was prepared by diluting 5 µL of the respective siRNA in 50 µL of 1× Gibco's Opti-MEM Reduced Serum Medium (Invitrogen) on ice and the diluted samples were immediately transferred to the respective wells of the 96-well plate. Plates were gently rocked back and forth for a few minutes and then incubated for an additional 16 h prior to cell lysis.

Cell Lysis

16 hours post-transfection, culture plates were removed from the incubator. In a biosafety cabinet, the medium was removed from each well and cells were washed with PBS. 1 µL of 1X passive lysis buffer were added to each well for a 96-well plate. Culture plates were placed on a rocking platform at room temperature for 30 minutes. Lysates were transferred to labeled microcentrifuge tubes. 10 µL cell lysate was transferred to a Costar 96 well plate (making triplicates of each lysate) immediately and a Synergy HT (Bio-Tek) plate luminometer was used to measure fluorescence. Fluorescence studies were done using the Dual-Luciferase Reporter Assay kit (Promega). According to the kit's protocol, 50 µL of LAR II substrate was first added to induce firefly luciferase luminescence followed by the addition of 50 µL of Stop&Glo™ to quench firefly luciferase and induce *Renilla* luciferase luminescence. The firefly luciferase signal was normalized

with the *Renilla* luciferase signal and the signal for the cells transfected with no siRNA were taken as 100% expression to which the other strands are compared

Chapter 3: Results and Discussion

3.1 Organic Synthesis of Phosphoramidites

In this study, a small library of propyl-triazole sphingosine modified siRNAs were synthesized to investigate their gene silencing abilities in the presence and absence of a transfection carrier. To achieve this, our first objective was to prepare a compound called azidosphingosine shown in **Scheme 3.1**. Azidosphingosine is used as a building block to generate a variety of compounds with various chemical modifications.

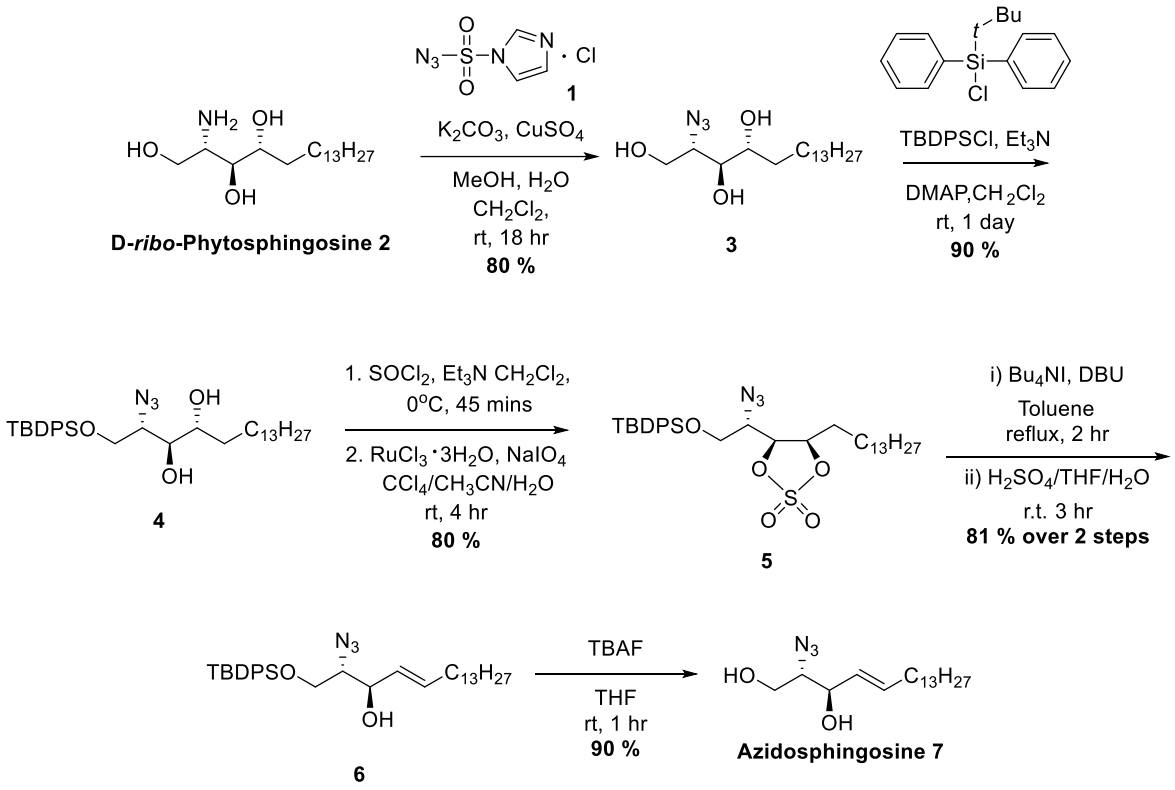

Scheme 3.1. Synthesis of azidosphingosine.

In order to obtain the desired compound, azidosphingosine **7**, the amino and primary alcohol groups of D-*ribo*-phytosphingosine **2** must be protected. The synthesis begins with the installation of an azide group to protect the amine group. Although other published procedures use triflyl azide as an azide source[100], our approach opted for a safer and cost-efficient route by using imidazole-1-sulfonyl azide hydrochloride **1**.[100, 101] Following a published procedure, we reacted sulfuryl chloride in an ice-cooled suspension of sodium azide in acetonitrile overnight at room temperature, and imidazole was added portion-wise the next day. From this procedure, we obtained similar yields that were published by Stick *et al*, in 2005.[101]

Azides are a popular class of compounds due to their diverse reactivity with many substrates. For example, azides play key roles in various chemical modifications such as the notable copper assisted azide-alkyne cycloaddition (CuAAc) reaction (often nicknamed the 'click' reaction) and their role as amine protecting groups.[102-106]

To prepare azido-phytosphingosine **3**, it was vital for the reaction to avoid the loss of stereochemistry. A previous study performed by Pandiakumar. AK *et al*, in 2014, suggests that the reaction undergoes a diazo (N_2) transfer reaction to form an azide.[107] Shown in **Figure 3.1** is a plausible mechanism involving the nucleophilic attack of the amine on the middle nitrogen of imidazole-1-sulfonyl azide hydrochloride. The known azido-phytosphingosine was prepared with column chromatography according to published procedures in fair yields of 80%.[108-110]

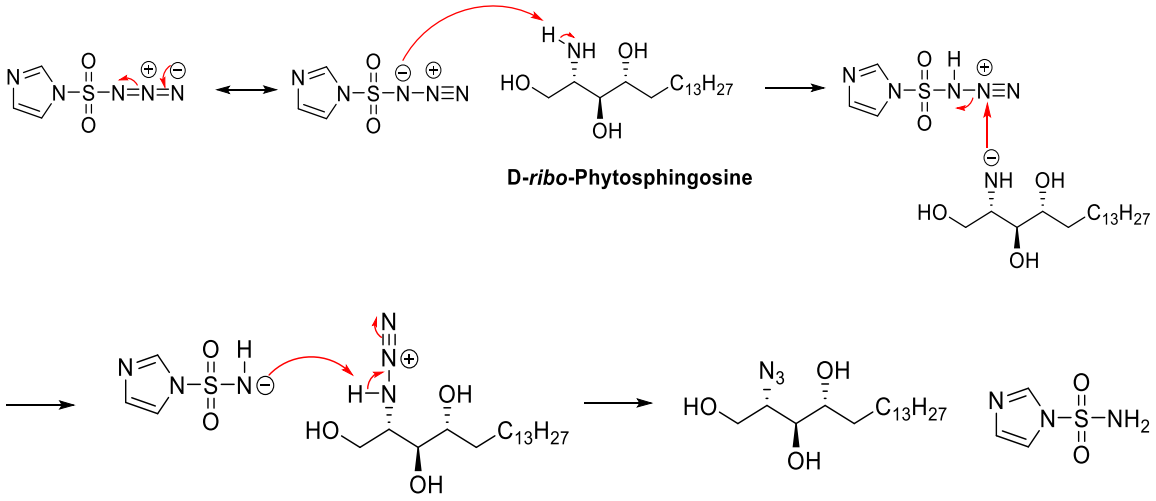

Figure 3.1. Proposed mechanism to generate azidophytosphingosine.

After the protection of the amine group, the primary alcohol must be protected in order to produce **4** generating high yields (90%) to avoid unwanted side reactions. The protecting group chosen is *tert*-butyldiphenylsilyl (TBDPS) and this protecting group is commonly used to protect alcohols. It is crucial to use less than two equivalents of TBDPS-Cl to protect the primary alcohol to avoid protecting the two secondary alcohols that are present on compound **4**. The vicinal diols on compound **4** are the only nucleophiles present on the compound, and they will undergo a substitution nucleophilic intramolecular (S_Ni) reaction to form a cis-1,2-cyclic sulfite compound **5** through the addition of thionyl chloride in the presence of triethyl amine.[111, 112] The proposed mechanism to transform the vicinal diols on compound **4** to a cis cyclic sulfite can be depicted in **Figure 3-2**.

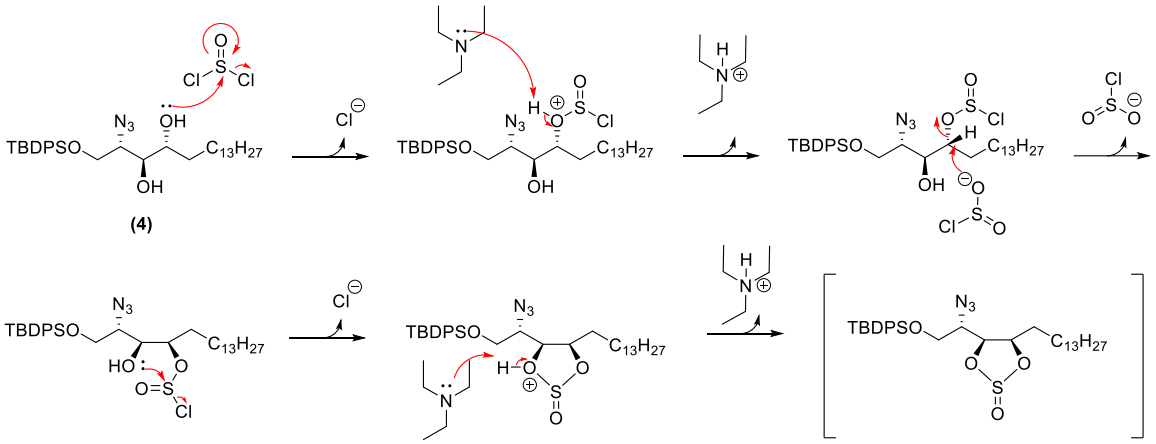

Figure 3.2. Proposed mechanism for the formation of the intermediate cyclic sulfite.

The secondary alcohol attacks the sulfur of thionyl chloride ($SOCl_2$), after the loss of Cl and deprotonation of oxygen, a good leaving group chlorosulfite is generated. From here, a bimolecular nucleophilic substitution (S_N2) occurs. The lone pair of electrons on oxygen, nucleophilically attacks the carbon center, resulting in chlorosulfite to leave and an inversion of configuration. Next the lone pair of electrons on the secondary alcohol attack the sulfur atom and chlorine acts as a leaving group. TEA deprotonates the oxygen, resulting in the formation of the intermediate. [113, 114]

The generation of the intermediary sulfite is followed by an oxidation step developed by Sharpless *et al*, 1988, using ruthenium (III) chloride trihydrate and sodium periodate to afford 1,2-cyclic sulfate with fair yields of 78-86% with various scales.[115]

To afford compound **6**, compound **5** must undergo an acid-catalyzed ring-opening and dehydrohalogenation to form an internal alkene and the re-exposure of a secondary alcohol. Following a literature procedure by Kim *et al.*, that required a reflux solution containing DBU and tetra-butyl ammonium iodide (NBu_4I), followed by sulfuric acid, THF and water, proved to be ineffective because compound **6** was not synthesized.[100] It was hypothesized that a sulfate ester formed after compound **5** during refluxing conditions with DBU and NBu_4I. After isolating the intermediate using column chromatography, our hypothesized compound was fully converted to the hypothesized intermediate and was confirmed with ^1H NMR and ^{13}C NMR. This led to the

second step potentially being the issue; no removal of the sulfate ester and re-exposure of the secondary alcohol. The reaction was monitored via TLC, however, there were no indications of the desired product being produced as the intermediate was still present and no new compounds had formed. We began to investigate other solvents that would push the reaction further such as THF. Changing the solvent to THF instead of toluene resulted in a poor yield of 32%. Despite the low yield, this was a starting point to optimize the reaction conditions. The difference between the two solvents is their structure and polarity.[116] THF is more polar than toluene due to the non-bonding electrons on oxygen, this can provide hydrogen bonding. In hopes to increase the yields further, we investigated the sulfuric acid equivalence shown in **Table 3-1**.

Table 3.1. Optimization of the ring opening and dehydrohalogenation reaction of compound 6 from intermediate.

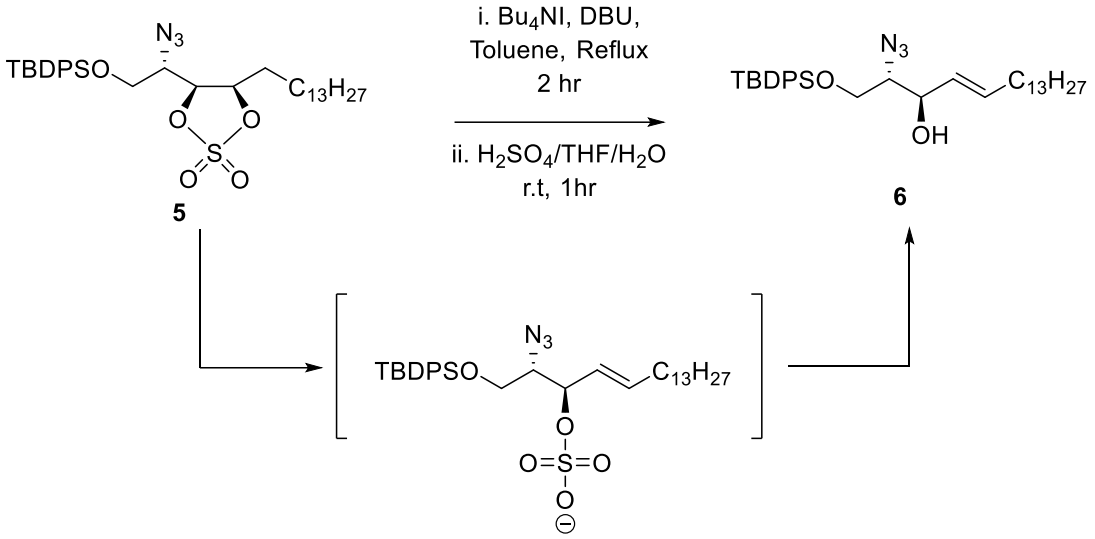

Entry	Solvent	H_2SO_4 (eq.)	Temperature	Time (h)	Yield %
1	Toluene	0.3	r.t	1	n.r
2	Toluene	0.3	r.t	2	n.r
3	Toluene	0.3	r.t	3	n.r
4	THF	0.3	r.t	3	32
5	THF	0.4	r.t	3	55
6	THF	0.5	r.t	3	43
7	THF	0.6	r.t	3	50
8	THF	0.7	r.t	3	51
9	THF	0.8	r.t	3	54
10	THF	0.9	r.t	3	67
11	THF	1.0	r.t	3	63
12	THF	1.1	r.t	3	41
13	THF	1.2	r.t	3	50
14	THF	1.3	r.t	3	44
15	THF	0.9	30 ºC	3	41
16	THF	0.9	35 ºC	3	42
17	THF	1.0	30 ºC	3	47
18	THF	1.0	35 ºC	3	48

We continued to optimize the reaction conditions further by investigating sulfuric acid equivalence up to 1.3 equivalence in increments of 0.1 while keeping the solvent, temperature, and time constant. For entries 4 to 10, a trend was noticed; as the acid equivalence increases the yield also increases. However, a threshold is reached with 1.0 equivalents of sulfuric acid as the yields begin to decrease. Now that we have found the desirable equivalence 0.9 and 1.0 equivalents resulting in yields of 67% and 63 % respectively, we investigated whether changes in temperature would increase the reaction yields. As is shown in entries 15 to 18, we increased the temperatures to 30 ºC and 35 ºC. Unfortunately, as the temperatures increased the yields decreased. This could be because the increase in heat may thermodynamically not favor the generation of compound **6**. With the optimized conditions, compound **5** can achieve a yield of 81% over 2 steps to afford compound **6.**

The final step to achieving our building block, azidosphingosine **7**, requires a deprotection of the alcohol protecting group on **6**, this is achieved with tetrabutylammonium fluoride (TBAF) in the presence of THF. TBAF is used as a fluoride source as the fluoride anion undergoes a fluoride-mediated deprotection of the silyl protecting group through a pentavalent silicon pathway.[117] Due to silicon's vacant d-orbitals, the pentavalent silicon center can exist, the silicon-oxygen bond is cleaved while forming a stable silicon-fluorine bond producing **7** in a yield of 90%.

The next objective is to undergo DMT-phosphoramidite chemistry and undergo a 1,3-triazole transformation shown in **Scheme 3-2**. Triphenylmethyl (trityl) groups such as 4,4-dimethoxytrityl (DMT) protecting groups are widely used for protecting alcohols in organic synthesis, especially during oligonucleotide synthesis.[118] Trityl protecting groups are stable under basic conditions, and can be readily removed in the presence of a mild acid. The installation of the DMT group on the terminal alcohol caused a couple of challenges. It was important to avoid protecting the secondary alcohol while keeping the reaction conditions basic enough. This resulted in generating optimized reaction conditions of 1.1 equivalent of DMT, catalytic amount of 4-(dimethylamino)pyridine (4-DMAP) and pyridine as the solvent to afford compound **8** in 51%.

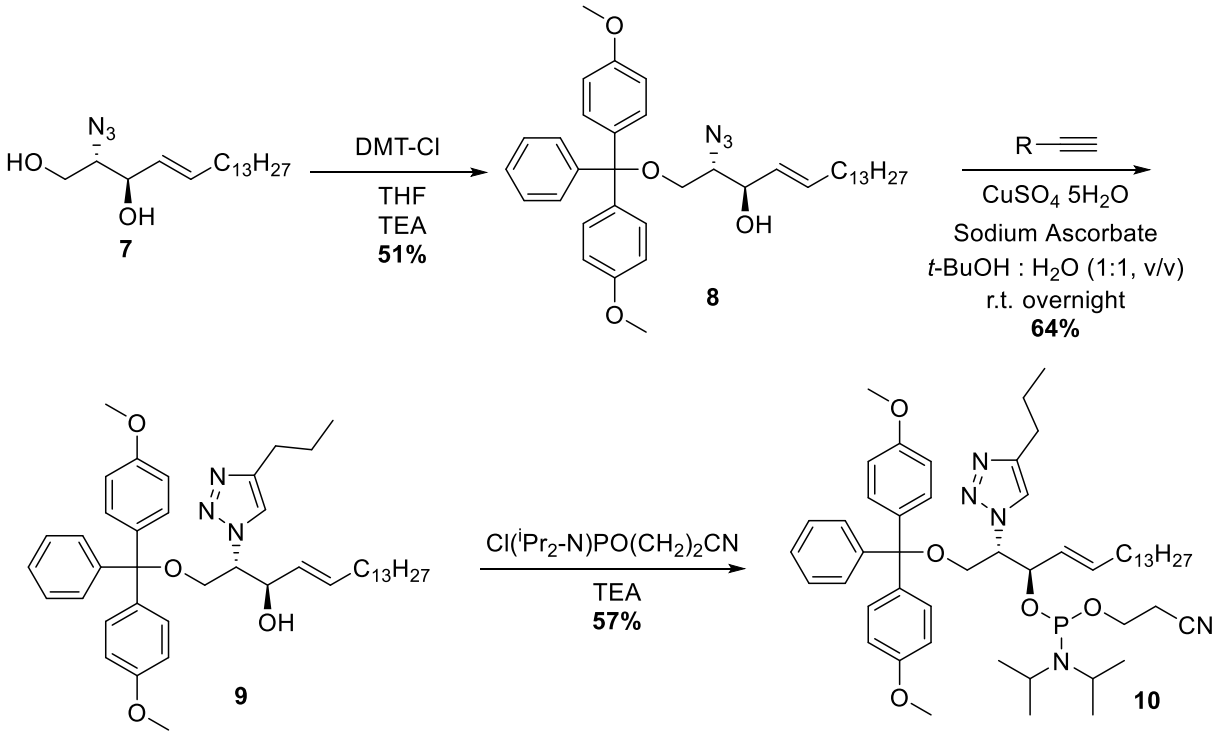

Scheme 3-2. Synthesis of propyl-triazole sphingosine DMT-phosphoramidite modifications.

The azide present on compound **8** creates a platform to undergo a variety of chemical modifications. In our case, we can reduce the azide to an amine or subject the azide the formation of a 1,4-triazole ring. Various 1,4-triazole functionalities have shown to be tolerated as a nucleic acid modification, to achieve this transformation it undergoes the Cu-catalyzed Azide-Alkyne Cycloaddition (CuAAC) reaction. To generate the triazole ring a well-established method was followed, a copper (I) catalyst is required; $Cu_2SO_4 \bullet 5H_2O$ was best suited for this reaction with sodium ascorbate as an *in situ* reducing agent.[119] Since there is a DMT protecting group present on compound **8**, it was vital to keep the reaction mixture basic as it can be cleaved under mild acidic conditions. To accomplish this, 2 equivalents of TEA were added to the reaction to generate compound **9a** in a 63% yield.

To form the triazole ring the reaction requires the reduction of Cu(II) to Cu(I) by the addition of the reducing agent, sodium ascorbate. The first Cu(I) generates a bond with the terminal

alkyne to form the copper acetylide intermediate, here Cu(I) acts as a strong σ-bound ligand. The introduction of the second copper atom coordinates with the alkyne through a weak π-complexation. The β-carbon of the acetylide undergoes a nucleophilic attack at the terminal-nitrogen of the azide to form the first carbon-nitrogen bond. From here, the intermediate undergoes a ligand exchange generating triazolide. Lastly, the triazolide intermediate, undergoes protonolysis to achieve the desired triazole ring to complete the catalytic cycle. [120, 121] The synthetic cycle is depicted below in **Figure 3-3**.

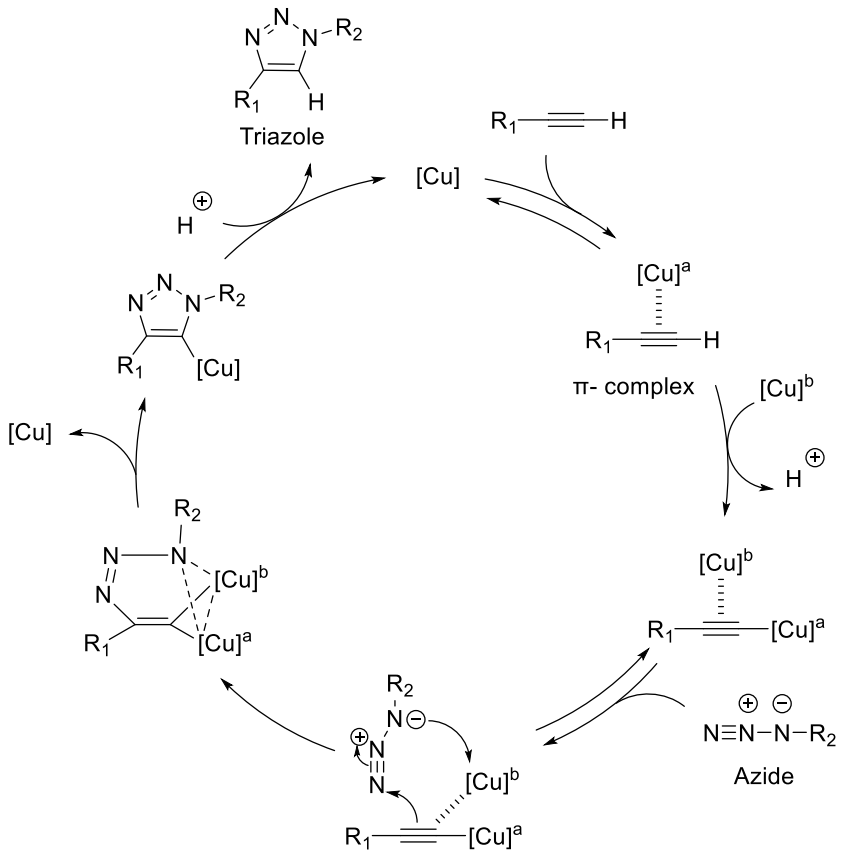

Figure 3.3: Catalytic cycle of Cu(I) catalyzed azide-alkyne cycloaddition catalytic cycle forming 1,3-triazole.

The final step is the attachment of the phosphite group, and this reaction is challenging due to the high sensitivity of the phosphite group towards moisture. The phosphite group undergoes a reaction with the secondary alcohol of compound **9a** using a TEA to generate compound 10 in 57% yield. During the oligonucleotide synthesis, the phosphite group will become oxidized to a phosphate.

To confirm the success of the phosphoramidites into the RNA, mass spectrometry was performed on each sequence strand and the results are summarized in **Table 3-2**.

Table 3-2.

Table 3-2. Negative ESI of sense strand oligonucleotides. **X** represents the propyl-triazole sphingosine modification

Code	Sequence	m/z Calculated	m/z Found
S-1	5’ CUU ACG CUG AGU ACU UCG AX 3’ (S)	6451.0936	6451.7883
S-2	5’ CUU ACG CUG AGU ACU UXG ATT 3’ (S)	6756.1600	6755.5989
S-3	5’ CUU ACG CUG XGU ACU UCG ATT 3’ (S)	6732.1444	6732.4007
S-4	5’ XUU ACG CUG AGU ACU UCG ATT 3’ (S)	6756.1600	6756.4147
S-5	3’ XG AAU GCG ACU CAU GAA GCU 5’ (AS)	6619.1361	6619.4267

3.2 Thermal Stability of siRNAs

The siRNA helix is stabilized by two main types of interactions: hydrogen bonding and base stacking.[122] The melting temperature (T_m) is the temperature at which point the two strands become unstable and dissociate and this, provides an insight to the duplex’s infection point. Due to the nucleobases’ high absorption at 260 nm, absorption is measured as a function of temperature, which allows T_m to be calculated since the exposed nucleobases have higher absorption than equivalent bases in their double stranded nucleic acid form.[123] **Table 3-3** displays the synthesized sequences, modification position and T_m values. Terminal modifications resulted in improving thermal stabilization. Placing the modification at the 3’ end of the antisense or sense strand (S-1 and S-5), replaces the dTdT overhang, and this did not have a destabilization effect. This similar result is seen in placing the modification at the 5’ end of the sense strand. A similar study done by Kubo *et al*., in 2021, which uses saturated and unsaturated fatty acid modifications on the 5’ end of the sense strand, displays no significant difference compared to their unmodified sequence.[124] At this position, the sphingosine modification is no thermally destabilizing but rather is stabilizing. This could be due to the modification improving hydrogen bonding and/or stacking interactions at the end of the RNA strand. Internal modifications did not result in significant thermal destabilization in comparison to previous bulkier modifications reported by the Desaulniers lab on

the central region.[125, 126] Placing the modification at positions 10 or 17 from the sense strand 5' end resulted in ΔT_m values of - 3.9 and - 7.9, respectively. This could be due do

These results were expected as the internal region of siRNA is less tolerable to large chemical modifications than the 3'-end and 5'-ends of the RNA strands.

Placing the chemical modification on the sense and the antisense strand showed similar trends in comparison to a single modification on the sense or antisense strand. The siRNA modified sequences D-1 and D-3 both have the sphingosine modification at the 3'end of the antisense strand. On the sense strand, D-1 has the sphingosine modification at the 3' end of the sense strand. While D-3 has the sphingosine modification at the 5' end of the sense, respectively. The modifications on the terminal ends show improving thermal stabilization, in comparison to WT. A potential reason as to why the D-1 shows stabilization could be due to the interaction between the triazole and long hydrophobic chain with the RNA sequences. In regard to the stabilization results of D-3, there are two sphingosine modifications on the same side of the siRNA, this could lead to a strong interaction between the two long hydrophobic chains. The interaction between the long alkyl chains could be strong enough to exhibit stabilization.

Comparing the double modifications D-1 and D-3 to the single modifications (S-1, S-4 and S-5), there is no drastic improvement. However, sequence D-2 has improved thermal stabilization in comparison to S-3 by about 5.5 ºC. As previously mentioned, internal modifications are less tolerable, however, adding the modification on the 5'-end of the antisense strand helps stabilize the duplex. The D-1 siRNA has the sphingosine modification at the 3'-ends of the sense strand shows improved thermal stabilization. As an example, a previous study placed various biaryl units such as benzene, naphthalene, phenanthrene or pyrene residues at the 3'-terminus ends of the sense and antisense strands, and they exhibited improved nuclease resistant with ΔT_m values of +0.8, +1.6, +3.1, and +3.7, respectively.[127]

Table 3-3. Sequences of anti-luciferase siRNAs and T_m's of siRNAs containing the propyl-triazole sphingosine modification.

siRNA	Duplex Sequences	[a]T_m(°C)	ΔT_m(°C)
	5' CUU ACG CUG AGU ACU UCG ATT 3' (S)	76.1	--
WT	3' TTG AAU GCG ACU CAU GAA GCU 5' (AS)		
	5' CUU ACG CUG AGU ACU UCG A**X** 3' (S)	78.23	+ 2.2
S-1	3' TTG AAU GCG ACU CAU GAA GCU 5' (AS)		
	5' CUU ACG CUG AGU ACU U**X**G ATT 3' (S)	72.2	- 3.9
S-2	3' TTG AAU GCG ACU CAU GAA GCU 5' (AS)		
	5' CUU ACG CUG **X**GU ACU UCG ATT 3' (S)	68.2	- 7.9
S-3	3' TTG AAU GCG ACU CAU GAA GCU 5' (AS)		
	5' **X**UU ACG CUG AGU ACU UCG ATT 3' (S)	77.2	+ 1.1
S-4	3' TTG AAU GCG ACU CAU GAA GCU 5' (AS)		
	5' CUU ACG CUG AGU ACU UCG ATT 3' (S)	78.2	+ 2.1
S-5	3' **X**G AAU GCG ACU CAU GAA GCU 5' (AS)		
	5' CUU ACG CUG AGU ACU UCG A**X** 3' (S)	81.8	+ 3.0
D-1	3' **X**G AAU GCG ACU CAU GAA GCU 5' (AS)		
	5' CUU ACG CUG **X**GU ACU UCG ATT 3' (S)	76.4	- 2.4
D-2	3' **X**G AAU GCG ACU CAU GAA GCU 5' (AS)		
	5' XUU ACG CUG AGU ACU UCG ATT 3' (S)	80.5	+ 1.7
D-3	3' XG AAU GCG ACU CAU GAA GCU 5' (AS)		

T_m values were measured in a sodium phosphate buffer (90 mM NaCl, 10 mM Na_2HPO_4, 1 mM EDTA, pH 7) at 260 nm, from 10 to 95 °C. **X** represents the propyl-triazole sphingosine modification.

3.3 Circular Dichroism Conformation of siRNA Helical Structure

To determine whether the siRNAs can retain activity, they must be in the A-form helical conformation to be a suitable substrate for RISC.[128] One way to characterize A-form helical conformation is to use a technique called circular dichroism (CD). CD generates polarized light that provides distinct absorption patterns based on the secondary structure of nucleic acids and proteins.[129] Various helices such as A, B and Z have similar but distinct absorption profiles as A-form helices present shallow troughs at around 210 nm and an absorption maximum at 260 nm. B-form helices are often observed by DNA duplexes and are similar, however they have a 10-20 nm shift to the right resulting in a shallow trough at 220 nm and an absorption maximum at 280 nm. [130] Lastly the Z-form helices is less common than the other two helices, they generate a trough at 205 nm, a large peak at 260 nm and a small trough at 290 nm.[130] Examining the two figures, **Figure 3-4** and **Figure 3-5**, both present A-Form helical conformations. **Figure 3-4** shows the CD spectra of the propyl-triazole sphingosine single-modified duplexes (S-1 to S-5) demonstrating the expected absorption profile of an A-form helix. **Figure 3-5** shows the CD spectra of the propyl triazole sphingosine double-modified duplexes (D-1 to D-3). Observing the CD spectra, the modified siRNAs retain the A-form helical conformation as the characteristic trough is present at 210 nm and the absorption maxima at 264 nm, this means that they will be active substrates for RISC.[131]

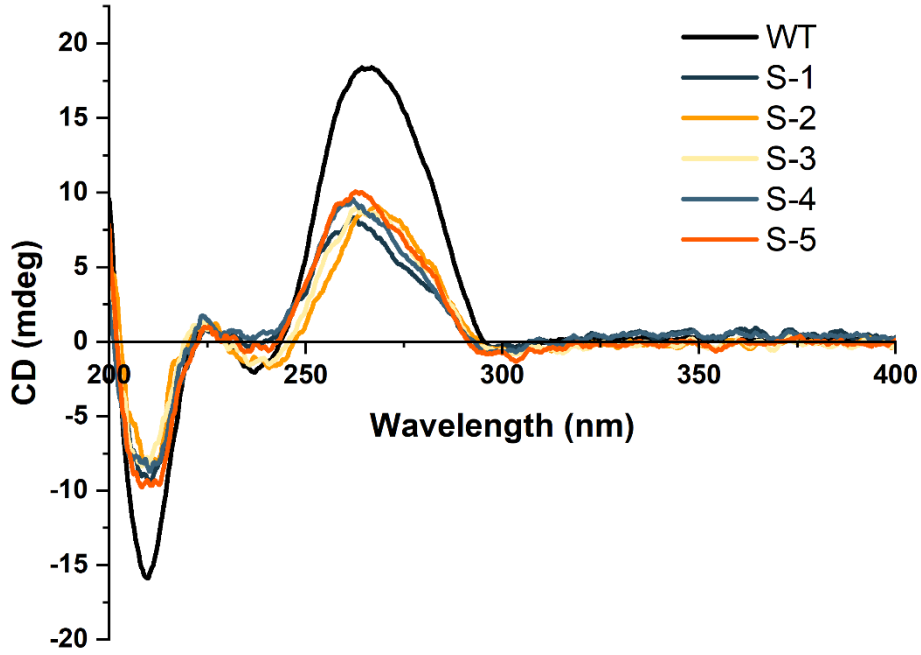

Figure 3-4. CD Spectra of propyl-triazole sphingosine single modified siRNAs targeting firefly luciferase.

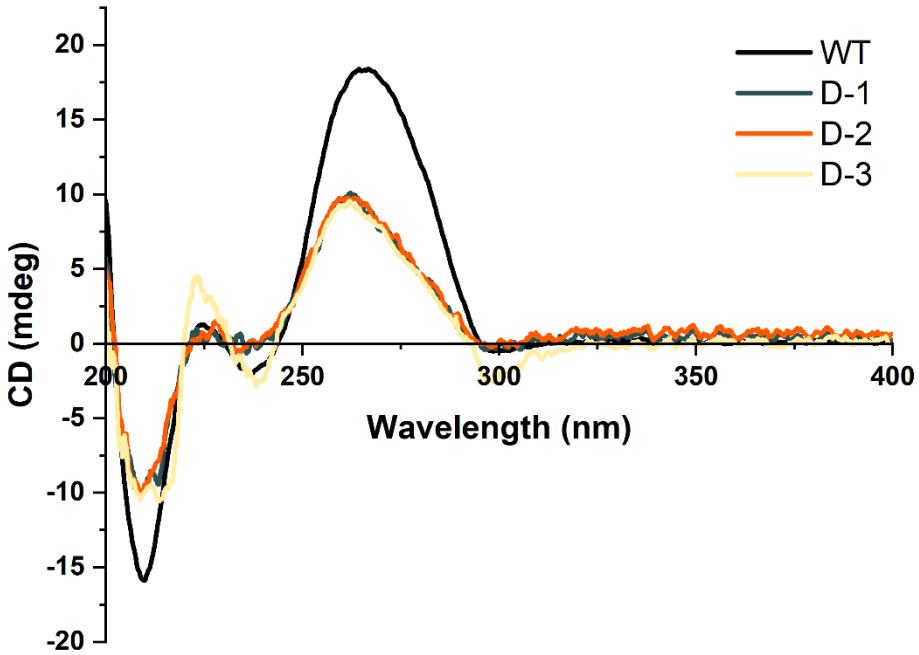

Figure 3-5. CD Spectra of propyl-triazole sphingosine double modified siRNAs targeting firefly luciferase.

3.4 Silencing Capability of the Endogenous Firefly Luciferase Gene

The biophysical characterization results of the sphingosine modified siRNAs suggests that they would be compatible with RNAi. The dual luciferase assay is a widely used assay for the purpose of screening new modifications for position and concentration dependent gene-silencing activity. The modified siRNAs target firefly luciferase mRNA, expressed from the transfected pGL3 plasmid, while Renilla luciferase, expressed as the pRLSV40 plasmid is used as an internal control to normalize the signal. Both luciferase enzymes are added to the substrate, luciferin, catalyzing a reaction that produces light as a by-product which is used to assess expression levels as luminescence.[132, 133] A control well was utilized on each plate by co-transfecting a well with both plasmids with no siRNA. The control was used to express luciferase luminescence as a percent of the control. The results are seen in **Figure 3-6** with the siRNAs being tested at various concentrations.

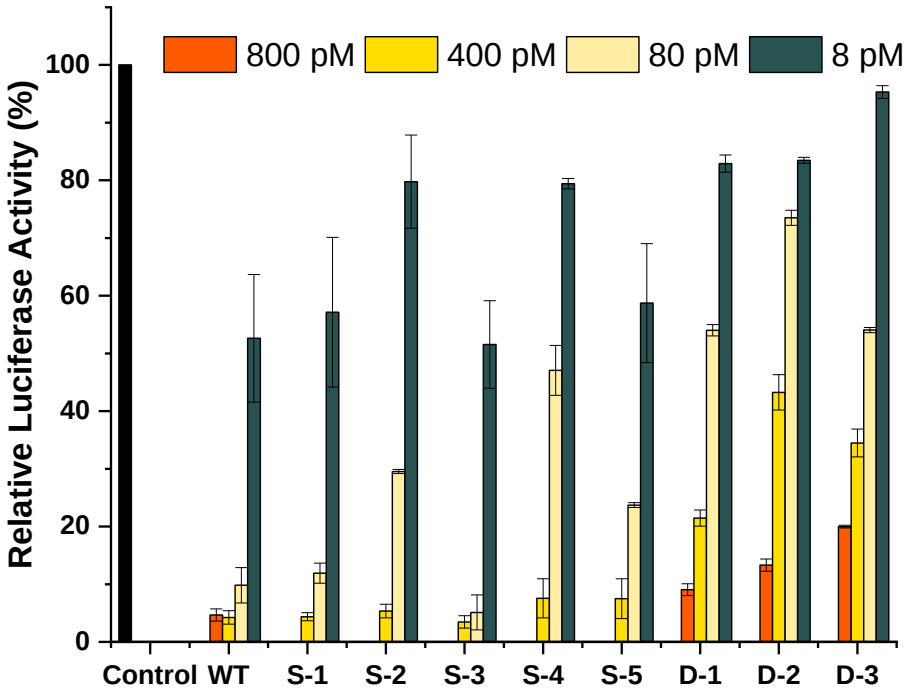

Figure 3-6. Gene-silencing ability from sphingosine-modified siRNAs transfected into HeLa cells targeting *firefly* luciferase mRNA and normalized to *Renilla* luciferase. Average of 3 technical replicates and 3 biological replicates.

The first five strands that were tested, S-1 to S-5, contain a single propyl-triazole sphingosine modification of the sense or antisense strand targeting *firefly* luciferase. All modified siRNA exhibited a dose-dependent gene-silencing. S-1 and S-3 are most comparable to wt at all concentrations. S-2 and S-3 show that the modification is well tolerated within the central region despite the fact that its destabilizing. The effect of destabilization is comparable with the work performed in the Desaulniers group.[99, 134] Overall, this shows that with destabilization of the duplex, these sphingosines-modified siRNAs are well tolerated within the RISC as a substrate.[135] siRNA S-5 contains the modification on the 3' terminus antisense strand. Previous reports suggests that the binding affinity of the guide strand with Ago2 protein is related with the silencing activity as the 3' overhang is not always bound to the PAZ domain as it dislodges upon base pairing with the complementary strand and again engages to the domain. siRNA S-5 contains the modification on the 3' terminus of the antisense strand and exhibits improved silencing abilities in comparison to other terminal modifications such as siRNA S-4. These results are consistent with previous studies in modifying the 3' terminus or the antisense strand and exhibited potent gene silencing abilities.[136] Given that these modifications were well tolerated, we wanted to explore the effect of two sphingosine modifications within an siRNA duplex.

The chemical modification is placed on the 3' end of the antisense strand for all of the duplexes, however their location on the sense strand differs. The modification is placed on the 3'-end (D-1), the central region (D-2) and the 5' end of (D-3). Placing the modifications on both the sense and antisense strand (siRNAs D-1 to D-3) also displayed dose-dependant knockdown (**Figure 3.6**). Comparing the double-modified series to the single-modified series, they still exhibit dose-dependant knockdown. However, comparing the double-modified series to wt, they are not as comparable. With a single chemical modification there is not a dramatic change on the siRNA resulting in comparable gene-silencing to wt. Placing a chemical modification on the sense and antisense strands will have an impact on its gene-silencing ability due to the dramatic change in modifications. The addition of two fatty acids on the siRNA strands may have impacted the binding

of RISC and its gene-silencing abilities. This results in the double-modified series not being comparable to the wt activity.

This is in contrast to a previous study by Yoshikawa *et al*., in which the double modified biaryl siRNAs were more effective compared to single-modified siRNAs.[127] The PAZ component of Ago2, recognizes the 3'-overhang region of a guide strand and is accommodated by a binding pocket composed of amino acids. The additional modification on the 3' terminal end of D-1 to D-3, should have enhanced gene-silencing in comparison to single modified siRNAs. However, when we compare our potency profile of our sphingosine-labeled siRNAs, siRNAs D-1 to D-3 present more effective gene silencing towards *firefly* luciferase in comparison to the biaryl modified siRNAs, this could be due to the less rigid characteristics of the sphingosine derivative. Overall, the single-modified siRNAs are comparable to wt as they are able to bind to RISC more effectively in comparison to the double-modified siRNAs.

3.5 Delivery Capability of Carrier-Free Firefly Luciferase Gene

Once we confirmed the biological activity of all siRNAs in HeLa cells after transfection with Lipofectamine reagent (Lipofectamine 2000™), we wanted to investigate the cellular uptake and delivery of the modified siRNAs. The dual luciferase assay is a good screening method for new modified siRNAs for their gene-silencing abilities in the presence or absence of a transfection carrier. Other lipid conjugates have shown success with increasing siRNA lipophilicity and improving cellular uptake without the need of transfection carriers.[99, 137] We focused on the terminal ends and central region of the siRNAs, S-1, S-3, S-4, D-1 to D-3, and investigated their gene-silencing abilities in the absence of a transfection carrier. A control well was utilized on each plate by co-transfecting a well with both plasmids, during the transfection period, with no siRNA. The control was used to express luciferase luminescence as a percent of the control. The results are seen in **Figure 3.7** with the siRNAs being tested at various concentrations.

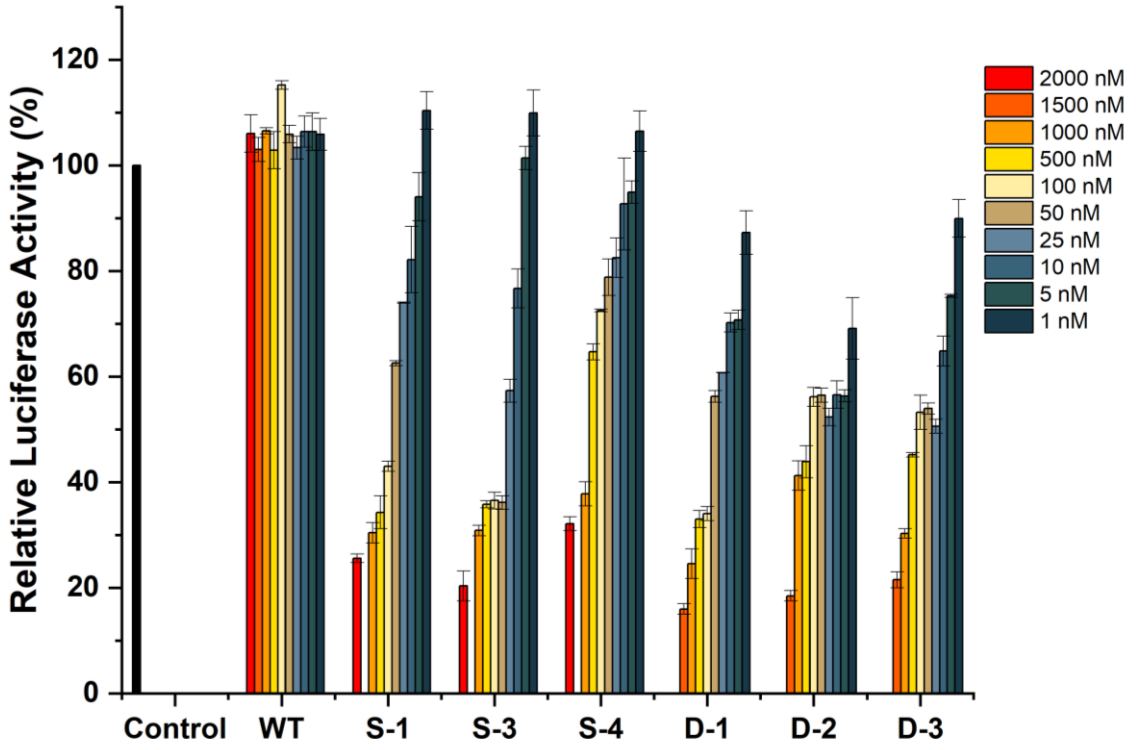

Figure 3.7: Reduction in *Firefly* luciferase expression in HeLa cells as a function of siRNA activity ranging from 1 to 2000 nM in the absence of a transfection carrier. Average of 2 technical replicates and 3 biological replicates.

Following the carrier-free protocol previously described (in the experimental chapter), as observed in **Figure 3.7**. This experiment provided an insight to the cellular permeability of the chemically modified siRNAs and accumulation in the cell.

The wt, which lacks a propyl-triazole modification, did not display any gene-silencing activity in this carrier-free study. This did not come as a surprise as unmodified siRNAs are known to have difficulties in crossing the cellular membrane unassisted. In contrast, all of the chemically modified siRNAs show a dose-dependant knockdown. The single modified propyl-triazole sphingosine siRNAs (S-1, S-3, and S-4) exhibit potent gene silencing. With siRNA S-4 showed 62-68 % knockdown reduction in *firefly* luciferase activity in high concentrations of 1000 to 2000 nM. It exhibited in a dose-dependent knockdown, however it required higher concentrations to observe gene silencing in comparison to S-1 and S-3. While siRNAs S-1 and S-3 exhibit potent gene silencing, with 60-80 % reduction in *firefly* luciferase activity in 50 to 2000 nM concentration

range. The effective carrier-free gene silencing activity of S-1 and S-3 as the sphingosine modification is placed on the 3' and central region of the sense strand, respectively. Overall, the single modified series show good gene-silencing knockdown and are able to cross the cellular membrane without a transfection carrier. A potential reason as to why these siRNAs are able to bypass the cellular membrane could be due to their ability to anchor themselves into the cellular membrane. The cellular membrane is a lipid bilayer that is composed of amphipathic molecules and the most abundant lipids are phospholipids. Various lipids are able to spontaneously aggregate to bury their hydrophobic tails in the interior and expose their hydrophilic heads to the aqueous environment. Utilizing this delivery mechanism, the various single-modified siRNAs enter the cytoplasm, then undergo the RNAi pathway. It's interesting to note how the different locations are able to impact the results of the carrier-free dual luciferase. Placing the chemical modification on the terminal ends would result in a better delivery mechanism as the lipid would anchor itself and the siRNA would be vertical. In contrast to the central modification, the sphingosine would anchor itself into the cellular membrane resulting in the RNA being horizontal. Overall, they are all able to cross the cellular membrane the difference in silencing activity is reflected on their ability to bind to RISC. The activity in the dual luciferase assay (**Figure 3.6**) with siRNA S-3 exhibiting the most effective gene-silencing activity with S-4 being the lease effective, and S-1 being in between. Further investigation into dose dependency generated the IC_{50} (Inhibitor Concentration) values shown in **Figure 3.8** summarized in **Table 3-4**. The IC_{50} values were determined using Graphpad Prism 9 software.

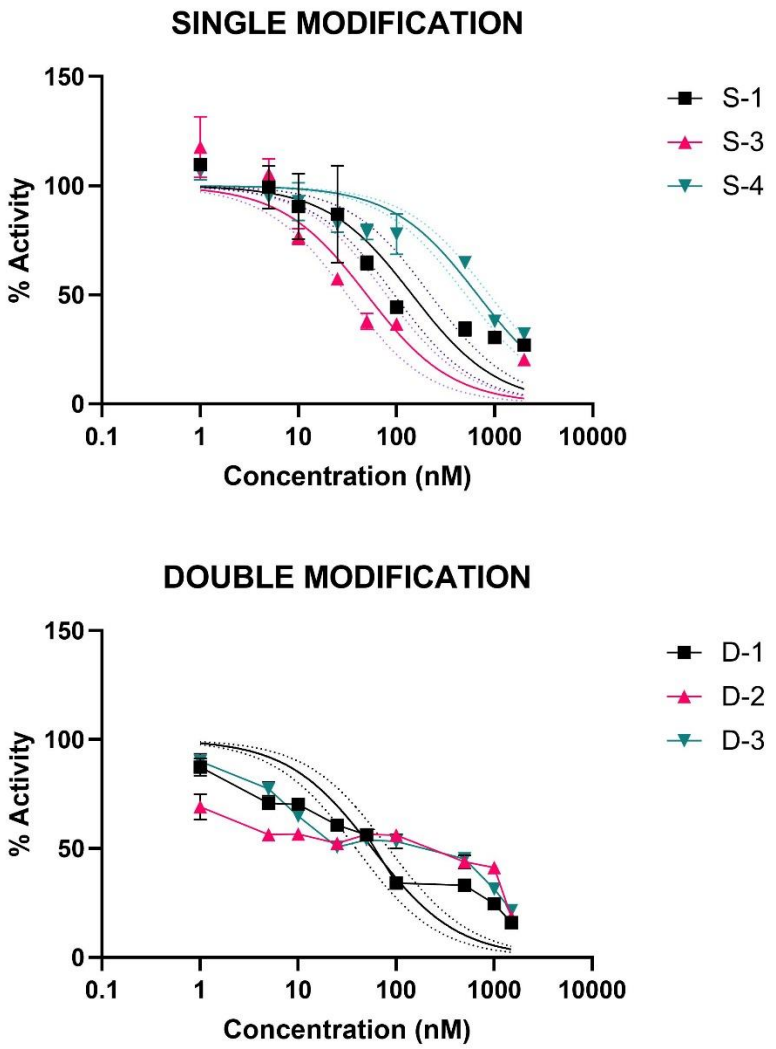

Figure 3.8: Inhibitory dose-response curves for propyl-triazole sphingosine-conjugated siRNAs targeting exogenous firefly luciferase in HeLa cells following a carrier-free transfection protocol. **Top:** Nonlinear regression curve of single-modified siRNAs; S-1, S-3, and S-4 with 95% CI. Average of 3 technical replicates and 3 biological replicates. **Bottom:** Nonlinear regression curve of double-modified siRNAs; D-1 to D-3 with 95% CI. Average of 2 technical replicates and 3 biological replicates.

Table 3.4: Summarized IC_{50} values of siRNAs S-1, S-3, S-4, and D-1 to D-3.

siRNA	**IC_{50} (nM)**
S-1	144.9
S-3	49.9
S-4	670.7
D-1	49.9
D-2	60.6
D-3	66.4

The IC_{50} values for S-1 and S-3 are 144.9 nM and 49.86 nM, respectively, while S-4's IC_{50} value is 670.7 nM. The statistical analysis suggests the curves are different, resulting in the assumption that placing the modification on various locations on the RNA sequence results in different activity. Comparing the observed IC_{50} values to previous work performed in the Desaulniers group. In 2018, Salim *et al.* implemented a cholesterol-triazole linked to various regions of the siRNA and investigated the cellular uptake without the presence of a transfection carrier. Placing the cholesterol-triazole conjugate on the 3' end (X5) and the central region (X2) generated IC_{50} values of 189.2 nM and 307.1 nM, respectively.[99] In comparison, the propyl-triazole sphingosine conjugates are slightly more potent on the 3' terminus of the sense strand and significantly more potent on the central region. This could be due to sphingosine being dramatically less bulky and more flexible than the cholesterol-triazole conjugate. siRNA S-4 resulted in an IC_{50} of 670.7 nM, which is significantly higher than S-1 and S-3, this could be due to the placement of the modification. Placing a chemical modification on the 5' terminus of the sense strand may disrupt the binding efficiency of Ago2, ultimately requiring higher concentrations to observe effective gene silencing.[135]

The double modified series show improved cellular uptake and gene-silencing activity compared to the single modified series and wt. Utilizing the same delivery mechanism previously mentioned for the single-modified series, the installation of a second lipid results in enhanced

cellular permeability. The double modified siRNAs D-1 to D-3 exhibited potent and improved gene silencing in the absence of a transfection carrier in comparison to the single modifications. siRNA D-1 resulted in 65- 84% knockdown with a concentration range of 100 to 1500 nM and continued to have 30 to 44 % knockdown with low concentrations of 5 to 50 nM. siRNA D-2 resulted in 80 % knockdown with 1500 nM, and 44-60 % knockdown with concentration range of 5 nM to 1000 nM. While siRNA D-3 exhibited 70-80 % knockdown with concentrations of 1000 to 1500 nM, and 45-55 % knockdown with low concentrations of 25 nM to 500 nM. The double-modified siRNAs exhibited more potent gene silencing as their IC_{50} values were 57.4 nM, 57.8 nM and 90.2 nM for D-1, D-2, and D-3, respectively. siRNA D-3 consists of the sphingolipid on the 3' end of the antisense strand and on the 5'end of the sense strand, this has the potential of both hydrophobic chains forming a strong interaction. This strong interaction is reflected in their Tm values (**Table 3.3**), as it is stabilizing the RNA. As a result of this interaction, the two hydrophobic tails are able to anchor themselves into the cellular membrane and introduce the siRNA in a more effective manner. Comparing the double modified siRNAs to one another, they are all quite comparable as they are close in IC_{50} values. The reason as to their discrepancy can be related back to their dual luciferase assay activity. Shown in the dual luciferase assay (**Figure 3.6**), D-1 is the most effective, followed by D-2 and D-3, and this trend is similar in the carrier-free assay. Implementing a sphingosine modification on the 3' end only has an impact on the cellular uptake and cellular permeability, however it does not impact the silencing activity.

Comparing the gene silencing abilities of siRNAs S-1 and D-1, siRNA D-1's IC_{50} value is lower than S-1. This may be due to the 3' overhang modifications on the sense and antisense strand, which improves stabilization and the interaction between the siRNA and PAZ instead of a single modification on the 3' terminal sense strand. Interestingly, siRNA D-2 contains the propyl-triazole sphingosine conjugate on the central region of the sense strand and on the 3' terminus of the antisense strand and does not exhibit a dramatic potency difference in comparison to S-3. Although implementing the chemical modification on the 3' terminus of the antisense strand, there is potential

for destabilization on the central region.[138] The doubly-modified siRNAs are comparable with IC_{50} values ranging from 49.9 nM and 66.4 nM. The double modified sphingosine siRNAs exhibit more potent gene silencing when compared to the single modified siRNAs. There is a dramatic improvement implementing a second modification which is observed between S4 and D3. Implementing the modification on the 3' terminus of the antisense strand improves the stabilization and interaction between the siRNA and the PAZ domain of Ago2, resulting in a significant decrease in IC_{50}. Overall, the addition of a sphingosine modification on the 3' end of the antisense strand is able to enhance cellular permeability and cellular uptake but does not have an impact on the silencing activity in RISC.

Chapter 4: Future Directions and Conclusions

With the success of the silencing abilities of propyl triazole sphingosine modified siRNAs in the presence and absence of a transfection carrier, additional chemical modifications and biological evaluations should be further explored. In the context of chemical modifications, there are variety of chemical routes with utilizing azidosphingosine as a building block shown in **Figure 4.1**. First, triazole modifications should be further investigated especially with the addition of a phenyl triazole. Exploring the aromatic addition would be an interesting 3' overhang modification on the sense strand as the bulkier modifications are well tolerated in this region. Second, the reduction of azide to nitrogen generates opportunity to link various alkyl chains or aromatic groups. Investigating the addition of a second long alkyl chain would be an interesting study as it has not been further explored. Lastly, creating various amide linked sphingosine derivatives would further expand the library of modified sphingosines. As well as integrating various fatty acids that have shown promise such as docosanoic acid and myristic acid through an amide bond reaction. Due to the interesting results of implementing a second sphingosine on the 3' end of the antisense strand and its ability to improve cellular uptake by anchoring itself in the cellular membrane, investigating the addition of multiple long carbons chains would be an interesting route. Instead of a sphingosine

on the same end of an siRNA, it would be interesting to implement one sphingosine with diacyl or triacyl glycerides may have the potential of improving delivery. This addition could be more effect as it would result in implementing the chemical modification on one position rather than two.

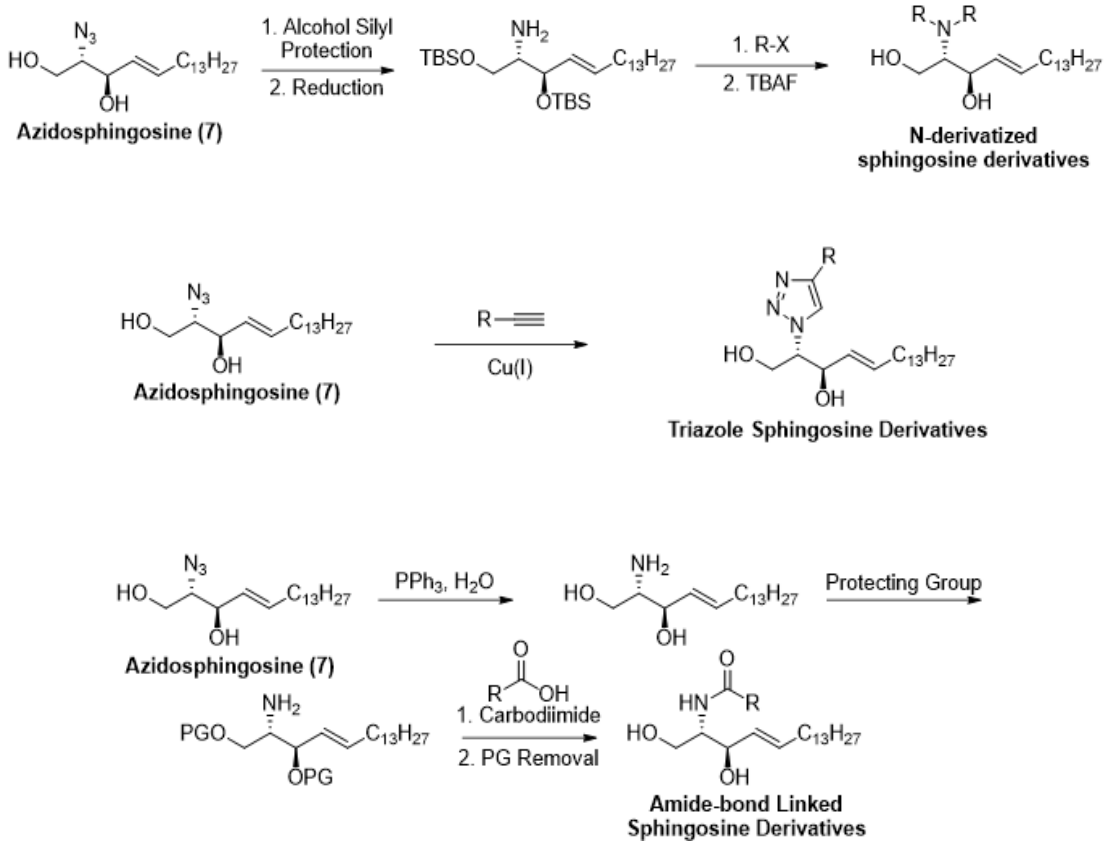

Figure 4.1: Summary of various routes to modify sphingosine.

In regard to biological evaluations, the sphingosine modified siRNAs should be further explored in other cell types such as B-cell lymphoma 2 (Bcl-2), an important anti-apoptotic gene. This oncogene is overexpressed in 50-70% of all human cancers and is a desirable target for siRNA therapeutics.[139, 140] Recently, the Desaulniers group developed centrally modified folic acid-siRNA conjugates that exhibited targeted delivery and enhanced gene silencing ability.[134] Similarly, exploring sphingosine modified siRNAs in other cell types can broaden its delivery application by determining if they are still productive in various cell types.

To further explore the delivery applications of this class of sphingolipids, we can conduct the dual luciferase assay and carrier-free assay in other cell types. Sphingolipids make up 20% of the nervous system and 25% of myelin sheaths which are found in the brain, spinal cord, and optic nerves.[141] Delivering therapeutics to these tissue sites have been challenging due the blood-brain barrier (BBB), which limits the access of drugs to the brain substance. We can investigate accumulation and gene silencing abilities of the sphingosine modified siRNAs various cells that are typically located in the nervous system. A couple of cells of interest are Schwann cells, oligodendrocyte cells and astrocytes. The most important function of the Schwann cell is to maintain and myelinate the axons of the peripheral nervous system (PNS).[142] Oligodendrocyte cells are commonly found in the central nervous system (CNS) such as the brain and spinal cord. Similar to Schwann cells, oligodendrocyte cells are primarily responsible for maintenance and generation of them myelin sheath that surrounds axons.[143] Lastly, astrocytes are the most numerous cell type within the CNS and perform a variety of tasks such as controlling the blood brain barrier and blood flow.[144] The potential of sphingolipid based conjugated systems exhibiting promising gene silencing activity and accumulation in tissues located in the nervous system would unlock a door to treating various neurodegenerative diseases.

A second pathway of investigation would be to further explore sphingosine modifications targeting myostatin *in vitro*. Myostatin (Mstn) has been shown to be a negative regulator of skeletal

muscle development and growth. A previous study utilized highly modified cholesterol conjugated siRNAs designed to induce muscle growth in mice models. In this study, Acosta *et al.*, designed 84 unique siRNAs targeting mouse Mstn mRNA, and were screened in a luciferase reporter assay in Hepa1-6 cells.[145] The potent siRNAs were tested further in *in vivo* efficacy studies in mice models. Utilizing the luciferase screening method with sphingosine modified siRNAs, it can generate preliminary results for further testing in mice models. Lastly, sphingosine modified siRNAs can be compared to the successful docosanoic acid conjugated siRNAs designed by Biscans *et al.*[146]

In summary, this study presents a safer, cost-effective, and reproducible synthesis of sphingosine molecules. As well as the generation of a small library of propyl triazole sphingosine siRNAs targeting *firefly* luciferase. In the presence of a transfection carrier both single and double modified siRNAs exhibit effective gene silencing abilities. In the absence of a transfection carrier the double modified siRNAs exhibited more potent gene silencing abilities in comparison to single sphingosine modified siRNAs and cholesterol modified siRNAs. With these promising preliminary results further modifications and placements on the RNA should be explored in an effort to overcome delivery and delivery specificity issues.

References

1. Bruce Alberts, A. J., Julian Lewis, Martin Raff, Keith Roberts, and Peter Walter., *Molecular Biology of the Cell*. 4th ed.; Garland Science: New York, 2002.
2. Jeremy M Berg, J. L. T., and Lubert Stryer., *Biochemistry*. 5th ed.; W.H. Freeman: New York, 2002.
3. Hu, B.; Zhong, L.; Weng, Y.; Peng, L.; Huang, Y. A.-O.; Zhao, Y.; Liang, X. J., Therapeutic siRNA: state of the art. (2059-3635 (Electronic)).
4. Diop-Frimpong, B.; Prakash, T. P.; Rajeev, K. G.; Manoharan, M.; Egli, M., Stabilizing contributions of sulfur-modified nucleotides: crystal structure of a DNA duplex with 2'-O-[2-(methoxy)ethyl]-2-thiothymidines. *Nucleic acids research* **2005,** *33* (16), 5297-5307.
5. Sood, A. J.; Viner, C.; Hoffman, M. M., DNAmod: the DNA modification database. Cold Spring Harbor Laboratory: 2016.
6. Boccaletto, P.; Machnicka, M. A.; Purta, E.; Piątkowski, P.; Bagiński, B.; Wirecki, T. K.; Valérie; Ross, R.; Limbach, P. A.; Kotter, A.; Helm, M.; Bujnicki, J. M., MODOMICS: a database of RNA modification pathways. 2017 update. *Nucleic Acids Research* **2018,** *46* (D1), D303-D307.
7. Wilson, R. C.; Doudna, J. A., Molecular Mechanisms of RNA Interference. *Annual Review of Biophysics* **2013,** *42* (1), 217-239.
8. Sarett, S. M.; Werfel, T. A.; Lee, L.; Jackson, M. A.; Kilchrist, K. V.; Brantley-Sieders, D.; Duvall, C. L., Lipophilic siRNA targets albumin in situ and promotes bioavailability, tumor penetration, and carrier-free gene silencing. *Proceedings of the National Academy of Sciences* **2017,** *114* (32), E6490.
9. Cerutti, H.; Casas-Mollano, J. A., On the origin and functions of RNA-mediated silencing: from protists to man. *Current Genetics* **2006,** *50* (2), 81-99.
10. Opalinska, J. B.; Gewirtz, A. M., Nucleic-acid therapeutics: basic principles and recent applications. *Nature Reviews Drug Discovery* **2002,** *1* (7), 503-514.
11. Zhang, B.; Pan, X.; Cobb, G. P.; Anderson, T. A., microRNAs as oncogenes and tumor suppressors. *Developmental Biology* **2007,** *302* (1), 1-12.
12. Fire, A.; Xu, S.; Montgomery, M. K.; Kostas, S. A.; Driver, S. E.; Mello, C. C., Potent and specific genetic interference by double-stranded RNA in Caenorhabditis elegans. *Nature* **1998,** *391* (6669), 806-811.
13. Gavrilov, K.; Saltzman, W. M., Therapeutic siRNA: principles, challenges, and strategies. *Yale J Biol Med* **2012,** *85* (2), 187-200.
14. Tomari, Y.; Matranga C Fau - Haley, B.; Haley B Fau - Martinez, N.; Martinez N Fau - Zamore, P. D.; Zamore, P. D., A protein sensor for siRNA asymmetry. (1095-9203 (Electronic)).
15. Rand, T. A.; Petersen S Fau - Du, F.; Du F Fau - Wang, X.; Wang, X., Argonaute2 cleaves the anti-guide strand of siRNA during RISC activation. (0092-8674 (Print)).
16. Matranga, C.; Tomari Y Fau - Shin, C.; Shin C Fau - Bartel, D. P.; Bartel Dp Fau - Zamore, P. D.; Zamore, P. D., Passenger-strand cleavage facilitates assembly of siRNA into Ago2-containing RNAi enzyme complexes. (0092-8674 (Print)).
17. Elbashir, S. M.; Harborth J Fau - Lendeckel, W.; Lendeckel W Fau - Yalcin, A.; Yalcin A Fau - Weber, K.; Weber K Fau - Tuschl, T.; Tuschl, T., Duplexes of 21-nucleotide RNAs mediate RNA interference in cultured mammalian cells. (0028-0836 (Print)).

18. Haley, B.; Zamore, P. D., Kinetic analysis of the RNAi enzyme complex. (1545-9993 (Print)).
19. Pickford, A.; Macino, G., 4 - Gene Silencing as a Tool for the Identification of Gene Function in Fungi. In *Applied Mycology and Biotechnology*, Arora, D. K.; Berka, R. M., Eds. Elsevier: 2005; Vol. 5, pp 93-116.
20. Masliah, G.; Barraud P Fau - Allain, F. H. T.; Allain, F. H., RNA recognition by double-stranded RNA binding domains: a matter of shape and sequence. (1420-9071 (Electronic)).
21. Jankowsky, E., RNA helicases at work: binding and rearranging. *Trends in Biochemical Sciences* **2011,** *36* (1), 19-29.
22. Meister, G.; Landthaler M Fau - Patkaniowska, A.; Patkaniowska A Fau - Dorsett, Y.; Dorsett Y Fau - Teng, G.; Teng G Fau - Tuschl, T.; Tuschl, T., Human Argonaute2 mediates RNA cleavage targeted by miRNAs and siRNAs. (1097-2765 (Print)).
23. van den Berg, A.; Mols, J.; Han, J., RISC-target interaction: cleavage and translational suppression. *Biochim Biophys Acta* **2008,** *1779* (11), 668-677.
24. Faehnle, C. R.; Elkayam E Fau - Haase, A. D.; Haase Ad Fau - Hannon, G. J.; Hannon Gj Fau - Joshua-Tor, L.; Joshua-Tor, L., The making of a slicer: activation of human Argonaute-1. (2211-1247 (Electronic)).
25. Nakanishi, K.; Ascano M Fau - Gogakos, T.; Gogakos T Fau - Ishibe-Murakami, S.; Ishibe-Murakami S Fau - Serganov, A. A.; Serganov Aa Fau - Briskin, D.; Briskin D Fau - Morozov, P.; Morozov P Fau - Tuschl, T.; Tuschl T Fau - Patel, D. J.; Patel, D. J., Eukaryote-specific insertion elements control human ARGONAUTE slicer activity. (2211-1247 (Electronic)).
26. Park, M. S.; Phan, H.-D.; Busch, F.; Hinckley, S. H.; Brackbill, J. A.; Wysocki, V. H.; Nakanishi, K., Human Argonaute3 has slicer activity. *Nucleic Acids Research* **2017,** *45* (20), 11867-11877.
27. Park, M. S.; Araya-Secchi, R.; Brackbill, J. A.; Phan, H.-D.; Kehling, A. C.; Abd El-Wahab, E. W.; Dayeh, D. M.; Sotomayor, M.; Nakanishi, K., Multidomain Convergence of Argonaute during RISC Assembly Correlates with the Formation of Internal Water Clusters. *Molecular Cell* **2019,** *75* (4), 725-740.e6.
28. Liu, J.; Carmell, M. A.; Rivas, F. V.; Marsden, C. G.; Thomson, J. M.; Song, J.-J.; Hammond, S. M.; Joshua-Tor, L.; Hannon, G. J., Argonaute2 Is the Catalytic Engine of Mammalian RNAi. *Science* **2004,** *305* (5689), 1437-1441.
29. Song, J. J.; Smith Sk Fau - Hannon, G. J.; Hannon Gj Fau - Joshua-Tor, L.; Joshua-Tor, L., Crystal structure of Argonaute and its implications for RISC slicer activity. (1095-9203 (Electronic)).
30. Frank, F.; Sonenberg, N.; Nagar, B., Structural basis for 5′-nucleotide base-specific recognition of guide RNA by human AGO2. *Nature* **2010,** *465* (7299), 818-822.
31. Frank, F.; Hauver, J.; Sonenberg, N.; Nagar, B., ArabidopsisArgonaute MID domains use their nucleotide specificity loop to sort small RNAs. *The EMBO Journal* **2012,** *31* (17), 3588-3595.
32. Ma, J.-B.; Ye, K.; Patel, D. J., Structural basis for overhang-specific small interfering RNA recognition by the PAZ domain. *Nature* **2004,** *429* (6989), 318-322.
33. Yan, K. S.; Yan, S.; Farooq, A.; Han, A.; Zeng, L.; Zhou, M.-M., Structure and conserved RNA binding of the PAZ domain. *Nature* **2003,** *426* (6965), 469-474.

34. Lingel, A.; Simon, B.; Izaurralde, E.; Sattler, M., Structure and nucleic-acid binding of the Drosophila Argonaute 2 PAZ domain. *Nature* **2003,** *426* (6965), 465-469.
35. Sheng, G.; Zhao, H.; Wang, J.; Rao, Y.; Tian, W.; Swarts, D. C.; van der Oost, J.; Patel, D. J.; Wang, Y., Structure-based cleavage mechanism of Thermus thermophilus Argonaute DNA guide strand-mediated DNA target cleavage. *Proceedings of the National Academy of Sciences* **2014,** *111* (2), 652.
36. Wang, Y.; Juranek, S.; Li, H.; Sheng, G.; Wardle, G. S.; Tuschl, T.; Patel, D. J., Nucleation, propagation and cleavage of target RNAs in Ago silencing complexes. *Nature* **2009,** *461* (7265), 754-761.
37. Kwak, P. B.; Tomari, Y., The N domain of Argonaute drives duplex unwinding during RISC assembly. *Nature Structural & Molecular Biology* **2012,** *19* (2), 145-151.
38. Sahin, U.; Karikó, K.; Türeci, Ö., mRNA-based therapeutics — developing a new class of drugs. *Nature Reviews Drug Discovery* **2014,** *13* (10), 759-780.
39. Collingwood, M. A.; Rose, S. D.; Huang, L.; Hillier, C.; Amarzguioui, M.; Wiiger, M. T.; Soifer, H. S.; Rossi, J. J.; Behlke, M. A., Chemical modification patterns compatible with high potency dicer-substrate small interfering RNAs. *Oligonucleotides* **2008,** *18* (2), 187-200.
40. Silnikov, V. N.; Vlassov, V. V., Design of site-specific RNA-cleaving reagents. *Russian Chemical Reviews* **2001,** *70* (6), 491-508.
41. Khvorova, A.; Watts, J. K., The chemical evolution of oligonucleotide therapies of clinical utility. (1546-1696 (Electronic)).
42. Jeong, J. H.; Mok, H.; Oh, Y.-K.; Park, T. G., siRNA Conjugate Delivery Systems. *Bioconjugate Chemistry* **2009,** *20* (1), 5-14.
43. Watts, J. K.; Deleavey, G. F.; Damha, M. J., Chemically modified siRNA: tools and applications. *Drug Discovery Today* **2008,** *13* (19), 842-855.
44. Deleavey, Glen F.; Damha, Masad J., Designing Chemically Modified Oligonucleotides for Targeted Gene Silencing. *Chemistry & Biology* **2012,** *19* (8), 937-954.
45. Jackson, A. L., Widespread siRNA "off-target" transcript silencing mediated by seed region sequence complementarity. *RNA* **2006,** *12* (7), 1179-1187.
46. Zhang, M. M.; Bahal, R.; Rasmussen, T. P.; Manautou, J. E.; Zhong, X.-b., The growth of siRNA-based therapeutics: Updated clinical studies. *Biochemical Pharmacology* **2021,** *189*, 114432.
47. Ohtsuka, E.; Ikehara, M.; Söll, D., Recent developments in the chemical synthesis of polynucleotides. *Nucleic acids research* **1982,** *10* (21), 6553-6570.
48. Dahl, B. H.; Nielsen, J.; Dahl, O., Mechanistic studies on the phosphoramidite coupling reaction in oligonucleotide synthesis. I. Evidence for nudeophilic catalysis by tetrazole and rate variations with the phosphorus substituents. *Nucleic Acids Research* **1987,** *15* (4), 1729-1743.
49. Serge, L. B., Strategies in the Preparation of DNA Oligonucleotide Arrays for Diagnostic Applications. *Current Medicinal Chemistry* **2001,** *8* (10), 1213-1244.
50. Muller, S.; Wolf, J.; Ivanov, S. A., Current Strategies for the Synthesis of RNA. *Current Organic Synthesis* **2004,** *1* (3), 293-307.
51. Bennett, C. F., Therapeutic Antisense Oligonucleotides Are Coming of Age. *Annual Review of Medicine* **2019,** *70* (1), 307-321.

52. Yu, R. Z.; Kim, T.-W.; Hong, A.; Watanabe, T. A.; Gaus, H. J.; Geary, R. S., Cross-Species Pharmacokinetic Comparison from Mouse to Man of a Second-Generation Antisense Oligonucleotide, ISIS 301012, Targeting Human Apolipoprotein B-100. *Drug Metabolism and Disposition* **2007,** *35* (3), 460.
53. Geselowitz, D. A.; Neckers, L. M., Bovine Serum Albumin Is a Major Oligonucleotide-Binding Protein Found on the Surface of Cultured Cells. *Antisense Research and Development* **1995,** *5* (3), 213-217.
54. Nguyen, D.; Zandarashvili, L.; White, M. A.; Iwahara, J., Stereospecific Effects of Oxygen-to-Sulfur Substitution in DNA Phosphate on Ion Pair Dynamics and Protein-DNA Affinity. *ChemBioChem* **2016,** *17* (17), 1636-1642.
55. Crooke, S. T.; Wang, S.; Vickers, T. A.; Shen, W.; Liang, X.-h., Cellular uptake and trafficking of antisense oligonucleotides. *Nature Biotechnology* **2017,** *35* (3), 230-237.
56. Liang, X.-h.; Sun, H.; Shen, W.; Crooke, S. T., Identification and characterization of intracellular proteins that bind oligonucleotides with phosphorothioate linkages. *Nucleic Acids Research* **2015,** *43* (5), 2927-2945.
57. Marshall, W. S.; Caruthers, M. H., Phosphorodithioate DNA as a Potential Therapeutic Drug. *Science* **1993,** *259* (5101), 1564-1570.
58. Migawa, M. T.; Shen, W.; Wan, W. B.; Vasquez, G.; Oestergaard, M. E.; Low, A.; De Hoyos, C. L.; Gupta, R.; Murray, S.; Tanowitz, M.; Bell, M.; Nichols, J. G.; Gaus, H.; Liang, X.-h.; Swayze, E. E.; Crooke, S. T.; Seth, P. P., Site-specific replacement of phosphorothioate with alkyl phosphonate linkages enhances the therapeutic profile of gapmer ASOs by modulating interactions with cellular proteins. *Nucleic Acids Research* **2019,** *47* (11), 5465-5479.
59. Ndeboko, B.; Ramamurthy, N.; Lemamy, G. J.; Jamard, C.; Nielsen, P. E.; Cova, L., Role of Cell-Penetrating Peptides in Intracellular Delivery of Peptide Nucleic Acids Targeting Hepadnaviral Replication. *Mol Ther Nucleic Acids* **2017,** *9*, 162-169.
60. Meade, B. R.; Gogoi, K.; Hamil, A. S.; Palm-Apergi, C.; Berg, A. V. D.; Hagopian, J. C.; Springer, A. D.; Eguchi, A.; Kacsinta, A. D.; Dowdy, C. F.; Presente, A.; Lönn, P.; Kaulich, M.; Yoshioka, N.; Gros, E.; Cui, X.-S.; Dowdy, S. F., Efficient delivery of RNAi prodrugs containing reversible charge-neutralizing phosphotriester backbone modifications. *Nature Biotechnology* **2014,** *32* (12), 1256-1261.
61. Singh, R. P.; Oh, B.-K.; Choi, J.-W., Application of peptide nucleic acid towards development of nanobiosensor arrays. *Bioelectrochemistry* **2010,** *79* (2), 153-161.
62. G. Blackburn, M. G. a. D. L., *DNA and RNA structure*. RSC Publishing: Cambridge, UK, 2006.
63. Evich, M.; Spring-Connell, A. M.; Germann, M. W., Impact of modified ribose sugars on nucleic acid conformation and function. *Heterocyclic Communications* **2017,** *23* (3), 155-165.
64. Sun, Y.; Zhao, Y.; Zhao, X.; Lee, R. J.; Teng, L.; Zhou, C., Enhancing the Therapeutic Delivery of Oligonucleotides by Chemical Modification and Nanoparticle Encapsulation. *Molecules* **2017,** *22* (10), 1724.
65. Chiu, Y. L., siRNA function in RNAi: A chemical modification analysis. *RNA* **2003,** *9* (9), 1034-1048.
66. Chernikov, I. V.; Vlassov, V. V.; Chernolovskaya, E. L., Current Development of siRNA Bioconjugates: From Research to the Clinic. *Frontiers in Pharmacology* **2019,** *10* (444).

67. Inoue, H.; Hayase, Y.; Imura, A.; Iwai, S.; Miura, K.; Ohtsuka, E., Synthesis and hybridization studies on two complementary nona(2'-O-methyl)ribonucleotides. *Nucleic acids research* **1987,** *15* (15), 6131-6148.
68. Prakash, T. P.; Allerson, C. R.; Dande, P.; Vickers, T. A.; Sioufi, N.; Jarres, R.; Baker, B. F.; Swayze, E. E.; Griffey, R. H.; Bhat, B., Positional Effect of Chemical Modifications on Short Interference RNA Activity in Mammalian Cells. *Journal of Medicinal Chemistry* **2005,** *48* (13), 4247-4253.
69. Snead, N. M.; Escamilla-Powers, J. R.; Rossi, J. J.; McCaffrey, A. P., 5' Unlocked Nucleic Acid Modification Improves siRNA Targeting. *Mol Ther Nucleic Acids* **2013,** *2* (7), e103-e103.
70. Zhang, L.; Peritz, A.; Meggers, E., A Simple Glycol Nucleic Acid. *Journal of the American Chemical Society* **2005,** *127* (12), 4174-4175.
71. Braasch, D. A.; Corey, D. R., Locked nucleic acid (LNA): fine-tuning the recognition of DNA and RNA. *Chemistry & Biology* **2001,** *8* (1), 1-7.
72. Herdewijn, P., Heterocyclic Modifications of Oligonucleotides and Antisense Technology. *Antisense and Nucleic Acid Drug Development* **2000,** *10* (4), 297-310.
73. Valenzuela, R. A. P.; Suter, S. R.; Ball-Jones, A. A.; Ibarra-Soza, J. M.; Zheng, Y.; Beal, P. A., Base Modification Strategies to Modulate Immune Stimulation by an siRNA. *ChemBioChem* **2015,** *16* (2), 262-267.
74. Ibarra-Soza, J. M.; Morris, A. A.; Jayalath, P.; Peacock, H.; Conrad, W. E.; Donald, M. B.; Kurth, M. J.; Beal, P. A., 7-Substituted 8-aza-7-deazaadenosines for modification of the siRNA major groove. *Org Biomol Chem* **2012,** *10* (32), 6491-7.
75. Peacock, H.; Fostvedt, E.; Beal, P. A., Minor-groove-modulating adenosine replacements control protein binding and RNAi activity in siRNAs. *ACS chemical biology* **2010,** *5* (12), 1115-1124.
76. Wahba, A. S.; Azizi, F.; Deleavey, G. F.; Brown, C.; Robert, F.; Carrier, M.; Kalota, A.; Gewirtz, A. M.; Pelletier, J.; Hudson, R. H. E.; Damha, M. J., Phenylpyrrolocytosine as an Unobtrusive Base Modification for Monitoring Activity and Cellular Trafficking of siRNA. *ACS Chemical Biology* **2011,** *6* (9), 912-919.
77. Peacock, H.; Kannan, A.; Beal, P. A.; Burrows, C. J., Chemical Modification of siRNA Bases To Probe and Enhance RNA Interference. *The Journal of Organic Chemistry* **2011,** *76* (18), 7295-7300.
78. Lu, Y.; Aimetti, A. A.; Langer, R.; Gu, Z., Bioresponsive materials. *Nature Reviews Materials* **2016,** *2* (1), 16075.
79. Whitehead, K. A.; Langer, R.; Anderson, D. G., Knocking down barriers: advances in siRNA delivery. *Nature Reviews Drug Discovery* **2009,** *8* (2), 129-138.
80. Thomas, M.; Lu, J. J.; Chen, J.; Klibanov, A. M., Non-viral siRNA delivery to the lung. *Advanced Drug Delivery Reviews* **2007,** *59* (2), 124-133.
81. Santel, A.; Aleku, M.; Keil, O.; Endruschat, J.; Esche, V.; Durieux, B.; Löffler, K.; Fechtner, M.; Röhl, T.; Fisch, G.; Dames, S.; Arnold, W.; Giese, K.; Klippel, A.; Kaufmann, J., RNA interference in the mouse vascular endothelium by systemic administration of siRNA-lipoplexes for cancer therapy. *Gene Therapy* **2006,** *13* (18), 1360-1370.
82. Seth, P. P.; Tanowitz, M.; Bennett, C. F., Selective tissue targeting of synthetic nucleic acid drugs. *The Journal of Clinical Investigation* **2019,** *129* (3), 915-925.

83. De Paula, D.; Bentley, M. V. L. B.; Mahato, R. I., Hydrophobization and bioconjugation for enhanced siRNA delivery and targeting. *RNA* **2007,** *13* (4), 431-456.
84. Zhang, X.; Goel, V.; Robbie, G. J., Pharmacokinetics of Patisiran, the First Approved RNA Interference Therapy in Patients With Hereditary Transthyretin-Mediated Amyloidosis. *The Journal of Clinical Pharmacology* **2019**.
85. Chenthamara, D.; Subramaniam, S.; Ramakrishnan, S. G.; Krishnaswamy, S.; Essa, M. M.; Lin, F.-H.; Qoronfleh, M. W., Therapeutic efficacy of nanoparticles and routes of administration. *Biomaterials Research* **2019,** *23* (1), 20.
86. Dowdy, S. F., Overcoming cellular barriers for RNA therapeutics. *Nature Biotechnology* **2017,** *35* (3), 222-229.
87. Huang, Y., Preclinical and Clinical Advances of GalNAc-Decorated Nucleic Acid Therapeutics. (2162-2531 (Print)).
88. A Highly Durable RNAi Therapeutic Inhibitor of PCSK9. *New England Journal of Medicine* **2017,** *376* (18), e38.
89. Osborn, M. F.; Khvorova, A., Improving siRNA DeliveryIn VivoThrough Lipid Conjugation. *Nucleic Acid Therapeutics* **2018,** *28* (3), 128-136.
90. Østergaard, M. E.; Jackson, M.; Low, A.; E Chappell, A.; G Lee, R.; Peralta, R. Q.; Yu, J.; Kinberger, G. A.; Dan, A.; Carty, R.; Tanowitz, M.; Anderson, P.; Kim, T.-W.; Fradkin, L.; Mullick, A. E.; Murray, S.; Rigo, F.; Prakash, T. P.; Bennett, C. F.; Swayze, E. E.; Gaus, H. J.; Seth, P. P., Conjugation of hydrophobic moieties enhances potency of antisense oligonucleotides in the muscle of rodents and non-human primates. *Nucleic acids research* **2019,** *47* (12), 6045-6058.
91. Prakash, T. P.; Mullick, A. E.; Lee, R. G.; Yu, J.; Yeh, S. T.; Low, A.; Chappell, A. E.; Østergaard, M. E.; Murray, S.; Gaus, H. J.; Swayze, E. E.; Seth, P. P., Fatty acid conjugation enhances potency of antisense oligonucleotides in muscle. *Nucleic Acids Research* **2019,** *47* (12), 6029-6044.
92. Alaamery, M.; Albesher, N.; Aljawini, N.; Alsuwailm, M.; Massadeh, S.; Wheeler, M. A.; Chao, C.-C.; Quintana, F. J., Role of sphingolipid metabolism in neurodegeneration. *Journal of Neurochemistry* **2021,** *158* (1), 25-35.
93. Pralhada Rao, R.; Vaidyanathan, N.; Rengasamy, M.; Mammen Oommen, A.; Somaiya, N.; Jagannath, M. R., Sphingolipid Metabolic Pathway: An Overview of Major Roles Played in Human Diseases. *Journal of Lipids* **2013,** *2013*, 178910.
94. Yang, L.; Zheng, L.-y.; Tian, Y.; Zhang, Z.-q.; Dong, W.-l.; Wang, X.-f.; Zhang, X.-y.; Cao, C., C6 ceramide dramatically enhances docetaxel-induced growth inhibition and apoptosis in cultured breast cancer cells: A mechanism study. *Experimental Cell Research* **2015,** *332* (1), 47-59.
95. Sassa, T.; Hirayama, T.; Kihara, A., Enzyme Activities of the Ceramide Synthases CERS2–6 Are Regulated by Phosphorylation in the C-terminal Region. *Journal of Biological Chemistry* **2016,** *291* (14), 7477-7487.
96. Hannun, Y. A.; Obeid, L. M., Principles of bioactive lipid signalling: lessons from sphingolipids. *Nature Reviews Molecular Cell Biology* **2008,** *9* (2), 139-150.
97. Kolter, T.; Sandhoff, K., Sphingolipid metabolism diseases. *Biochimica et Biophysica Acta (BBA) - Biomembranes* **2006,** *1758* (12), 2057-2079.
98. Saxena, K.; Duclos, R. I.; Zimmermann, P.; Schmidt, R. R.; Shipley, G. G., Structure and properties of totally synthetic galacto- and gluco-cerebrosides. *Journal of Lipid Research* **1999,** *40* (5), 839-849.

99. Salim, L.; McKim, C.; Desaulniers, J.-P., Effective carrier-free gene-silencing activity of cholesterol-modified siRNAs. *RSC Advances* **2018,** *8* (41), 22963-22966.
100. Kim, S.; Lee, S.; Lee, T.; Ko, H.; Kim, D., Efficient Synthesis of d-erythro-Sphingosine and d-erythro-Azidosphingosine from d-ribo-Phytosphingosine via a Cyclic Sulfate Intermediate. *The Journal of Organic Chemistry* **2006,** *71* (22), 8661-8664.
101. Goddard-Borger, E. D.; Stick, R. V., An Efficient, Inexpensive, and Shelf-Stable Diazotransfer Reagent: Imidazole-1-sulfonyl Azide Hydrochloride. *Organic Letters* **2007,** *9* (19), 3797-3800.
102. Kolb, H.; Prof, M.; Prof, K., Click Chemistry: Diverse Chemical Function from a Few Good Reactions. *Angewandte Chemie International Edition* **2001,** *40*, 2004-2021.
103. Diez-Gonzalez, S.; Nolan, S. P., [(NHC)2Cu]X Complexes as Efficient Catalysts for Azide–Alkyne Click Chemistry at Low Catalyst Loadings. *Angewandte Chemie* **2008,** *120*, 9013-9016.
104. Ariza, X.; Urpí, F.; Viladomat, C.; Vilarrasa, J., One-pot conversion of azides to Boc-protected amines with trimethylphosphine and Boc-ON. *Tetrahedron Letters* **1998,** *39* (49), 9101-9102.
105. Ariza, X.; Urpí, F.; Vilarrasa, J., A practical procedure for the preparation of carbamates from azides. *Tetrahedron Letters* **1999,** *40* (42), 7515-7517.
106. Scriven, E. F. V.; Turnbull, K., Azides: their preparation and synthetic uses. *Chemical Reviews* **1988,** *88* (2), 297-368.
107. Pandiakumar, A. K.; Sarma, S. P.; Samuelson, A. G., Mechanistic studies on the diazo transfer reaction. *Tetrahedron Letters* **2014,** *55* (18), 2917-2920.
108. van den Berg, R. J. B. H. N.; Boltje, T. J.; Verhagen, C. P.; Litjens, R. E. J. N.; van der Marel, G. A.; Overkleeft, H. S., An Efficient Synthesis of the Natural Tetrahydrofuran Pachastrissamine Starting from d-ribo-Phytosphingosine. *The Journal of Organic Chemistry* **2006,** *71* (2), 836-839.
109. Du, W.; Gervay-Hague, J., Efficient Synthesis of α-Galactosyl Ceramide Analogues Using Glycosyl Iodide Donors. *Organic Letters* **2005,** *7* (10), 2063-2065.
110. Berg, R.; Korevaar, C.; Marel, G.; Overkleeft, H.; Boom, J., A simple and low cost synthesis of D-erythro-sphingosine and D-erythro-azidosphingosine from D-ribo-phytosphingosine: Glycosphingolipid precursors. *Tetrahedron Letters* **2002,** *43*, 8409-8412.
111. Jackson, Y. A.; Townsend, N. O., 10.03 - Bicyclic 5-5 Systems: Four Heteroatoms 1:3. In *Comprehensive Heterocyclic Chemistry III*, Katritzky, A. R.; Ramsden, C. A.; Scriven, E. F. V.; Taylor, R. J. K., Eds. Elsevier: Oxford, 2008; pp 129-159.
112. Hardacre, C.; Messina, I.; Migaud, M. E.; Ness, K. A.; Norman, S. E., 1,2-Cyclic sulfite and sulfate furanoside diesters: improved syntheses and stability. *Tetrahedron* **2009,** *65* (32), 6341-6347.
113. Lewis, E. S.; Boozer, C. E., The Kinetics and Stereochemistry of the Decomposition of Secondary Alkyl Chlorosulfites1. *Journal of the American Chemical Society* **1952,** *74* (2), 308-311.
114. Bissinger, W. E.; Kung, F. E., A Study of the Reaction of Alcohols with Thionyl Chloride1. *Journal of the American Chemical Society* **1947,** *69* (9), 2158-2163.
115. Hu, X.; Yin, Z.; Guo, J.; Adamson, J.; Fujiki, M.; Borovkov, V., Stereospecific Synthesis of Cyclic Sulfite Esters with Sulfur-Centered Chirality via Diastereoselective

Strategy and Intramolecular H-Bonding Assistance. *The Journal of Organic Chemistry* **2021,** *86* (1), 379-387.
116. Weissberger, A.; Riddick, J. A.; Bunger, W. B.; Sakano, T. K., *Techniques of chemistry. - 2: Organic solvents. Physical properties and methods of purification. 4.ed*. Wiley: New York, N.Y., 1986.
117. Nelson, T. D.; Crouch, R. D., Selective Deprotection of Silyl Ethers. *Synthesis* **1996,** *1996* (09), 1031-1069.
118. Bessodes, M.; Komiotis, D.; Antonakis, K., Rapid and selective detritylation of primary alcohols using formic acid. *Tetrahedron Letters* **1986,** *27* (5), 579-580.
119. Kolb, H. C.; Sharpless, K. B., The growing impact of click chemistry on drug discovery. (1359-6446 (Print)).
120. Rostovtsev, V. V.; Green Lg Fau - Fokin, V. V.; Fokin Vv Fau - Sharpless, K. B.; Sharpless, K. B., A stepwise huisgen cycloaddition process: copper(I)-catalyzed regioselective "ligation" of azides and terminal alkynes. (1433-7851 (Print)).
121. Worrell, B. T.; Malik, J. A.; Fokin, V. V., Direct evidence of a dinuclear copper intermediate in Cu(I)-catalyzed azide-alkyne cycloadditions. *Science* **2013,** *340* (6131), 457-460.
122. Guckian, K. M.; Schweitzer, B. A.; Ren, R. X. F.; Sheils, C. J.; Paris, P. L.; Tahmassebi, D. C.; Kool, E. T., Experimental Measurement of Aromatic Stacking Affinities in the Context of Duplex DNA. *Journal of the American Chemical Society* **1996,** *118* (34), 8182-8183.
123. Nygaard Ap Fau - Hall, B. D.; Hall, B. D., A method for the detection of RNA-DNA complexes. (0006-291X (Print)).
124. Kubo, T.; Nishimura, Y.; Sato, Y.; Yanagihara, K.; Seyama, T., Sixteen Different Types of Lipid-Conjugated siRNAs Containing Saturated and Unsaturated Fatty Acids and Exhibiting Enhanced RNAi Potency. *ACS Chemical Biology* **2021,** *16* (1), 150-164.
125. Desaulniers, J.-P.; Hagen, G.; Anderson, J.; McKim, C.; Roberts, B., Effective gene-silencing of siRNAs that contain functionalized spacer linkages within the central region. *RSC Advances* **2017,** *7* (6), 3450-3454.
126. Hammill, M. L.; Isaacs-Trépanier, C.; Desaulniers, J.-P., siRNAzos: A New Class of Azobenzene-Containing siRNAs that Can Photochemically Regulate Gene Expression. *ChemistrySelect* **2017,** *2* (30), 9810-9814.
127. Yoshikawa, K.; Ogata, A.; Matsuda, C.; Kohara, M.; Iba, H.; Kitade, Y.; Ueno, Y., Incorporation of Biaryl Units into the 5′ and 3′ Ends of Sense and Antisense Strands of siRNA Duplexes Improves Strand Selectivity and Nuclease Resistance. *Bioconjugate Chemistry* **2011,** *22* (1), 42-49.
128. Gregory, R. I.; Chendrimada Tp Fau - Cooch, N.; Cooch N Fau - Shiekhattar, R.; Shiekhattar, R., Human RISC couples microRNA biogenesis and posttranscriptional gene silencing. (0092-8674 (Print)).
129. Macromolecules: Structure and function: By F. Wold. Prentice-Hall, 1971. 305 pages, £7.60. *Biochemical Education* **1978,** *6* (4), 99.
130. Saenger, W., *Principles of Nucleic Acid Structure*. Springer, New York, NY: 1984.
131. Berova, N.; Nakanishi, K.; Woody, R. W., *Circular Dichroism: Principles and Applications*. Wiley: 2000.

132. de Wet, J. R.; Wood, K. V.; DeLuca, M.; Helinski, D. R.; Subramani, S., Firefly luciferase gene: structure and expression in mammalian cells. *Mol Cell Biol* **1987,** *7* (2), 725-737.
133. Promega, Dual-Luciferase® Reporter Assay System Technical Manual. Revised June 2015.
134. Salim, L.; Islam, G.; Desaulniers, J.-P., Targeted delivery and enhanced gene-silencing activity of centrally modified folic acid–siRNA conjugates. *Nucleic Acids Research* **2020,** *48* (1), 75-85.
135. Soutschek, J.; Akinc, A.; Bramlage, B.; Charisse, K.; Constien, R.; Donoghue, M.; Elbashir, S.; Geick, A.; Hadwiger, P.; Harborth, J.; John, M.; Kesavan, V.; Lavine, G.; Pandey, R. K.; Racie, T.; Rajeev, K. G.; Röhl, I.; Toudjarska, I.; Wang, G.; Wuschko, S.; Bumcrot, D.; Koteliansky, V.; Limmer, S.; Manoharan, M.; Vornlocher, H.-P., Therapeutic silencing of an endogenous gene by systemic administration of modified siRNAs. *Nature* **2004,** *432* (7014), 173-178.
136. Chandela, A.; Watanabe, T.; Yamagishi, K.; Ueno, Y., Synthesis and characterization of small interfering RNAs with haloalkyl groups at their 3′-dangling ends. *Bioorganic & Medicinal Chemistry* **2019,** *27* (7), 1341-1349.
137. Willibald, J.; Harder, J.; Sparrer, K.; Conzelmann, K.-K.; Carell, T., Click-Modified Anandamide siRNA Enables Delivery and Gene Silencing in Neuronal and Immune Cells. *Journal of the American Chemical Society* **2012,** *134* (30), 12330-12333.
138. Efthymiou, T. C.; Peel, B.; Huynh, V.; Desaulniers, J.-P., Evaluation of siRNAs that contain internal variable-length spacer linkages. *Bioorganic & Medicinal Chemistry Letters* **2012,** *22* (17), 5590-5594.
139. Feng, L.-F.; Zhong, M.; Lei, X.-Y.; Zhu, B.-Y.; Tang, S.-S.; Liao, D.-F., Bcl-2 siRNA induced apoptosis and increased sensitivity to 5-fluorouracil and HCPT in HepG2 cells. *Journal of Drug Targeting* **2006,** *14* (1), 21-26.
140. Akar, U.; Chaves-Reyez, A.; Barria, M.; Tari, A.; Sanguino, A.; Kondo, Y.; Kondo, S.; Arun, B.; Lopez-Berestein, G.; Ozpolat, B., Silencing of Bcl-2 expression by small interfering RNA induces autophagic cell death in MCF-7 breast cancer cells. *Autophagy* **2008,** *4* (5), 669-679.
141. Bouscary, A.; Quessada, C.; René, F.; Spedding, M.; Turner, B. J.; Henriques, A.; Ngo, S. T.; Loeffler, J.-P., Sphingolipids metabolism alteration in the central nervous system: Amyotrophic lateral sclerosis (ALS) and other neurodegenerative diseases. *Seminars in Cell & Developmental Biology* **2021,** *112*, 82-91.
142. Bhatheja, K.; Field, J., Schwann cells: Origins and role in axonal maintenance and regeneration. *The International Journal of Biochemistry & Cell Biology* **2006,** *38* (12), 1995-1999.
143. Huntemer-Silveira, A.; Patil, N.; Brickner, M. A.; Parr, A. M., Strategies for Oligodendrocyte and Myelin Repair in Traumatic CNS Injury. *Frontiers in Cellular Neuroscience* **2021,** *14* (458).
144. Blackburn, D.; Sargsyan, S.; Monk, P. N.; Shaw, P. J., Astrocyte function and role in motor neuron disease: A future therapeutic target? *Glia* **2009,** *57* (12), 1251-1264.
145. Acosta, J.; Carpio, Y.; Borroto, I.; González, O.; Estrada, M. P., Myostatin gene silenced by RNAi show a zebrafish giant phenotype. *Journal of Biotechnology* **2005,** *119* (4), 324-331.

146. Biscans, A.; Caiazzi, J.; McHugh, N.; Hariharan, V.; Muhuri, M.; Khvorova, A., Docosanoic acid conjugation to siRNA enables functional and safe delivery to skeletal and cardiac muscles. *Molecular Therapy* **2020,** *29*.

Appendix

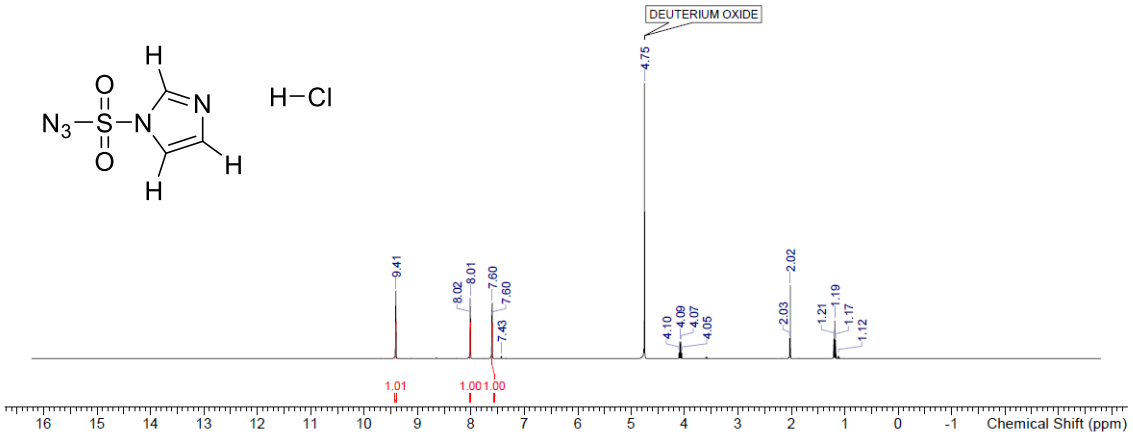

A1.1: ^{1}H NMR Spectrum of Imidazole-1-sulfonyl Azide Hydrochloride – Compound 1

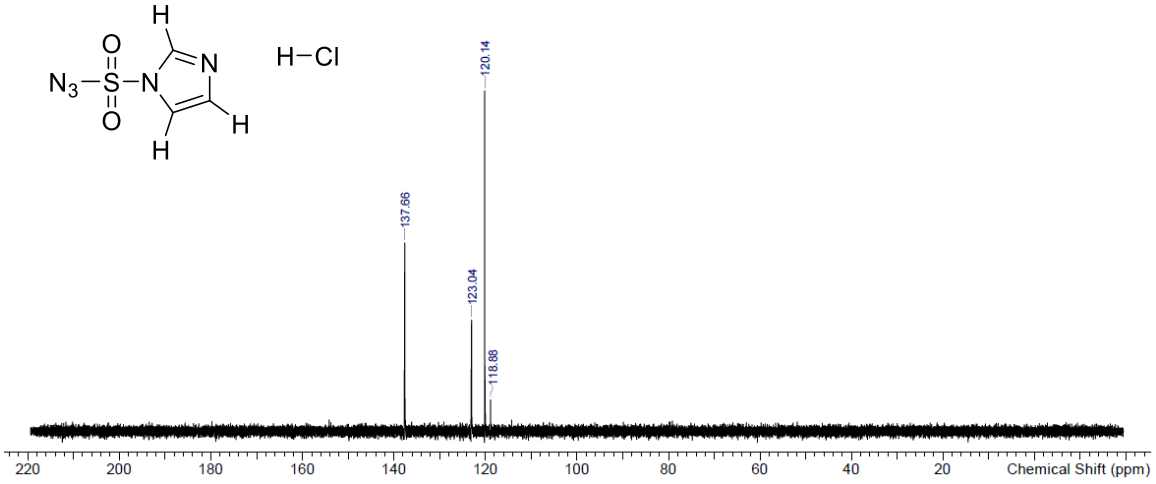

A1.2: ^{13}C NMR Spectrum of Imidazole-1-sulfonyl Azide Hydrochloride – Compound 1

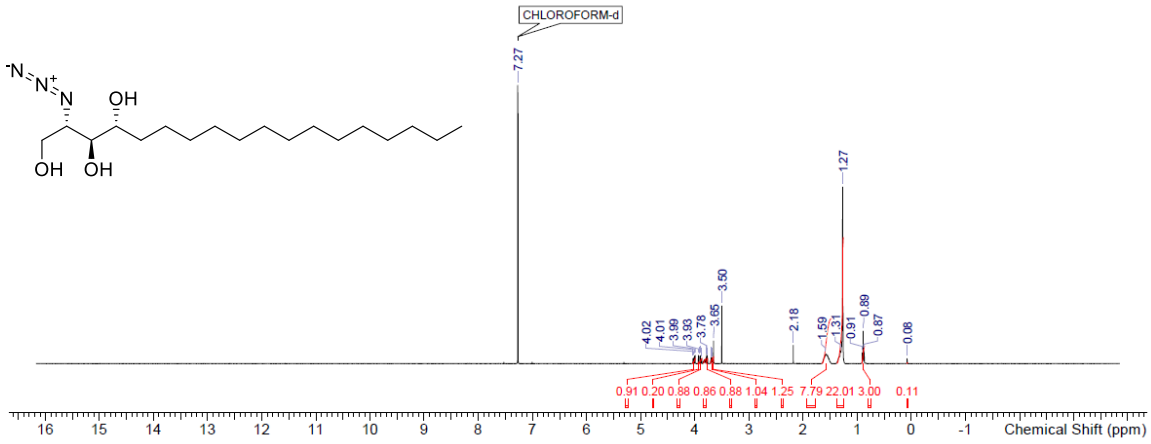

A1.3: ^{1}H NMR Spectrum of (*2S,3S,4R*)-2-azidooctadecane-1,3,4-triol – Compound 3

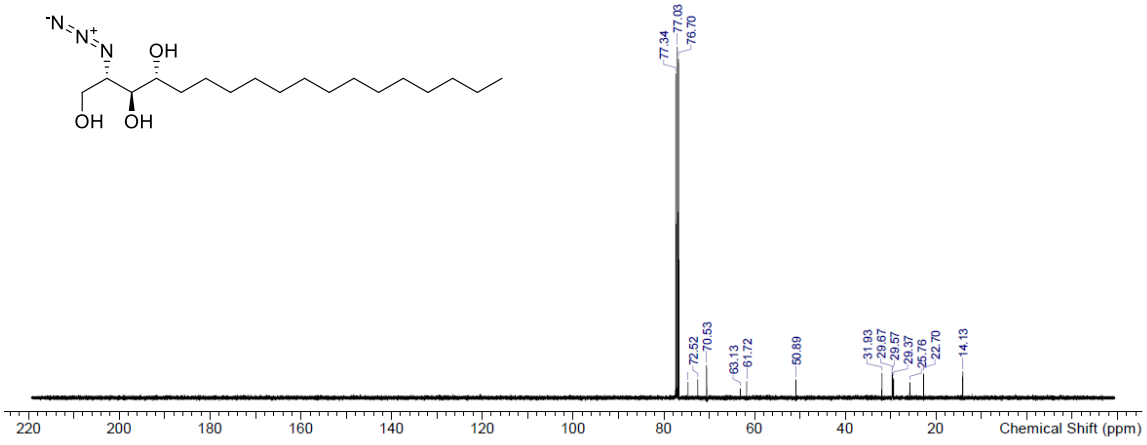

A1.4: ^{13}C NMR Spectrum of (*2S,3S,4R*)-2-azidooctadecane-1,3,4-triol – Compound 3

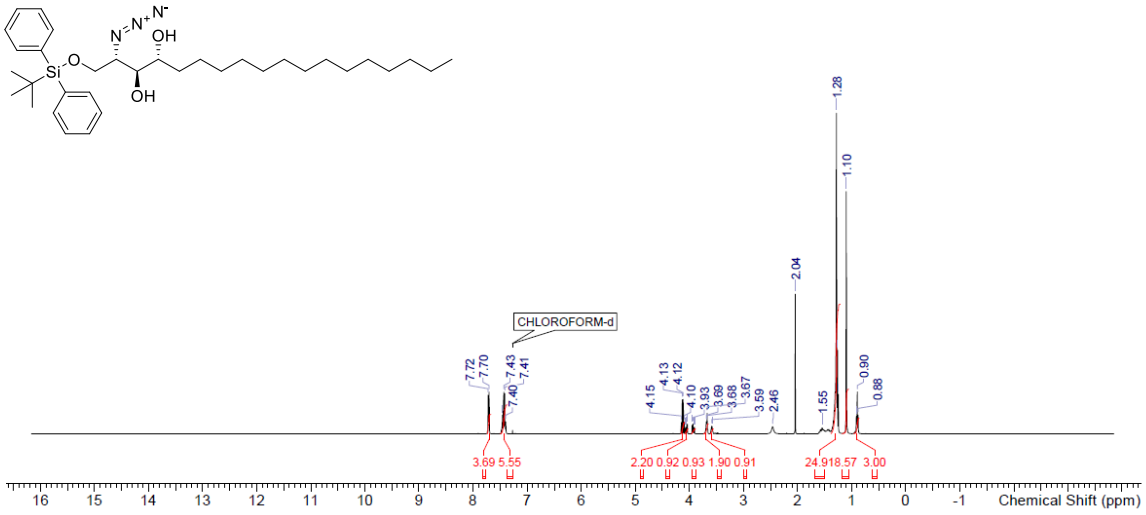

A1.5: ^{1}H NMR Spectrum of (*2S,3S,4R*)-2-Azido-1-(*tert*-butyldiphenylsilyoxy)octadecane-3,4-triol – Compound 4

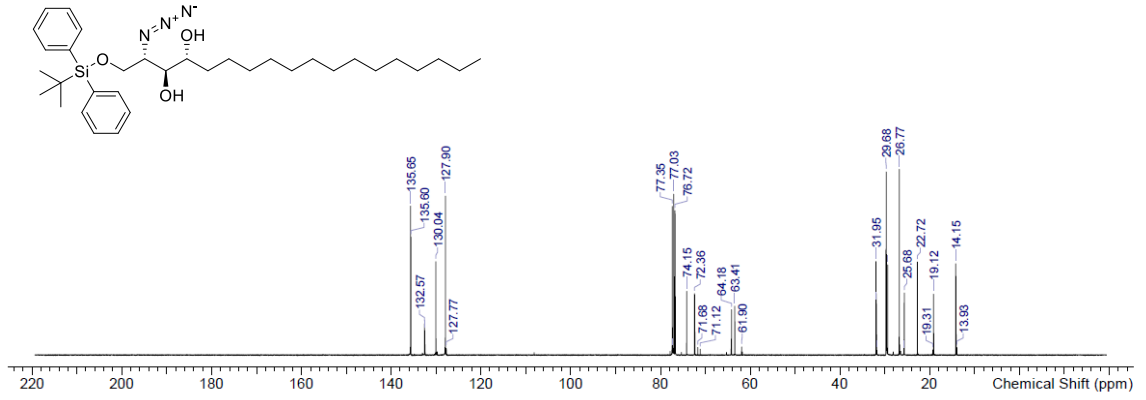

A1.6: ^{13}C NMR Spectrum of(*2S,3S,4R*)-2-Azido-1-(*tert*-butyldiphenylsilyoxy)octadecane-3,4-triol – Compound 4

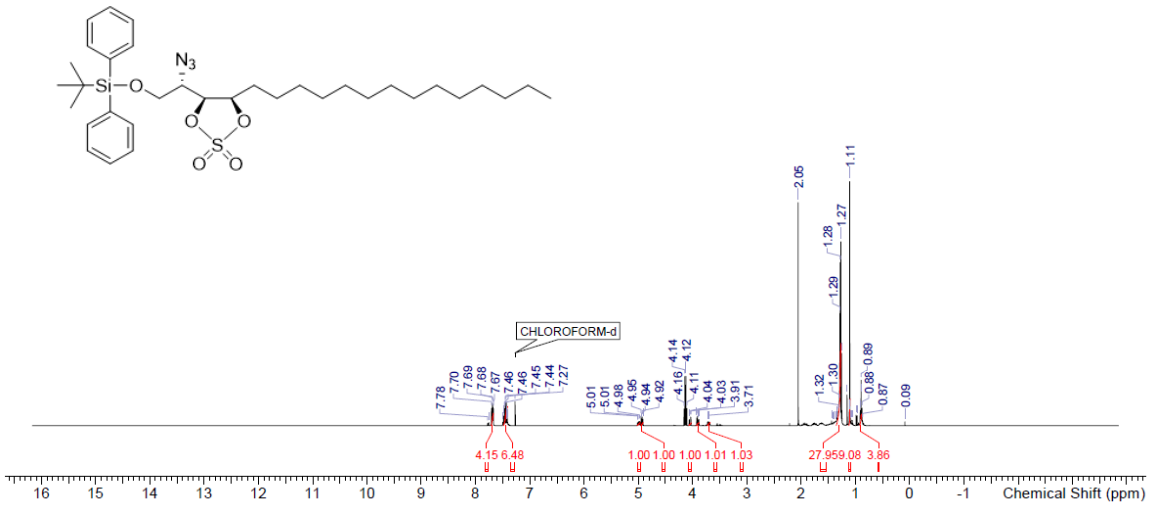

A1.7: ^{1}H NMR Spectrum of (2*S*,4*S*,5*R*)-[2-Azido-2-(2,2-dioxo-5-tetradecyl-2*ì*6-[1,3,2]dioxathiolan-4-yl)ethoxy]-*tert*-butyldiphenylsilane – Compound 5

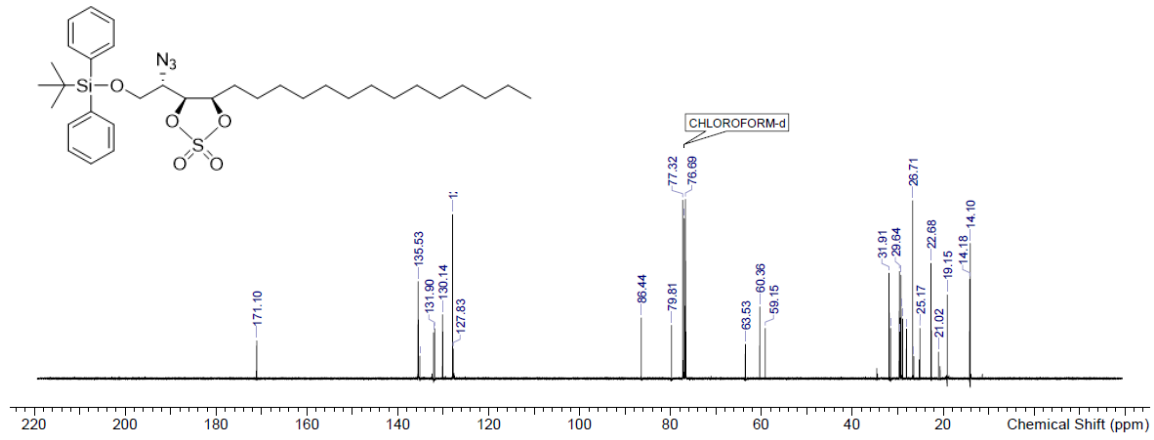

A1.8: ^{13}C NMR Spectrum of(2*S*,4*S*,5*R*)-[2-Azido-2-(2,2-dioxo-5-tetradecyl-2*ì*6-[1,3,2]dioxathiolan-4-yl)ethoxy]-*tert*-butyldiphenylsilane – Compound 5

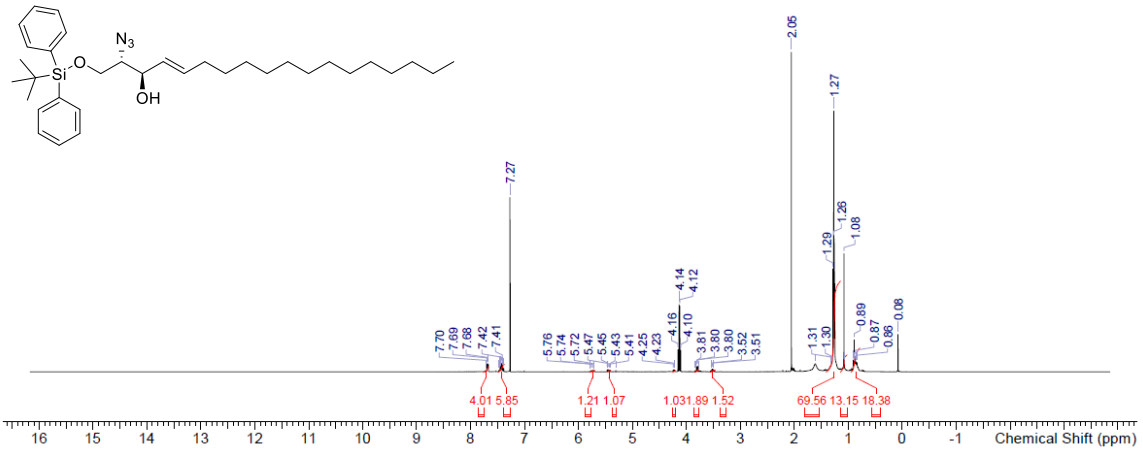

A1.9: ^{1}H NMR Spectrum of (*2S,3R)-(E*)-2-Azido-1-(*tert*-butyldiphenylsilyoxy)octadec-4-en-3-ol – Compound 6

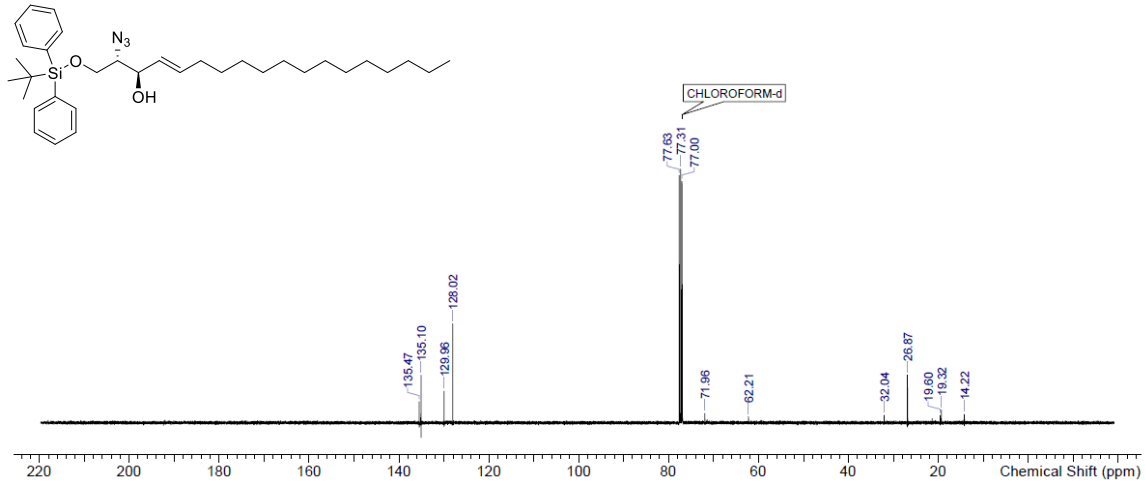

A1.10: ^{13}C NMR Spectrum of (*2S,3R)-(E*)-2-Azido-1-(*tert*-butyldiphenylsilyoxy)octadec-4-en-3-ol – Compound 6

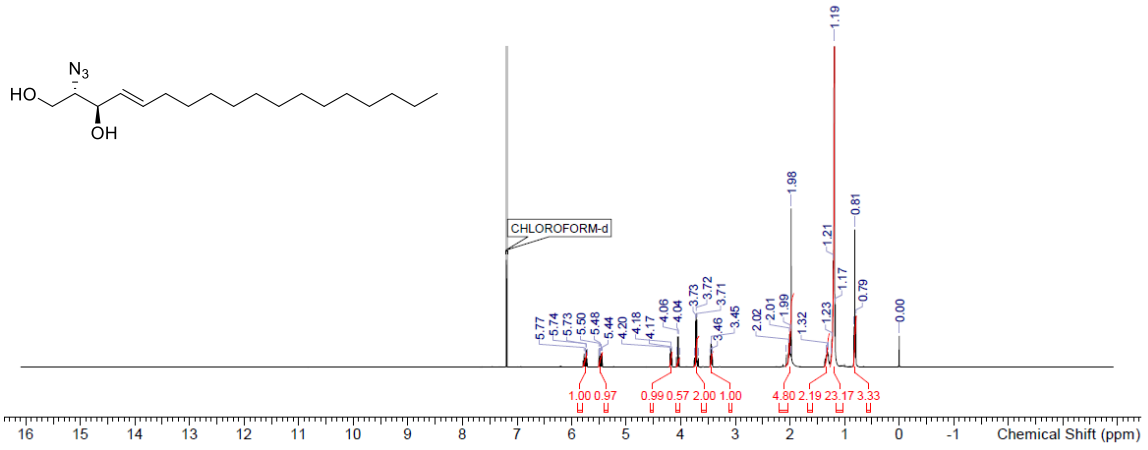

A1.11: ^{1}H NMR Spectrum of (2*S*,3*R*)-(*E*)-2-Azidooctadec-4-ene-1,3-diol – Compound 7

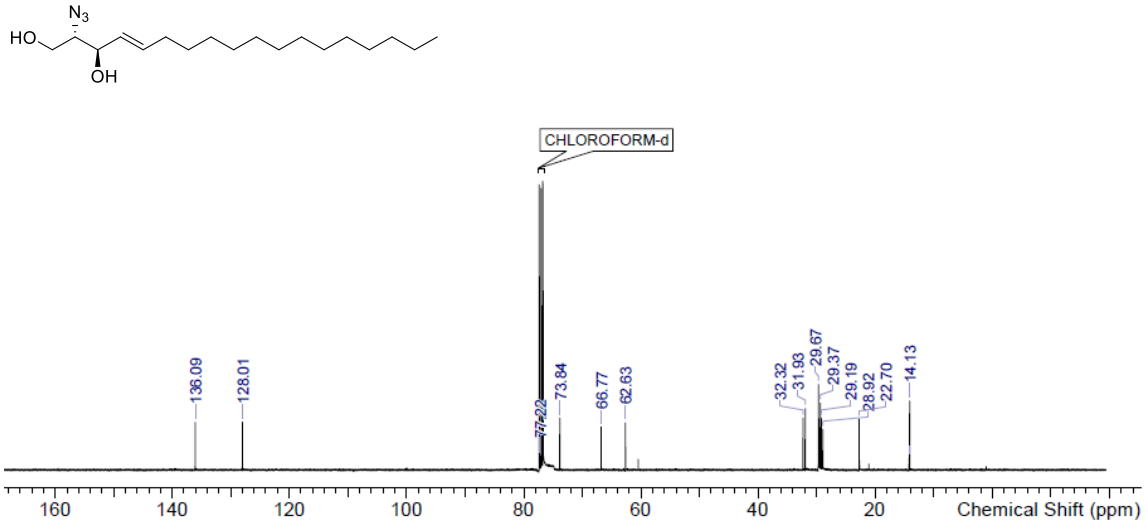

A1.12: ^{13}C NMR Spectrum of (2*S*,3*R*)-(*E*)-2-Azidooctadec-4-ene-1,3-diol – Compound 7

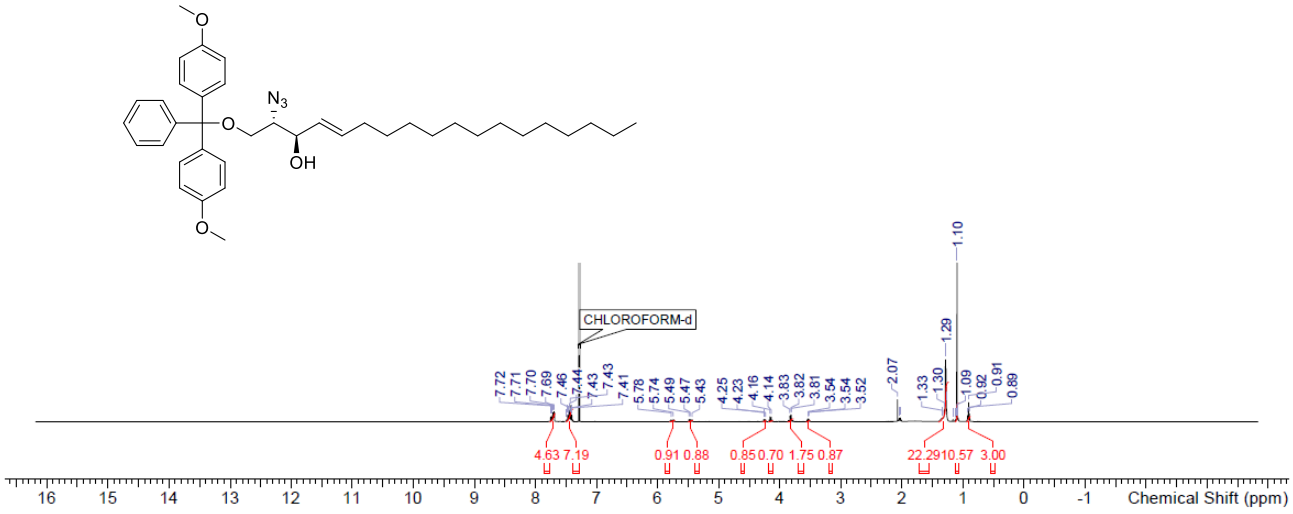

A1.13: ^{1}H NMR Spectrum of (2S,3R,E)-2-azido-1-(bis(4methoxyphenyl)(phenyl)methoxy)octadec-4-en-3-ol – Compound 8

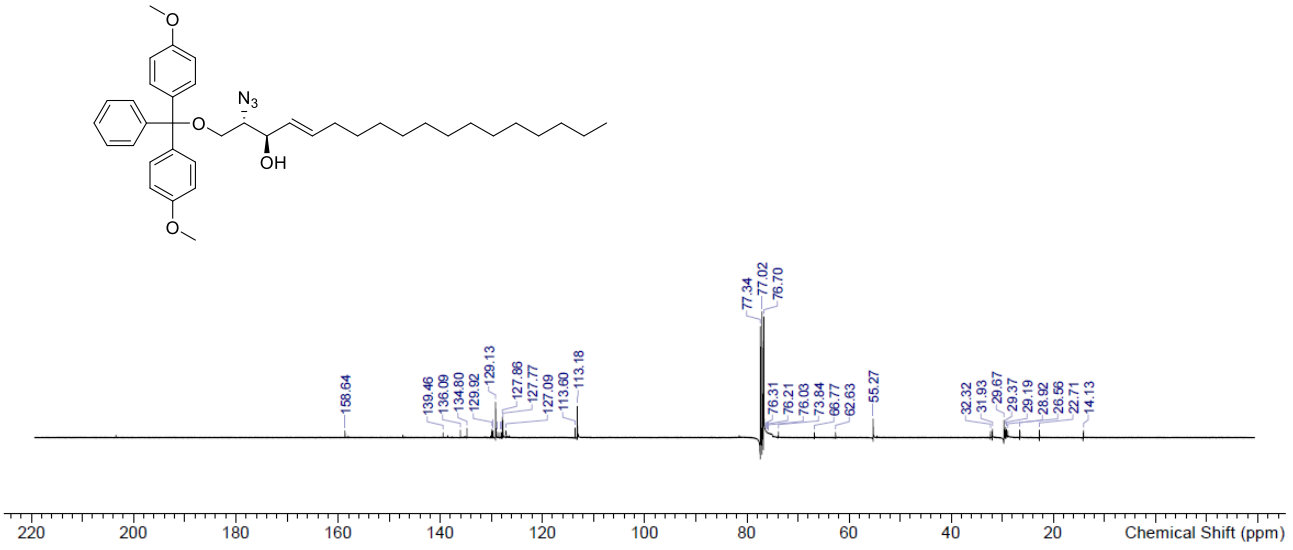

A1.14: ^{13}C NMR Spectrum of (2S,3R,E)-2-azido-1-(bis(4methoxyphenyl)(phenyl)methoxy)octadec-4-en-3-ol – Compound 8

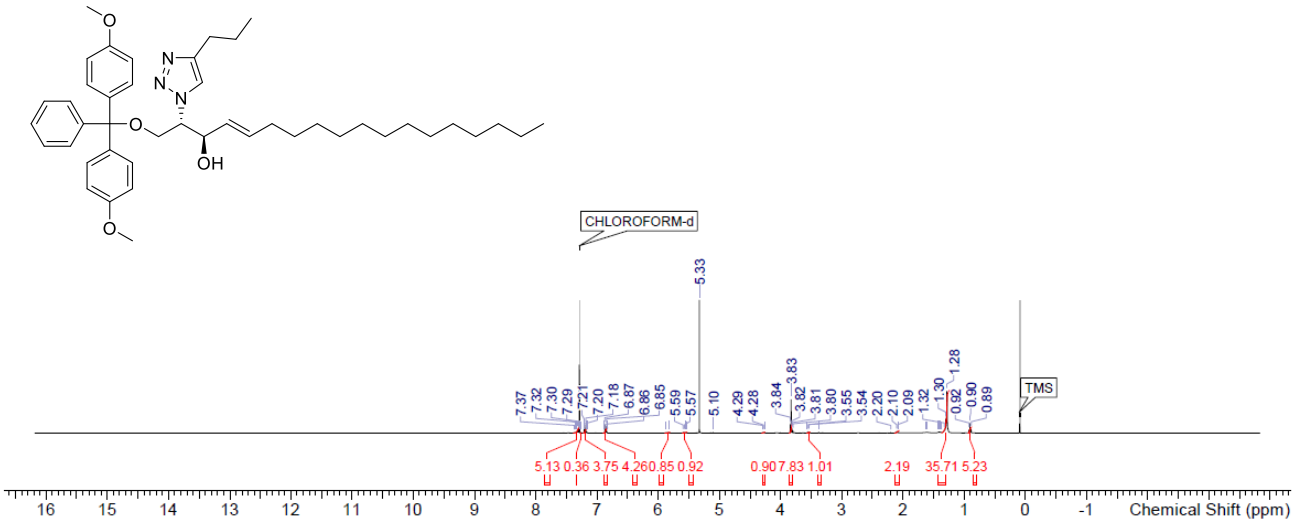

A1.15: ^{1}H NMR Spectrum of (2S,3R,E)-1-(bis(4-methoxyphenyl)(phenyl)methoxy)-2-(4-propyl-1H-1,2,3-triazol-1-yl)octadec-4-en-3-ol – Compound 9-PT

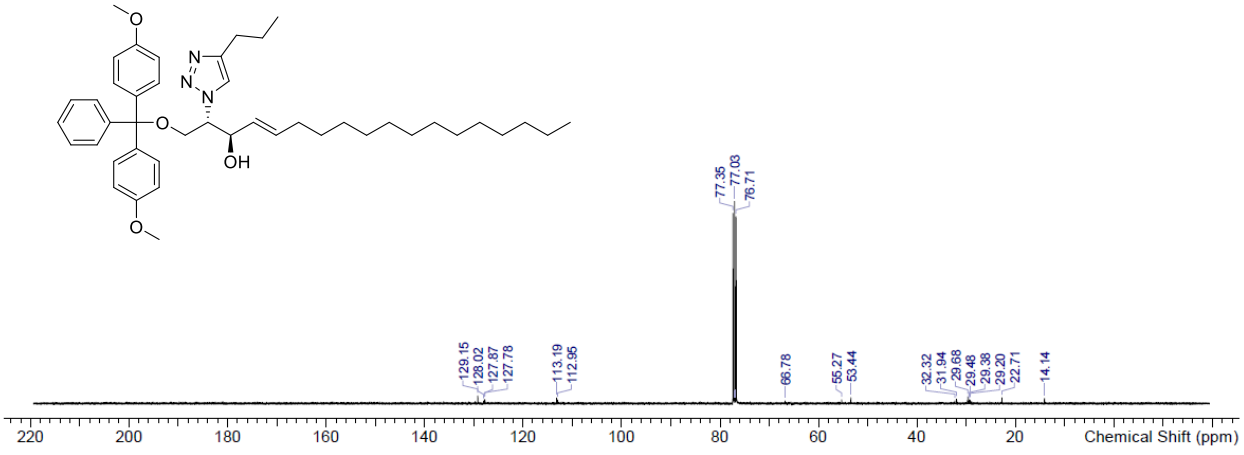

A1.16: ^{13}C NMR Spectrum of (2S,3R,E)-1-(bis(4-methoxyphenyl)(phenyl)methoxy)-2-(4-propyl-1H-1,2,3-triazol-1-yl)octadec-4-en-3-ol – Compound 9-PT

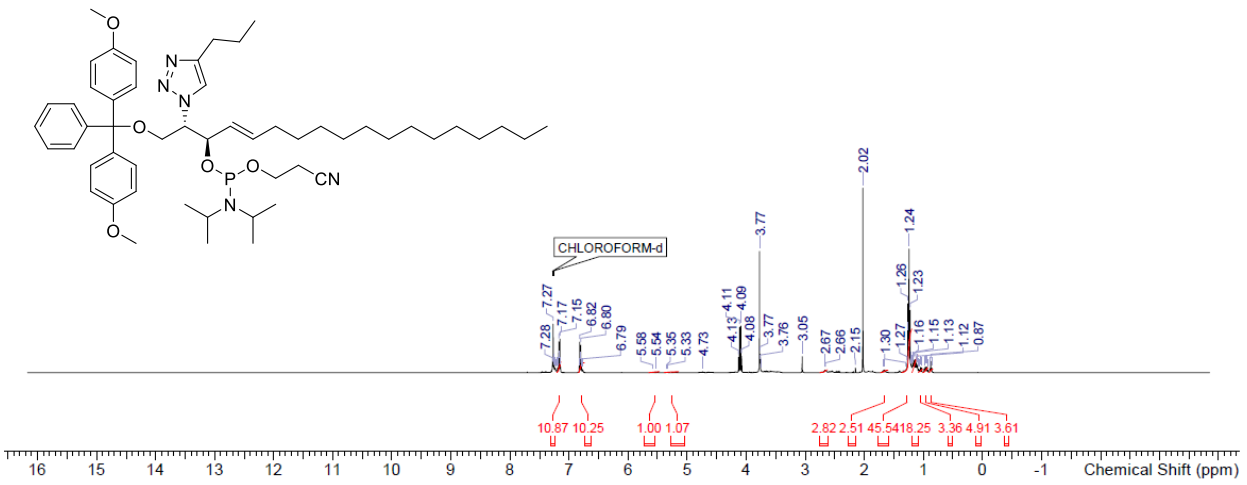

A1.19: ^{1}H NMR Spectrum of (2S,3R,E)-1-(bis(4-methoxyphenyl)(phenyl)methoxy)-2-(4-propyl-1H-1,2,3-triazol-1-yl)octadec-4-en-3-yl (2-cyanoethyl) diisopropylphosphoramidite – Compound 10-PT

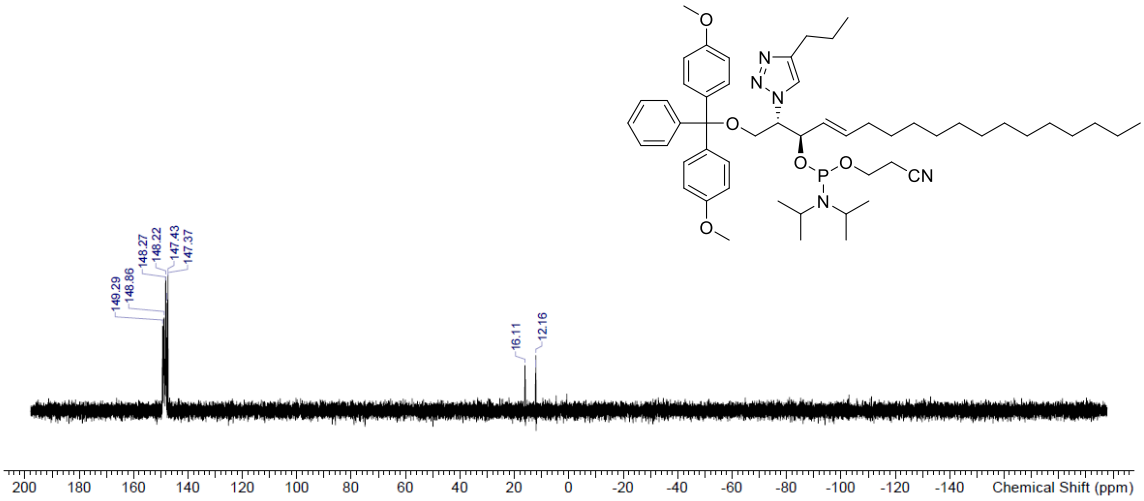

A1.20: ^{31}P NMR Spectrum of (2S,3R,E)-1-(bis(4-methoxyphenyl)(phenyl)methoxy)-2-(4-propyl-1H-1,2,3-triazol-1-yl)octadec-4-en-3-yl (2-cyanoethyl) diisopropylphosphoramidite – Compound 10-PT